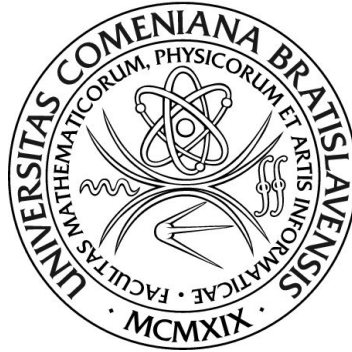


**COMENIUS UNIVERSITY IN BRATISLAVA**  
**FACULTY OF MATHEMATICS, PHYSICS AND INFORMATICS**



**Activation of the Mirror Neuron System  
by Emotional Facial Expressions: an fMRI Study**

DIPLOMA THESIS

Lucia Hrašková

Study programme:	Cognitive Science
Field of study:	2503 Cognitive Science
Department:	Department of Applied Informatics
Supervisor:	RNDr. Barbora Cimrová, PhD.
Consultant:	doc. Grega Repovš, PhD.

**Bratislava, 2018**



## THESIS ASSIGNMENT

**Name and Surname:** Lucia Hrašková  
**Study programme:** Cognitive Science (Single degree study, master II. deg., full time form)  
**Field of Study:** Cognitive Science  
**Type of Thesis:** Diploma Thesis  
**Language of Thesis:** English  
**Secondary language:** Slovak

**Title:** Activation of the Mirror Neuron System by Emotional Facial Expressions: An fMRI Study

**Annotation:** Following a thorough review of relevant literature, the goal of the thesis is to analyse an fMRI dataset and identify brain areas specific to processing emotional facial expressions, relate the results to existing findings about the mirror neuron system, and consider what conclusions can be made about the latter given the available data. Over the course of the work, a reflection on the process itself emerged as a secondary, yet increasingly substantial theme.

**Aim:** The goal of the thesis is to analyse an fMRI dataset and determine whether the studied task enables robust activation of the mirror neuron system.

**Literature:** Fusar-Poli, Paolo et al. (2009): Functional Atlas of Emotional Faces Processing: A Voxel-Based Meta-Analysis of 105 Functional Magnetic Resonance Imaging Studies, *Journal of Psychiatry & Neuroscience* 34(6): 418-432.  
Molenberghs, Pascal et al. (2012): Brain Regions with Mirror Properties: A Meta-Analysis of 125 Human fMRI Studies, *Neuroscience and Biobehavioral Reviews* 36: 341-349.  
Schraa-Tam, Caroline K.L. et al. (2012): fMRI Activities in the Emotional Cerebellum: A Preference for Negative Stimuli and Goal-Directed Behavior, *Cerebellum* 11: 233-245.

**Supervisor:** RNDr. Barbora Cimrová, PhD.  
**Consultant:** doc. Grega Repovš, PhD.  
**Department:** FMFI.KAI - Department of Applied Informatics  
**Head of department:** prof. Ing. Igor Farkaš, Dr.

**Assigned:** 15.02.2016

**Approved:** 22.12.2016  
prof. Ing. Igor Farkaš, Dr.  
Guarantor of Study Programme

---

Student

---

Supervisor



Univerzita Komenského v Bratislave  
Fakulta matematiky, fyziky a informatiky

## ZADANIE ZÁVEREČNEJ PRÁCE

**Meno a priezvisko študenta:** Lucia Hrašková  
**Študijný program:** kognitívna veda (Jednoodborové štúdium, magisterský II. st., denná forma)  
**Študijný odbor:** kognitívna veda  
**Typ záverečnej práce:** diplomová  
**Jazyk záverečnej práce:** anglický  
**Sekundárny jazyk:** slovenský

**Názov:** Activation of the Mirror Neuron System by Emotional Facial Expressions: An fMRI Study  
*Aktivácia systému zrkadliacich neurónov emotívnymi výrazmi tváre: fMRI štúdia*

**Anotácia:** Po dôkladnej revízii relevantnej literatúry analyzujeme súbor fMRI dát s cieľom identifikovať oblasti mozgu aktívne pri spracovávaní emocionálnych výrazov tváre, posúdiť výsledky v kontexte existujúcich zistení o systéme zrkadliacich neurónov a zvážiť, aké závery je o ňom možné urobiť na základe dostupných dát. Druhotnou témou je reflexia samotného procesu, ktorá sa v jej priebehu stávala čoraz podstatnejšou súčasťou práce.

**Cieľ:** Analýza súboru fMRI dát s cieľom určiť, či daná úloha umožňuje robustnú aktiváciu systému zrkadliacich neurónov.

**Literatúra:** Fusar-Poli, Paolo et al. (2009): Functional Atlas of Emotional Faces Processing: A Voxel-Based Meta-Analysis of 105 Functional Magnetic Resonance Imaging Studies, *Journal of Psychiatry & Neuroscience* 34(6): 418-432.  
Molenberghs, Pascal et al. (2012): Brain Regions with Mirror Properties: A Meta-Analysis of 125 Human fMRI Studies, *Neuroscience and Biobehavioral Reviews* 36: 341-349.  
Schraa-Tam, Caroline K.L. et al. (2012): fMRI Activities in the Emotional Cerebellum: A Preference for Negative Stimuli and Goal-Directed Behavior, *Cerebellum* 11: 233-245.

**Vedúci:** RNDr. Barbora Cimrová, PhD.  
**Konzultant:** doc. Grega Repovš, PhD.  
**Katedra:** FMFI.KAI - Katedra aplikovanej informatiky  
**Vedúci katedry:** prof. Ing. Igor Farkaš, Dr.  
**Dátum zadania:** 15.02.2016

**Dátum schválenia:** 22.12.2016

prof. Ing. Igor Farkaš, Dr.  
garant študijného programu

.....  
študent

.....  
vedúci práce

I hereby declare that this thesis was written by myself,  
without any unauthorised third-party support.  
Formulations and ideas taken from other sources are  
cited as such.

.....

The author would like to thank  
Grega and Anka for the data and time,  
Bajka for the support and nerves,  
Rišo for saving her when she got stuck,  
Honza, because he asked for it,  
and Kajco, for being the best.

# Abstrakt

Schopnosť dedukovať mentálne a emočné stavy iných, čiastočne facilitovaná emočnými výrazmi tváre, je kľúčová pre sociálnu interakciu. Zrkadliace neuróny - neuróny aktívne pri pozorovaní i vykonávaní rovnakého úkonu - sú potenciálnym základným mechanizmom tejto schopnosti. Cieľom tejto práce je pomocou funkčnej magnetickej rezonancie (fMRI) identifikovať oblasti mozgu, ktoré sú aktívne pri pozorovaní emočných výrazov tváre a potencionálne súčasťou systému zrkadliacich neurónov, a tak prehĺbiť poznatky o tomto mechanizme. Po dôkladnej revízii existujúcej literatúry o emóciách, empatii a zrkadliacich neurónoch, ako aj podobných štúdií, na ktorých táto práca stavia, opisuje techniku fMRI a následne samotnú analýzu. Výsledky naznačujú, že oblasti mozgu aktivované skúmaným experimentom zahŕňajú niektoré z kľúčových oblastí bežne považovaných za súčasť systému zrkadliacich neurónov - BA44 a BA45, dolný parietálny lalok, insulu, amygdalu a dolný frontálny gyrus - a potvrdzujú, že filmy, ktoré ich majú vyvolávať, sú efektívnejšie pre emócie s vyššou subjektívnou vzrušivosťou. Práca usiluje o transparentnosť o jej základných predpokladoch, obmedzeniach a rozhodnutiach urobených v jej priebehu. Ich detailný opis a reflexia samotného procesu sú jej integrálnou súčasťou. Vďaka podrobnému popisu samotnej fMRI analýzy pomocou FSL je tiež využiteľná ako príručka pre začiatočníkov.

**KLÚČOVÉ SLOVÁ:** emócie, výrazy tváre, fMRI, zrkadliace neuróny

# Abstract

The ability to make inferences about the mental and emotional state of others, partly enabled by reading emotional facial expressions, is crucial to social interaction. Mirror neurons, a class of neurons active both when observing and experiencing a motor act, have been argued to be its underlying mechanism. The goal of the present work is to deepen the understanding of this mechanism by identifying brain regions that are activated by observing emotional facial expressions, and potentially part of the mirror neuron system, using functional magnetic resonance imaging (fMRI). Following a thorough review of existing literature on emotions, empathy, and the mirror neuron system, as well as similar studies on which this work elaborates, we describe the technique of fMRI, before proceeding to the analysis itself. The results suggest that the brain regions activated by our experiment include some of the key areas commonly considered to be part of the mirror neuron system - BA44, BA45, the inferior parietal lobule, the insula, the amygdala, and the inferior frontal gyrus - and confirm that emotions with higher subjective arousal are more easily induced by films designed to elicit them. The work aims to be transparent about its underlying assumptions, limitations, and the decisions made over the course of it. The latter are described in considerable detail, with a reflection on the process itself constituting an integral part of it. The detailed description of fMRI analysis using FSL also makes it potentially useful as a tutorial for beginners.

**KEYWORDS:** emotions, facial expressions, fMRI, mirror neurons

# Contents

<b>Introduction</b>	<b>11</b>
<b>Emotions</b>	<b>12</b>
The subjective component	13
The physiological component	13
The behavioural component	14
Eliciting emotions	16
<b>Empathy</b>	<b>17</b>
Social perspective	18
Cognitive perspective	19
Biological perspective	20
<b>Mirror neuron system</b>	<b>20</b>
<b>Functional magnetic resonance imaging</b>	<b>26</b>
Basic principles of MR imaging	26
Functional MRI	27
<b>Materials and methods</b>	<b>29</b>
Participants	29
Stimuli, experimental design, and procedure	30
fMRI acquisition	33
Functional image analysis	33
Preprocessing	34
Detecting scanner artefacts	34
Distortion correction	34
Brain extraction	35
FSL FEAT	37
Motion correction	37
Slice-timing correction	41
Spatial smoothing	42
Intensity normalisation	43
High-pass temporal filtering	43
Registration	43
Output	45
ICA-AROMA and high-pass temporal filtering	45
First-level analysis	47
General linear model	47
Statistical inference	50

Output	51
Group-level analysis	52
Output	54
Statistical inference	54
<b>Results</b>	<b>57</b>
<b>Conclusion</b>	<b>58</b>
<b>Personal reflection</b>	<b>60</b>
<b>Bibliography</b>	<b>65</b>
<b>Appendix A</b>	<b>81</b>
<b>Appendix B</b>	<b>93</b>

# Abbreviations

**BBR** Boundary-Based Registration

**BET** Brain Extraction Tool

**BOLD** blood-oxygen level-dependent

**DOF** degrees of freedom

**EPI** echo-planar imaging

**FDR** false discovery rate

**FE** fixed-effects

**FEAT** fMRI Expert Analysis Tool

**FILM** FMRIB's Improved Linear Model

**FLAME** FMRIB's Local Analysis of Mixed Effects

**FLIRT** FMRIB's Linear Image Registration Tool

**fMRI** functional magnetic resonance imaging

**FWE** familywise-error rate

**FWHM** full width at half maximum

**FSL** Functional MRI of the Brain Software Library

**GLM** general linear model

**HRF** hemodynamic response function

**IAPS** International Affective Picture System

**ICA** independent component analysis

**ICA-AROMA** ICA-based Automatic Removal of Motion Artefacts

**ISI** inter-stimulus interval

**MCFLIRT** motion correction FMRIB's Linear Image Registration Tool

**MH MCMC** Metropolis-Hastings Markov Chain Monte Carlo

**ME** mixed-effects

**MELODIC** Multivariate Exploratory Linear Optimized Decomposition into Independent Components

**MNI** Montreal Neurological Institute

**MNS** mirror neuron system

**MRI** magnetic resonance imaging

**OLS** ordinary least squares

**PE** parameter estimate

**RF** radiofrequency

**RFT** random field theory

**STS** superior temporal sulcus

**SVD** singular value decomposition

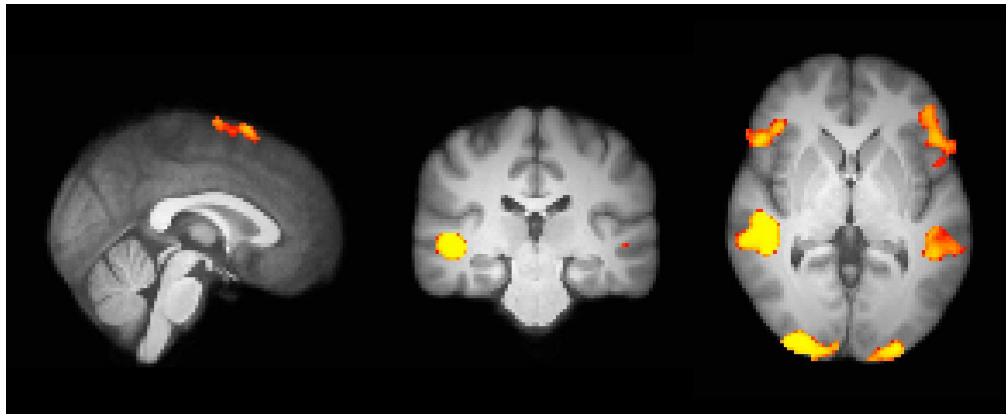
**TE** echo time

**TFCE** Threshold-Free Cluster Enhancement

**TMS** transcranial magnetic stimulation

**TR** repetition time

Research has found that using brain images to represent the level of brain activity associated with cognitive processes in a paper increases its perceived credibility (McCabe and Castel, 2008).



The following text leads up to an interpretation of the fMRI image above.

The judgment on its credibility is left up to the reader.

# Introduction

Humans are ‘social animals’, and their ability to convey and understand each other’s thoughts and feelings is key to social interaction (Dijksterhuis, 2005). Communication takes many forms, from words to body language, with the latter, arguably, forming a major part of it (Mehrabian, 1972). Whilst body language appears to differ between cultures, facial expressions - at least some of them - have been argued to be universal, and revealing of our internal states, often against our will (Ekman and Friesen, 1971). The supposedly universal and discrete nature of emotional facial expressions also makes them useful for studies of emotion. The face is, indeed, one of the richest and most powerful tools in social communication, and we are ‘very good at explicitly recognising and describing the emotion being expressed’ by it (Frith, 2009). We read, and even mimic, other people’s emotional facial expressions spontaneously, often without being aware of it. This facilitates and improves social relationships (Chartrand and Bargh; 1999). The recently discovered mirror neurons - a class of neurons that fire both when observing and performing a specific motor act - have been argued to be the underlying mechanism of this ability (Gallese et al., 1996; di Pellegrino et al., 1992).

The goal of the present work is to deepen the understanding of this mechanism by identifying brain regions activated by emotional facial expressions using functional magnetic resonance imaging (fMRI). It builds on existing studies, such as that of van der Gaag et al. (2007), who performed three experiments in which the participants had to either observe, discriminate, or imitate facial expressions presented through film clips. They found that ‘even passive viewing of facial expressions activates a wide network of brain regions that were also activated in the execution of similar expressions, including the IFG (inferior frontal gyrus)/insula, and the posterior parietal cortex’ (ibid.). Using similar stimuli, Bastiaansen et al. (2011) examined the hypoactivation of the same system in adults with autism-spectrum disorders, and found that, in this population, the activity of the IFG increases with age, and is accompanied by an improvement in social functioning.

Schraa-Tam et al. (2012) focused specifically on activation of the cerebellum, and how it differs for positive and negative emotions.

The present work begins with a survey of the complex notions of emotion and empathy, and a review of existing research on mirror neurons. It builds upon the above-mentioned studies, and uses similar stimuli, with the goal of identifying brain areas specific to processing emotional facial expressions that are potentially part of the mirror neuron system (MNS). A detailed description of the analysis and the decisions behind it, as well as a reflection on the process itself, constitute secondary, yet crucial parts of it.

## Emotions

Despite the fact that most people experience them and have an intuitive understanding of what they are, the concept of emotions has been notoriously difficult, perhaps impossible, to define in its entirety, let alone measure. The complexity of emotional processes and states is reflected in a variety of definitions and theories of emotion, each approaching the issue from a different point of view, and emphasising different primary characteristics. Back in 1980, Plutchik observed that ‘there is no sense of the definitions moving in a certain direction with time; the more recent definitions are as inconsistent as are the earlier ones’. Decades later, these statements appear to remain true. Having reviewed and classified a variety of them, Kleinginna and Kleinginna (1981: 355) concluded that ‘a formal definition of emotion should be broad enough to include all traditionally significant aspects of emotion, while attempting to differentiate it from other psychological processes’.

First of the significant aspects is evolutionary, with work on emotional expressions having been an integral part of Darwin’s research on human evolution, and one of his arguments

for the descent of humans from animals (Darwin et al., 1872). Plutchik (1980), too, argues that human emotions have deep evolutionary roots. As a ‘complex chain of loosely connected events that begins with a stimulus and includes feelings, psychological changes, impulses to action and specific, goal-directed behaviour’, they situate individuals within their environment, and allow them to act upon, interact with, and survive in the latter (ibid.). Although various theories have attempted to describe the way in which the aspects of emotional experience relate to each other, and the exact nature of these mechanisms remains unclear, there is, indeed, broad agreement that it consists of three major components: subjective (affective/cognitive), physiological, and behavioural (Cannon, 1927; Schachter and Singer, 1962).

## **The subjective component**

The bodily sensations provoked by a subjectively significant internal or external stimulus, together with perceptual and cognitive appraisal, or labeling of it, result in the subjective experience of emotions (Kleinginna and Kleinginna, 1981). Feelings, defined by Damasio and Carvalho (2013) as mental experiences of a body state, are the foundation for the more complex processes called emotion, and have been argued to be the essence of it (LeDoux and Hoffman, 2018). The subjective emotional experience is defined by its valence (positive/negative) and level of arousal, influenced by personal experience, beliefs, and memories, and best assessed through self-report (LeDoux and Hoffman, 2018). Due to their visceral, irrational nature, feelings are often considered in contrast to rational thinking. Emotions modulate our cognitive functions, including memory and attention, and allow for fast decision-making. Conversely, the ability of an organism to be cognitively aware of its emotional state is a key aspect of emotional experience (ibid.). Rather than being the opposite sides of a spectrum, emotions and cognition are therefore closely linked, and complementary.

## **The physiological component**

The series of physiological reactions provoked by the stimulus are mediated by neural-hormonal systems and can, to an extent, be observed and measured. Physiological measures commonly used for assessment of emotional states include electrodermal activity (EDA, also referred to as skin conductance, or galvanic skin response), blood pressure, heart rate, skin temperature, respiration rate, and body heat flux, among others. As argued by Boucsein (2012: 379), ‘different parameters could have different validities not only with respect to various emotional states, (...) but also with respect to different experimental settings.’

Cardiac activity is among the most widely used. Heart rate is closely associated to many basic human functions and can rise significantly during certain emotional events. Although interpreting the relevance of the signal can be challenging because many different bodily processes regulate the heart and circulatory systems, heart rate remains a popular measure, sensitive to cognitive demands, time restrictions, and uncertainty (Allanson and Fairclough, 2004). It has been used to assess not only emotional arousal and valence, but also attention, cognitive effort (or mental workload), stress, and orientation reflex during media viewing (Kivikangas et al., 2011). Skin conductance is associated with emotional arousal and can be considered a direct measure of sympathetic activity (Lang et al., 1993). Whilst its temporal resolution is rather low, it is less sensitive to noise and less ambiguous than some other measures, such as heart rate. It acts as a measure of stress and frustration, and is linearly correlated with arousal (Park, 2009; Ganglbauer et al., 2009; Bethel et al., 2007). Last but not least, brain imaging techniques are instrumental in revealing neural activity associated with various emotional states. Although there is no single method capable of accurately reading the inherently subjective emotional state of an individual, there is ‘growing evidence indeed that emotional states have their corresponding specific physiological signals that can be mapped respectively’ (Lisetti and Nasoz, 2004:1674).

## **The behavioural component**

The experience of an emotion is inextricably linked with a motor and behavioural reaction. Behaviour motivated by emotions is ‘often, but not always, expressive, goal-directed, and adaptive’ (Kleinginna and Kleinginna, 1981). It allows us to adapt to our environment, and survive in it, while also allowing others to assess our emotional state, and act accordingly. Indeed, while measures such as skin conductance or heart rate might be useful for the assessment of emotions in a research or clinical setting, humans do not normally measure each other’s physiological responses, and rely instead on motor expressions of emotions for everyday communication. The facial-feedback theory of emotions suggests that the motor expression of an emotion can, in fact, precede, and provoke, the experience of the associated physiological responses (James, 1890). Motor expressions such as body language, gestures, or facial expressions therefore act as proxies of emotional states, useful for social interaction.

Whilst emotions can also be expressed verbally, linguistic and semantic accounts are deliberate, and as such create more space for inaccuracy and deception than nonverbal communication. The melodic and rhythmic components of speech known as emotional prosody, however, do provide an insight into the speaker’s emotive disposition, and have also been shown to ‘play a critical role in how humans respond to related visual cues in the environment, such as facial expressions’ (Rigoulot and Pell, 2012). Facial perception, defined as ‘any higher-level processing of faces’, involves both perceptual processing and recognition of the emotional meaning of a stimulus (Fusar-Poli et al., 2009; Kanwisher et al., 1997). Of nonverbal displays of emotion, facial expressions are, arguably, the most powerful. Although they may vary across cultures, individuals, and time, Ekman and Friesen (1971) have argued that an understanding of certain facial expressions that reflect discrete, separate emotions, which they call basic, appears to be universal. The list initially included 6 basic emotions - happiness, sadness, anger, surprise, disgust and fear - and was later extended to include others (Ekman and Friesen, 1971; Ekman, 1999).

The very existence of a subset of basic emotions remains subject to ongoing debate (Clark-Polner et al., 2017; Cohen, 2005). While not rejecting the idea that there might be basic meaningful components out of which emotions are built, Ortony and Turner (1990) argue that ‘the complexity and the apparent limitlessness of different emotional feelings can be explained without recourse to a notion of basic emotions’. Moreover, whether emotions can truly be reduced to, or deduced from facial expressions, remains unclear. The notion that there is a straightforward link between emotions and facial expressions, and that the latter is culturally universal, has been questioned (Gendron et al., 2014; Jack et al., 2012). Reisenzein et al. (2013) have argued that ‘with the exception of amusement - which, as mentioned, is not commonly considered a prototypical emotion - there is, at present, no convincing evidence that people undergoing the ‘basic emotions’ (...) typically show the patterned facial expressions predicted by the theory’. Facial expressions thus might not always reflect the emotional states we believe they do. Experimental studies investigating brain activity, however, require a method that is readily standardised, and continue to employ facial expressions associated with basic emotions, presented in various forms, as their experimental stimuli, hoping to invoke the desired emotions in their participants.

Emotions supposedly ‘give evidence of dispositions in the individual that allow events to be appraised as pleasant and unpleasant - that is, to elicit positive or negative affect’ (Frijda, 1994). The notion of valence and emotional polarity, or ‘opposites’, has, however, been criticised. Solomon and Stone (2002) call the labelling of emotions as ‘positive’ or ‘negative’ ‘simple-minded and detrimental to serious research on the emotions’, arguing that it ‘blocks our appreciation of the subtlety and complexity of emotions’ and ‘leads us to misleading ‘oppositional’ thinking which belies the complex relationships among emotions’. Nevertheless, rather than studying individual emotions, studies of the latter commonly group them by their valence, for the sake of simplicity and significant results.

## Eliciting emotions

Procedures used to elicit various emotional states in a laboratory setting range from hypnosis, repeating phrases, imagery, and music to narrative text, pictures, and film clips, with the latter being, arguably, more reliable and preferred (Bower, 1983; Velten, 1968; Lang, 1979; Sutherland et al., 1982). Standardised databases of pictures for studying emotions exist, with the International Affective Picture System (IAPS) being perhaps the best known and widely used (Lang et al., 2008). Uhrig et al. (2016) have found pictorial stimuli to be, perhaps unexpectedly, more effective in producing the corresponding emotional states than film clips, while admitting that this might have been caused by the length of the clips they used, rather than an inherent stimulus quality. Two-dimensional photographs, however, are 'not amenable to manipulations of angle and orientation and raise methodological concerns when applied to examination of facial asymmetries that could be related to hemispheric specialization' (Fusar-Poli et al., 2009). 3-D stimuli, such as those developed by Gur et al. (2002), were therefore designed to address these shortcomings.

Conversely, Zupan and Babbage (2017) have shown film clips to be a more effective technique of emotion elicitation than narrative text, and films also continue to be commonly preferred over pictorial stimuli. Horvat et al. (2015) found that 'carefully designed video sequences induce a stronger and more accurate emotional reaction than pictures.' Whilst Philippot (1993) has confirmed that 'film segments can elicit a diversity of predictable emotions, in the same way, in a majority of individuals', Fernández et al. (2012) argue that 'physiological activation would be more easily induced by emotion-eliciting films that tap into emotions with higher subjective arousal, such as anger and fear'. Films also have the advantage of being readily standardised and having 'a relatively high degree of ecological validity, in so far as emotions are often evoked by dynamic visual and auditory stimuli that are external to the individual' (Gross and Levenson, 1995). For practical reasons, films used to elicit emotions normally use actors rather than genuine, spontaneous facial expressions. Whilst posed expressions might be easier to discern, it is important to remember that, albeit not always accurately, humans -

and even machines - might be able to distinguish authentic from ambiguous or contrived facial expressions, and the latter might not have the same effect as the former, i.e. what is usually desirable in a psychological study (Calvo et al., 2013; Hoque et al., 2012).

## Empathy

Reading facial expressions contributes to our ability to infer the emotional state - or empathise - with another person (Zhou et al., 2017). Empathy is crucial for our social functioning and co-existence and it does, indeed, ‘in some sense cut right to the heart of what it means to be human’ (Rameson and Lieberman, 2009:94). Nevertheless, despite years of research, the complex construct of empathy has evaded a single, all-encompassing definition. Numerous conceptions of empathy have been proposed by researchers in various disciplines. The concept can be approached from a number of perspectives offering a range of insights that complete and enrich, rather than contradict each other, and is perhaps best understood if these are combined.

### **Social perspective**

Humans are social animals, and empathy, defined by Decety and Lamm (2001:199) as a ‘sense of similarity in feeling experienced between self and the other, without confusion between the two’, is crucial for their functioning as such. People affected by disorders characteristic by a lack of empathy tend to have difficulties with social interaction. It is an important component of interpersonal communication, and survival, and might also play a significant role in moral understanding and agency (Watson and Greenberg, 2001; Kennett, 2002). Segal (2011:268) goes as far as arguing that social empathy, which she defines as ‘the conjunction of individual empathy and deep contextual understanding of inequalities and disparities’, can enhance civic engagement, social action, and justice. Empathy might thus be crucial not only in sustaining, but also in improving our society.

Motor imitation, a low-level version of empathy, is part of nonverbal communication, which has been argued to be more important than verbal communication (van Baaren et al., 2001; Mehrabian, 1972). Imitation, called ‘social glue’ by Dijksterhuis (2005), is therefore crucial to social interactions. Interestingly, rather than being a supplement to regular communication, imitation appears to be automatic, and the default (ibid.). A complete lack of it is perceived as odd. Conversely, if deliberate and contrived, imitation becomes obtrusive. Crucially, spontaneous imitation is not only of significance for the bond between the mimicker and the mimicked individual. It affects how we perceive and interact with our social environment in general, and makes us more prosocial (ibid.).

However, whilst empathy can inspire compassion, defined by Singer and Klimecki (2014: 875) as ‘a feeling of concern for another person’s suffering which is accompanied by the motivation to help’, it can also, paradoxically, have the opposite effect. Personal distress, ‘a strong aversive and self-oriented response to the suffering of others’ can result in the desire to ‘protect oneself from excessive negative feelings’, and withdraw, rather than help others (ibid.). The quality and extent of the experience of empathy thus appear to be crucial for its effect on the individual and, consequently, on their environment.

## **Cognitive perspective**

The distinction between cognitive and emotional empathy helps further elucidate the different effects of empathy on the individual and their behaviour. According to Blair and Blair (2001:141), ‘*cognitive empathy* refers to the process by which an individual represents the internal mental state of another individual’, with the latter also being the definition of theory of mind. Such rational perspective-taking and the ‘metacognitive process of thinking about the contents of other people’s minds’ is also referred to as mentalising (Rameson and Lieberman, 2009:98).

Conversely, *affective empathy* ‘also includes sharing of those feelings, at least at the level of gross affect’ (Shamay-Tsoory, 2001). It is underlaid by simulation theory, which argues that we understand the minds of others by using our own mind as a model (Rameson and Lieberman, 2009). The latter has, arguably, been supported by the discovery of mirror neurons that are activated by both our own actions and the actions of another person, and have also been invoked in discussions of imitation. Empathy thus appears to involve both cognitive and affective components (Pfeifer and Dapretto, 2001). Shamay-Tsoory (2001:228) argues that mentalising and simulation are served by separate, though interacting, neural networks, and that ‘a balanced activation of these two networks is required for appropriate social behaviour’.

## **Biological perspective**

Recent research in neuroscience has confirmed that the way empathy has been conceptualised can be mediated by dedicated neural networks, and supported by the cognitive and affective processes activated when people experience it (Shamay-Tsoory, 2001:215, Watson and Greenberg, 2001:126). Simply observing another individual in pain has been shown to ‘activate the neural network associated with the coding of the motivational-affective dimension of pain in oneself’ (Decety and Lamm, 2001:201). Eisenberg and Eggum (2001:76) suggest that ‘the neurological processes involved in self-regulation play an important role in empathy-related responding.’ Interestingly, the degree of connection between observer and target in psychophysiological indicators ‘predicts better understanding of the target’s emotional state’ (ibid.).

Studies using fMRI indicate that whilst mentalising involves the medial prefrontal cortex, the temporoparietal junction, and the temporal poles, affective empathic response involves regions that mediate emotional experiences (Blair and Blair, 2001; Shamay-Tsoory, 2001). Moreover, there is evidence that the ventral regions of the medial prefrontal cortex ‘may be important for affective processing while more dorsal regions may be primarily involved in

cognitive processes' (Rameson and Lieberman, 2009:99). In line with the view that the two kinds of empathy are not mutually exclusive, they appear to engage common, as well as distinct neuronal networks. Finally, whilst their relationship remains ambivalent, over the last few decades, discussions of empathy and its neural correlates almost invariably allude to the - already mentioned - mirror neurons (Lamm and Majdandžić, 2015).

## Mirror neuron system

The relatively recent discovery of a class of neurons that are activated both by executing and observing an action, called mirror neurons due to this 'mirroring' property, has caused a revolution in neuroscience (Gallese et al., 1996; di Pellegrino et al., 1992). Back in 2000, Ramachandran predicted that mirror neurons would do for psychology what DNA had for biology. Whilst the neurons were first discovered in macaques, over the last 25 years countless studies devoted to identifying analogous neurons in humans, and relating them to everything from the degree of an erection to motor learning, social cognition, and the theory of mind, have emerged (Decety and Meyer, 2008; Gallese, 2013; Iacoboni, 2009; Mouras et al., 2008; Ramachandran and Oberman, 2006; Rizzolatti and Fabbri-Destro, 2008; Rizzolatti et al., 1996; Vanderwert et al., 2013). First discovered in the ventral premotor cortex of the macaque brain, mirror neurons have since been reported in various different brain areas (Rizzolatti and Fadiga, 1998). The complex network of functionally distinct areas containing mirror neurons has become known as the mirror neuron system (Rizzolatti and Craighero, 2004). There appears to be agreement that the MNS includes area F5, a region of the ventral premotor cortex, and the inferior parietal lobule (ibid.). In addition, although not a direct part of it, the superior temporal sulcus (STS) is also strictly related to it.

The appeal of the theory lies in its apparent simplicity which has, arguably, led to numerous oversimplifications, bold claims, and far-reaching conclusions being made. The

amount of interest and the scope of the questions they supposedly provide an answer to calls the extent to which Ramachandran's prophecy was valid, or merely self-fulfilling, wishful thinking, into question. The lure of a tangible neural substrate explaining a variety of psychological phenomena has resulted in them being tweaked to fit various theories, and becoming 'the most hyped concept in neuroscience' (Jarrett, 2012). A critical examination of the existing research suggests that mirror neurons might, in fact, be too good to be true, and the enthusiasm with which psychologists have embraced them as their own Rosetta stone a manifestation of their need to find one.

Although there appears to be wide agreement about the importance of mirror neurons, similarly to their location, their exact functioning and significance remain surprisingly unclear. The meaning of mirror neurons has been extended to cover such vague concepts as 'understanding an action from the inside', or even understanding the intention behind it (Iacoboni et al., 2005; Rizzolatti and Sinigaglia, 2010; Sinigaglia and Rizzolatti, 2011). More moderate interpretations relate mirror neurons to 'motor resonance', a concept which fits well with Prinz's (1997) common coding theory according to which 'perceived events and planned actions share a common representational domain', and perceiving an action automatically activates its representation, given that one is able to perform it (Uithol et al., 2011). In addition to motor resonance, a mechanism referred to as limbic or emotional resonance has been studied (Decety and Meyer, 2008). Brain regions including the anterior cingulate cortex, anterior insula, and inferior frontal gyrus appear to be activated both while experiencing an emotional state and observing it in another person. Van der Gaag et al. (2007) argue that the IFG and posterior parietal cortex compose a MNS for 'the motor components of facial expressions, while the amygdala and insula may represent an additional MNS for emotional states'. These areas appear to provide the missing link between motor cognition and theory of mind, supposedly underlying our ability to empathise with others and infer their mental states (Avenanti et al., 2009; Botvinick et al., 2005; Decety and Jackson, 2004; Wicker et al., 2003).

While those ascribing to the adaptation hypothesis suggest that mirror neurons have become genetically universal through natural selection, and that experience plays a minor role in their development, others deny their evolutionary significance and view them as motor neurons endowed with matching properties forged through correlated experience of observing and executing an action (Heyes, 2014; Tkach et al., 2007). It has, indeed, been demonstrated that training and experience play a role in the activation of the MNS (Catmur et al., 2007; Orgs et al., 2008). Press et al. (2012) were even able to ‘reprogram’ mirror activity by training a subset of hand-specific mirror neurons to respond to observation of arbitrary geometric shapes, thus casting more doubt on the view that they have evolved as a genetic adaptation for social interaction. Moreover, the very necessity of the MNS for the phenomena of which they are supposedly the underlying mechanism has been questioned. Rizzolatti and Craighero (2004), despite arguing for the evolutionary importance of mirror neurons, admit that they might not be the only mechanism underlying action understanding.

Of the 532 neurons measured in macaques by Gallese et al. (1996), only 92 were mirror neurons, with 51 active during observation of only a single action, 38 responding to two or three actions, and 3 being active when the monkey observed the experimenter grasping with his hand or mouth. Whilst the original study used single-cell recordings, such methods and, by extension, such specific conclusions, cannot commonly be made with human subjects. The only single-neuron study in humans concluded that ‘multiple systems in humans may be endowed with neural mechanisms of mirroring for both the integration and differentiation of perceptual and motor aspects of actions performed by self and others’, with their role varying according to location, and ranging from movement initiation and sequencing, and memory recollection to emotions (Mukamel et al., 2010). Whilst the non-invasive methods normally used in mirror neuron studies on humans, such as transcranial magnetic stimulation (TMS) or fMRI, have comparably good spatial resolution, they cannot compete with single-cell recordings, or help identify specific mirror neurons (Fadiga et al., 1995).

Extending the original findings to humans is, therefore, problematic. Moreover, some believe that the original study was, itself, controversial, and its conclusions not consistent with the measured data. Specifically, Pascolo et al. (2009) argue that, rather than mirroring them, the measured responses reflected an anticipation of the experimenter's actions and were an epiphenomenon of a group of neurons observed in a certain time frame, not a cell-defining property. In 2013, Pascolo et al. went as far as criticising the authors of the early studies for their 'over-eagerness to construct a mind theory, even from the earliest experiments'. An exhaustive summary or criticism of existing findings is beyond the scope of the present work. Entire books could be, and have been, written about the latter. For a detailed critical examination, see Hickock (2014). Such overviews, however, suggest that the above-mentioned 'over-eagerness' continues to surround the concept of mirror neurons. Astonishingly, over two decades of research have seemingly done little to dissipate the vagueness surrounding the theory, with the latter providing even more space for another of its main shortcomings: exaggeration. The conclusions made about mirror neurons are often based on speculative assumptions, a desire to prove a point, confirm one's expectations, and contribute to a new, exciting field, rather than rigorous interpretation of data.

The issue of bias is not specific to research on mirror neurons, neither is it, of course, specific to research. It is, however, more of a concern when science, the human endeavour that we rely on for acquiring knowledge, is at stake. Speaking specifically of medical science, Ioannidis (2005) has, in a thought-provoking essay, argued that 'it can be proven that most claimed research findings are false'. He later explained that 'the current system values publications, grants, academic titles, and previously accumulated power' and does not 'reward replication—it often even penalizes people who want to rigorously replicate previous work, and it pushes investigators to claim that their work is highly novel and significant' (Ioannidis, 2014). '[T]he highly competitive environment for funding and career promotion that incites researchers to submit predominantly positive results' is fuelled by editors, for whom 'it is the competition for citation index and the financial survival of journals that makes it more attractive to publish positive findings' (Joobar et al., 2012). Moreover, publication bias, despite having been known and documented for

decades, appears to be increasing (ibid.). These well-known phenomena have ‘an escalating and damaging effect on the integrity of knowledge’, contribute to many published research findings being ‘false or exaggerated, and an estimated 85% of research resources (being) wasted’, and mark the quality of research, including that on mirror neurons (Ioannidis, 2014; Joober et al., 2012).

It has been shown that simply including neuroscience data in an explanation of a psychological phenomenon ‘may interfere with people’s abilities to critically consider the underlying logic of this explanation’ (Weisberg et al., 2008:470). Moreover, part of the scientific credibility of brain imaging as a research technique appears to lie in the images themselves. McCabe and Castel (2008:344) argue that tangible, physical representations of cognitive processes, such as brain images, and papers that include them, are intuitively interpreted as more credible due to ‘people’s natural affinity for reductionist explanations of cognitive phenomena’. Both scientists and media covering brain imaging research should refrain from oversimplification while also explaining and emphasising the limitations of brain imaging techniques, such as fMRI.

Consequences of wishful thinking and the desire to have results published to further one’s career, or at least survive in a ‘publish or perish’ environment, include hard evidence being overlooked or misinterpreted - consciously or not - and almost two thirds of psychological studies not being reproducible (Open Science Collaboration, 2015). Scientists are, of course, aware of how the system functions and therefore likely to adjust the way they work, effectively censoring themselves before a reviewer is provided the opportunity to do so. The biases inherent in the institutions of science therefore fuel and reinforce human ones. Cognitive biases commonly affecting scientists include so-called ‘hypothesis myopia’ (collecting evidence to support a hypothesis, not looking for evidence against it), ‘texas sharpshooter’ (seizing on random patterns in the data and mistaking them for interesting findings), ‘asymmetric attention’ (rigorously checking unexpected results but giving expected ones a free pass), and ‘just-so storytelling’ (finding stories after the fact to rationalise the results) (Nuzzo, 2015). In science, confirmation bias, ‘the seeking or

interpreting of evidence in ways that are partial to existing beliefs, expectations, or a hypothesis at hand', is ubiquitous (Nickerson, 1998).

Nosek (Ball, 2015) argues that such 'motivated reasoning' and rationalisation is, in fact, the most common and problematic source of bias in science. It provides ground for less rigorous methodological, interpretation, and presentation choices, and results in inconspicuous shifts in hypotheses and goals, circular and erroneous analyses, 'puzzlingly high correlations', and inflated false-positive rates, as reported in - albeit not exclusive to - fMRI studies (Eklund et al., 2016; Kriegeskorte et al., 2009; Nieuwenhuis et al., 2011; Vul et al., 2009). User-friendly software that makes it easy to analyse extensive datasets, whilst useful, contributes to the issue by allowing complex analyses to be performed by less experienced researchers without a full understanding of the methods. Moreover, whilst the self-correcting nature of science should, arguably, compensate for these issues, peer review seems to be a 'fallible instrument - especially in areas such as medicine and psychology' (Ball, 2015). Confirmation bias is equally common in mirror neuron theory, as illustrated by the example of Rizzolatti and Sinigaglia (2008) adjusting and exaggerating figures adapted from a different study in order to support their cause (Pascolo et al., 2013). Methods of fighting against it exist and include proper reporting, meta-analyses, and replication. The willingness of the authors to overcome such bias, and establish a clear, data-driven definition of the mirror neuron system, is key for the future of the theory.

We believe that a mechanism allowing humans to 'resonate' with others appears, instinctively, to be necessary for communication and social interaction, and understand the appeal of the mirror neuron theory. Whilst we agree that the latter might, in fact, explain the former to an extent, we avoid making grand conclusions about the function or significance of mirror neurons, and strive to see them for what they are - or have reliably been demonstrated to be. The truth is that numerous studies have identified brain regions that are activated both when observing and experiencing a motor act, including emotional states expressed through facial expressions. Our goal is to try and replicate such results.

The present study was designed with the goal of locating brain regions that are part of the MNS, using fMRI.

## Functional magnetic resonance imaging

### **Basic principles of MR imaging**

Magnetic resonance imaging (MRI) is a non-invasive imaging technique that relies on strong magnetic fields and radio waves to generate detailed three-dimensional anatomical images. Under normal circumstances, the magnetic moments of hydrogenic nuclei, abundant in water and fat, are oriented randomly. Once placed in a strong, uniform magnetic field, the nuclei align with it, thus creating a net longitudinal magnetisation in the direction of the field. Subsequent application of a radiofrequency (RF) pulse decreases the longitudinal magnetisation and establishes a transversal one. Upon removal of the RF pulse, the system seeks to return to its equilibrium. MRI imaging takes advantage of the fact that the time it takes to return to equilibrium differs by tissue type, and that the signal created by longitudinal relaxation (described by time constant T1) and transverse relaxation (T2) can be measured using a receiver coil. As shown in Figure 1.1, by altering the time between subsequent excitation of the nuclei (repetition time, TR) and how soon following the excitation data is collected (echo time, TE), different characteristics of the brain tissue can be emphasised (Huettel et al., 2008).

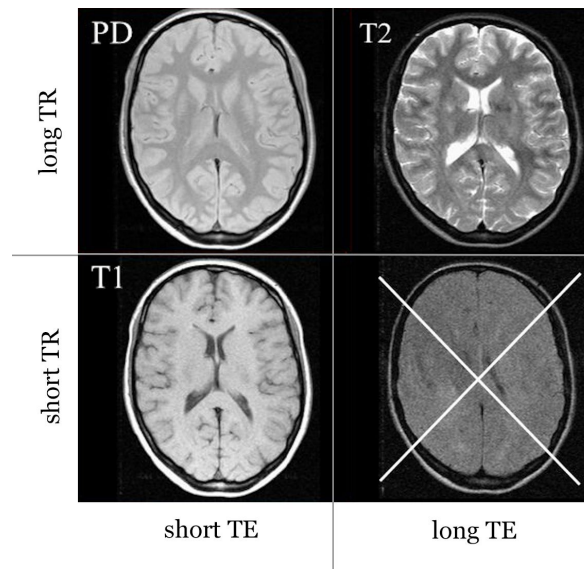


**Figure 1.1:** By altering TR and TE, different tissue characteristics can be emphasised. T2\* (not depicted in the figure) is sensitive to the flow of oxygenation, can be acquired simultaneously with T1 and T2-weighted images, and distinguishes fMRI from MRI.

## Functional MRI

In addition to generating structural images of the brain, *functional* MRI (fMRI) measures brain activity by depicting ‘changes in deoxyhemoglobin concentration consequent to task-induced or spontaneous modulation of neural metabolism’ (Glover, 2011). For reasons that are still not quite understood, the amount of blood that flows to a brain region following neuronal activity exceeds the amount necessary to replenish the oxygen used by it, resulting in an increased ratio of oxygenated to deoxygenated hemoglobin. In 1990, Ogawa discovered that the latter have different magnetic properties leading to magnetic signal variation which can be detected using an MR scanner. The ratio of oxygenated to deoxygenated hemoglobin in blood, known as the blood-oxygen-level dependent (BOLD) contrast, has since become the most common approach to fMRI, with its popularity growing exponentially, and revolutionising research on brain function.

The increase in blood flow following a period of neuronal activity is represented by the hemodynamic response function (HRF). Several properties of the HRF are crucial for

fMRI analysis. Firstly, as explained above, BOLD fMRI is an indirect method. Rather than measuring neuronal activity itself, it measures the metabolic demands of active neurons. Although the two are coupled, the relationship between them is neither straightforward, nor perfectly understood (Ekstrom, 2010; Gore, 2003). The BOLD contrast ‘reflects the input and intracortical processing of a given area rather than its spiking output’ (Logothetis et al., 2001). It cannot separate feedforward and feedback active networks, and is a sum of the entire region’s network (Huettel et al., 2009). Whilst the spatial resolution of fMRI is, indeed, high (voxel size  $\sim 1\text{-}2\text{mm}$ ), it is not capable of detecting signal at the level of a single neuron.

Second, unlike the neuronal activity by which it is triggered, the HRF is slow to peak (see Figure 1.2). It takes about 5 seconds to reach its maximum. Following the peak there is a sluggish undershoot - a fall below the baseline, to which the BOLD signal does not fully return for another 15 to 20 seconds (Poldrack et al., 2011). The slowness of the hemodynamic response, together with temporal acquisition of consecutive scans being generally rather sparse ( $\text{TR} = 2\text{-}3$  seconds), makes the temporal resolution of fMRI comparably low.

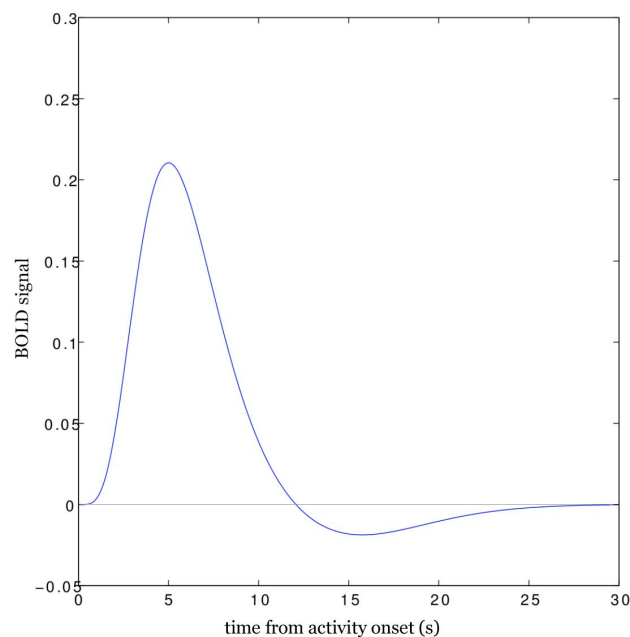


**Figure 1.2:** Hemodynamic response function modelled by the canonical double-gamma function.

Lastly, the fact that the HRF can be treated as a linear time-invariant system makes it possible to ‘create a straightforward statistical model that describes the time course of hemodynamic signals that would be expected given a particular time course of neuronal activity, using the mathematical operation of convolution’ (Boynton et al., 1996; Poldrack et al., 2011:2). For each individual, however, hundreds of consecutive volumes, each consisting of tens of thousands of voxels, are acquired. Moreover, the nature of the response varies across individuals, and even brain regions. A variety of other factors, such as anxiety, medications, disease, and attention also have an impact on it (Logothetis, 2008). This makes fMRI data a challenge to analyse. Nevertheless, given optimal experimental design, many repetitions of a task, and careful preprocessing, statistical methods can be used to reliably determine brain regions that are most active during a particular task (Glover, 2011; Dale, 1999). These properties, together with its high spatial resolution, non-invasive nature, and availability, make BOLD fMRI a dominant method for measuring behaviour-related neural activity, and a popular choice for neuroscientific studies, including ours.

## Materials and methods

### Participants

Written informed consent was obtained from each participant prior to the study. Like the study itself, the informed consent was approved by the Faculty of Arts Ethical Committee (University of Ljubljana). Out of the thirty-one healthy volunteers that participated in the experiment, one did not complete the mirror task, and was therefore excluded from the analysis. The age of the remaining 30 participants (15 female; 2 left- and 13 right-handed, and 15 male; 3 left- and 12 right-handed) ranged from 24 to 52 years ( $M = 36.53$ ,  $SD = 8.37$ ). All participants were experienced accounting and finance managers. The choice of this particular population was given by the fact that the experiment was part of a larger study of decision-making in managers.

## Stimuli, experimental design, and procedure

The experimental stimuli consisted of 3-second full-face full-colour video clips of five male and five female actors, all Caucasian, displaying various emotional states (anger, disgust, surprise, happiness), and neutrality, and of clips of moving geometric shapes. Each experimental condition was presented 3 times in pseudo-randomised (counterbalanced between subjects) blocks lasting 24 seconds. Each block comprised of 6 video clips, separated by a 1-second inter-stimulus interval (ISI). Consecutive blocks were separated by a 20-second ISI during which a fixation point was presented. Figure 2.1 depicts the time course of the experimental procedure for a selected participant, in order to make it clearer.

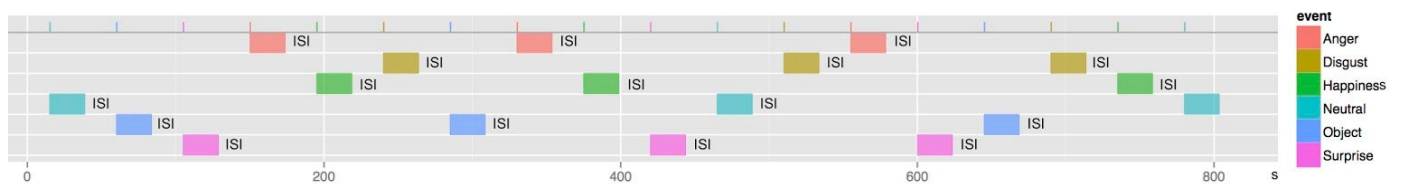


**Figure 2.1:** Scheme of the experimental procedure, with time in s depicted on the x-axis. The blocks were pseudo-randomised - presented in a different order for each participant.

The video clips of emotional states were the same as those used by van der Gaag et al. (2007), and others. To ensure faithful depiction and maximize their capacity to induce emotions, they either presented spontaneous reactions - as in the case of happiness, triggered by jokes - or the result of instructing the actors to display the prototypical expression of the given emotion. 20 naturalistic specimen were first filmed for each condition, then rated by an independent group of 15 participants on a 7-point intensity scale, as well as on how genuine the emotions appeared. Finally, a subset of video clips of actors that displayed the various emotions with similar intensity was selected, and used in experiments including ours (*ibid.*). While van der Gaag et al. (2007) presented the neutral condition with videos of actors blowing up their cheeks, the neutral facial expressions used in our experiment involved very little to no facial muscle movement. Both the latter and the moving geometric shapes were therefore considered control conditions, in order to discount areas activated simply by faces, without emotional valence, or simply by movement. We presume that this is comparable to also controlling for the motor component of facial expressions. This allowed us to isolate the impact of the emotional

facial expressions, and compare various conditions to answer our research question. See Figure 2.2 for example screenshots of the videos we used to depict various emotional states.



**Figure 2.2:** Example screenshots of video clips depicting emotional states. Left to right: anger, disgust, happiness, surprise.

The fMRI acquisition took place at the Centre of Clinical Physiology, Medical Faculty, University of Ljubljana, Slovenia. The participants were given instructions about the task, and placed in an MRI scanner. Structural images were recorded first, then a number of BOLD images was acquired while the participants performed a series of cognitive control tasks. In the ‘mirror neuron task’ itself, the participants were told that short videos of people will be displayed on the screen, and asked to passively observe these, without further explicit tasks, while undergoing fMRI scanning. A resting state BOLD run was also recorded.

Van der Gaag et al. (2007) used an event-related design, meaning the stimuli were presented in random order rather than an alternating pattern. Such designs allow to compare the response to each individual condition but result in a weak detection power. Schraa-Tam et al. (2012) thus made use of a blocked-design with negative and positive emotions. Combining disgust with anger, and happiness with surprise made their design ‘likely to be more sensitive in isolating activations associated with negative emotions’ (ibid.). It did not, however, allow them to distinguish the effects of individual emotions. By contrast, our study refrains from grouping emotions of the same valence into blocks. Whilst our main focus is on mean activation across all of the emotions involved, our design will also allow us to separate them, and study the effect of each of them individually.

Bastiaansen et al. (2011) used disgusted and pleased facial expressions and contrasted them to neutral ones. The stimuli used by van der Gaag et al. (2007) consisted of neutral, happy, fearful and disgusted expressions. To control for the specificity of both facial and biological movements, two control conditions were presented - neutral facial expressions with actors blowing up their cheeks, and an additional condition displaying abstract pattern motions. By contrast, Schraa-Tam et al. (2012) contrasted positive (happy and surprised), negative (angry and disgusted), and neutral faces to moving geometric objects. We use the same range of emotional stimuli as Schraa-Tam et al. (2012) but approach the control conditions in a slightly different manner; study 30 participants, instead of 20, and do not restrict ourselves to a specific brain region. In short, our study mimics similar studies, with its experimental design presenting several comparative advantages.

The experimental design allows us to identify areas of activation specific to emotions - as compared to the control conditions - and common to all considered emotions. However, whilst we might speculate that these are part of the mirror neuron system, we argue that the present dataset is not sufficient for making inferences about the latter. The fact that these regions are activated by emotional facial expressions, and more so than by the control conditions, does not necessarily imply that they are part of the MNS. Various other systems might be common to emotional facial expressions processing. By definition, the MNS is activated both by observing and experiencing a specific motor act. Our experimental design, however, did not include a control experiment that would enable us to distinguish regions activated *both* by observing various emotional states in others and by *experiencing* them. The design will therefore not allow us to discard motor or sensory neurons that are active during one task but not the other. It will merely enable us to conclude that the areas found to be active are common to all emotions and are *potentially* - or include those that are - part of the MNS. A brief comparison with existing studies of the MNS, and similar studies that did include a control experiment, should reveal an overlap in results. To truly reach a conclusion about the MNS, however, a similar study would have to be performed, with the same participants undergoing both the present experiment, and a control one.

## **fMRI acquisition**

Neuroimaging data were acquired with a Philips Achieva 3.0T TX scanner. One T1-weighted and one T2-weighted high-resolution, whole-brain anatomical scans were acquired (both: 236 sagittal slices, matrix =  $336 \times 336$ , voxel size =  $0.7 \times 0.7 \times 0.7$  mm; T1: TE = 5.7 ms, TR = 12 ms, flip angle =  $8^\circ$ ; T2: TE = 414 ms, TR = 2500 ms, flip angle =  $90^\circ$ ). Whole-brain functional volumes (BOLD) were acquired with a T2\*-weighted echo-planar imaging (EPI) sequence (48 axial slices, voxel size =  $3 \times 3 \times 3$  mm, matrix =  $80 \times 80$ , TR = 2.5 s, TE = 27 ms, flip angle =  $90^\circ$  SENSE factor 2) in one BOLD run (330 frames, 13.75 minutes). In addition, to support distortion correction of both structural and functional images, two spin-echo images (48 axial slices, voxel size =  $3 \times 3 \times 3$  mm, matrix =  $80 \times 80$ , TR = 2.8 s, TE = 27 ms, flip angle =  $90^\circ$  SENSE factor 2) were acquired with opposite frequency readout directions (anterior-to-posterior and posterior-to-anterior).

## **Functional image analysis**

The functional imaging data were analysed using the Functional MRI of the Brain Software Library (FSL; [www.fmrib.ox.ac.uk/fsl](http://www.fmrib.ox.ac.uk/fsl)) 5.0.9 software package developed at Oxford University (Smith et al., 2004). The data were preprocessed using standard preprocessing methods. These, in short, include non-brain tissue removal, motion correction, slice-timing correction, spatial smoothing, grand-mean intensity normalisation of the entire 4D dataset by a single multiplicative factor, high-pass temporal filtering, and linear registration to high-resolution structural space and standard space images, followed by nonlinear registration from high-resolution structural to standard space.

The choice of specific preprocessing steps, as well as the order in which they are performed, varies, and is largely determined by the software that is used to process the data (Poldrack et al., 2011: 34). Given that there is no truly standard preprocessing pipeline, and since the author had no prior experience with fMRI analysis, a description of the choices, and a full disclosure of the considerations made over the course of the analysis follows.

## Preprocessing

The input data for each participant consisted of a set of three images - a T1-weighted image (the main, high-resolution, structural image), a T2-weighted image (a low-resolution structural image) and a four-dimensional BOLD image. The images had been converted to a common format known as NiFTI. Conveniently, compressed NiFTI files (.nii.gz) can be directly read and written by FSL. The structural images were oriented according to the neurological convention (left-to-right), while the functional images followed the radiological convention (right-to-left). It is normally important to ensure that all images are reoriented to the standard Montreal Neurological Institute (MNI) orientation, or following the same convention. However, since FSL is capable of dealing with a mixture of the two, no measures were taken to reorient the images.

## Detecting scanner artefacts

Each image was first visually assessed for gross artefacts that would require scanner-specific corrections. This involved both viewing the structural images and watching videos of the functional images in FSLEyes (FSL's image viewer). Artefacts that may occur due to issues with the scanner include spikes, reflected by large, regular, diagonal stripes of different brightness levels across the images; or so-called 'ghosting', caused by a slight offset in phase in echo-planar acquisition, manifested as a dim shadow of the brain on each side of the image (Poldrack et al., 2011: 35-36). No such artefacts were present in our data.

## Distortion correction

Gradient-echo echo-planar imaging, the most common method for fMRI acquisition, suffers from artefacts caused by inhomogeneity of the main magnetic field near regions where air and tissue meet, such as the orbitofrontal cortex and the lateral temporal lobe (ibid.). These can either take the form of a spatial distortion, or of dropout - reduced signal, which makes it difficult to align functional data with structural images, or make

conclusions about (de)activation in the affected areas (see Figure 2.3). Such distortions can be corrected, to a degree, provided that a field map which characterizes the main magnetic field (known as B0) was acquired at the time of fMRI acquisition. So-called B0 unwarping can then be run as part of preprocessing within FSL. The visual assessment of our data further revealed that, in the 4D images, a portion of the orbitofrontal cortex appeared to be missing for two of the participants. However, in this particular case field maps had not been acquired, and the signal dropout was therefore left uncorrected.

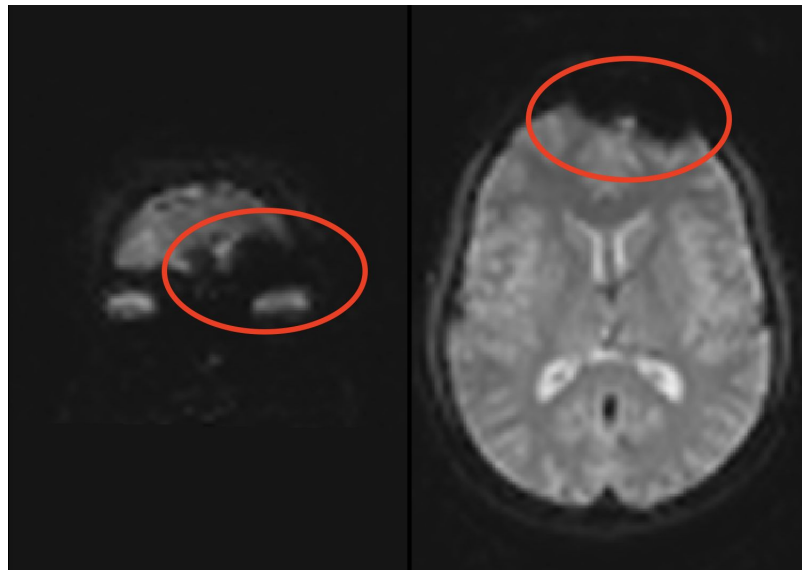


**Figure 2.3:** Signal dropout, apparent in a 4D image of registered to a high-resolution structural image.

### Brain extraction

Prior to doing any analysis on the brain, it is necessary to separate it from non-brain tissue that is not of interest, including membranes and sinuses. Brain extraction, also known as brain/non-brain segmentation, or skull-stripping, improves the robustness of later preprocessing stages, namely registration. Various comparable automated methods for brain extraction exist (Boesen et al., 2004). We relied on FSL's Brain Extraction Tool (BET) v2.1, which 'uses a deformable model that evolves to fit the brain's surface by the application of a set of locally adaptive model forces' (Smith, 2002). It first makes a rough intensity-based estimation of the brain/non-brain threshold, and finds the size and center of

gravity of the head. Based on the latter, an initial sphere is defined, and a triangular tessellation of the sphere is gradually deformed towards the outer edges of the brain (ibid.). Figure 2.4 shows an example result of BET.



**Figure 2.4:** Example of a brain-extracted image (coloured red) including an outline, with the original high-resolution structural image at the background.

Brain extraction was performed on each structural image of each participant. Although brain-extraction algorithms make this step significantly less time-consuming, as with all stages of fMRI analysis, it is important to assess the quality of the output, and rerun the algorithm if necessary. Whilst minor imperfections should not cause concern, especially if performing BET for registration purposes, substandard brain extraction could lead to issues with spatial normalisation, and corrupt the results of the analysis (Poldrack et al., 2011).

Having first tried using the default settings for each image, we eventually ran standard brain extraction using *bet2* on all low-resolution structural images, and a more advanced, robust brain-center estimation that iterates *bet2* up to 10 times, for the high-resolution images. (The latter did not appear to lead to better results for low-resolution images, rather the opposite.) For each image, a brain mask, as well as a brain outline were output in addition to the brain-extracted image, and made the assessment of the quality of the result easier. Although BET generally segments brain tissue from non-brain relatively well, a

compromise is often necessary. When forced to decide between leaving a small portion of non-brain tissue, or removing a portion of brain tissue, we generally opted for the latter, since not losing signal of interest appeared to be of more importance. For most images, various iterations with different fractional intensity thresholds - a parameter that determines the size of the brain outline estimate, and is adjustable in BET - were run before a satisfactory result was achieved.

Brain extraction is of particular importance for structural images, where tissue outside of the brain also tends to exhibit strong signal. BET on functional images was done as part of the preprocessing steps described below, in an unsupervised, and more liberal way. Similarly to other data processing steps, BET was initially performed using the FSL GUI, and later automated. For the sake of transparency and a simple, visual overview of the entire analysis, screenshots of FSL GUI settings, as well as key command lines, are included in the Appendix in chronological order.

## FSL FEAT

Following brain extraction, fMRI data preprocessing was carried out using FSL's fMRI Expert Analysis Tool (FEAT) Version 6.00. All of the following preprocessing steps were carried out in the FEAT GUI. Upon entering the functional image in the GUI, FEAT detects the repetition time (TR), as well as the number of fMRI volumes in the time series from the metadata stored in the header of the input NiFTI file. Entering a simple command (*fslinfo <filename>*) into the terminal allowed us to verify that these numbers were, indeed, correct. FEAT further calculates the brain/background threshold as the percentage of the maximum input image intensity, used at various points of the analysis. Typically, an experiment does not begin until after a number of initial 'dummy scans' that ought to be omitted from the analysis because steady-state imaging had not yet been reached. The number of these volumes is decided at the time of fMRI acquisition. Whilst four such scans preceded our experiment, none of them were saved, and the number of volumes to be deleted was thus left at 0.

## Motion correction

The noise commonly found in fMRI data is largely due to an extreme low-frequency variation commonly referred to as drift. Although relatively poorly understood, this drift is believed to be caused by a combination of physiological effects and scanner instabilities (Smith et al., 1999; Zarahn et al., 1997; Aguirre et al., 1997). Having input the functional image, we clicked on *Estimate from data* in order to get an estimate of the noise level (the standard deviation for a typical voxel over time, expressed as a percentage of the baseline signal level), and the temporal smoothness (the smoothness coefficient in a simple autocorrelation model) - an approximation of the noise characteristics that would remain in the fully preprocessed data, excluding motion correction. Whilst the estimated level of noise in our data varied across participants, it was generally rather high. Some of the measures described below should also contribute towards improving the signal-to-noise ratio.

Head motion, another major source of noise in fMRI data, can result in a ‘mismatch of the location of subsequent images in the time series’, as well as disruption of the MRI signal itself, and ‘have drastic effects on fMRI data’ (Poldrack et al., 2011:43). A visual assessment of the quality of the functional images revealed that a portion of the participants appeared to move significantly throughout the experiment. Various methods of addressing, and minimizing, the adverse effects of motion exist, and entire images should therefore only be thrown away in extreme cases. Since physiological motion was not monitored at the time of the fMRI acquisition, several post-hoc, data-based cleanup methods were employed to assess the level of, and correct for, confounds arising from motion, including cardiac and respiratory motion (Poldrack et al., 2011:42-42).

First, *fsl\_motion\_outliers*, a tool designed to deal with intermediate to large motion, including nonlinear artefacts, was used. The script performs motion correction on the input functional image using MCFLIRT, ‘an intra-modal motion correction tool based on optimisation and registration techniques used in FMRIB's Linear Image Registration Tool

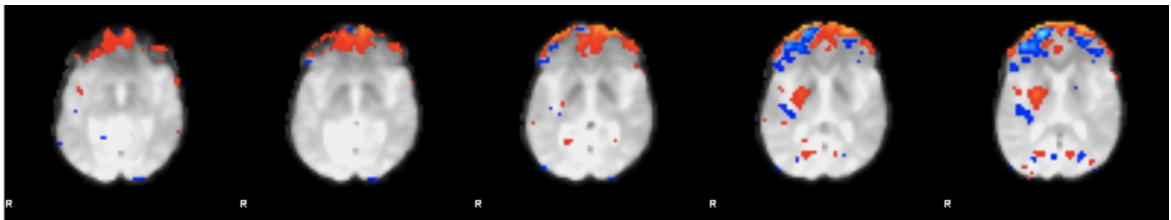
(FLIRT)' (Webster, 2015). MCFLIRT attempts to remove the effects of head motion by applying rigid-body transformations and detecting timepoints that corrupt the image beyond what linear motion parameter regression methods can fix (Jenkinson and Smith, 2001; Jenkinson et al., 2002). Rather than deleting such timepoints, it creates a confound matrix that can later be used in the general linear model (GLM) to remove their effect from the estimation of effects of interest, 'without any adverse effects in the statistics' (Jenkinson, 2012). We opted for the default metric - *refrms* - which uses root mean square intensity difference of volume N to the reference volume (ibid.).

Whilst *fsl\_motion\_outliers* is, indeed, useful for dealing with motion, and allowed us to get an idea of the amount of motion-related spikes in our data, the outputs of the script were not ultimately included in the general linear model. Neither were the head motion parameters estimated using MCFLIRT, since Webster (2017a) describes this solution as simplistic, and not well understood. Instead, denoising based on independent component analysis (ICA), an alternative method for motion correction, was performed. Unlike rigid-body transformations, ICA-based denoising is also capable of correcting for sudden motion, as well as structured noise that is not related to motion, thus making spike-regression redundant.

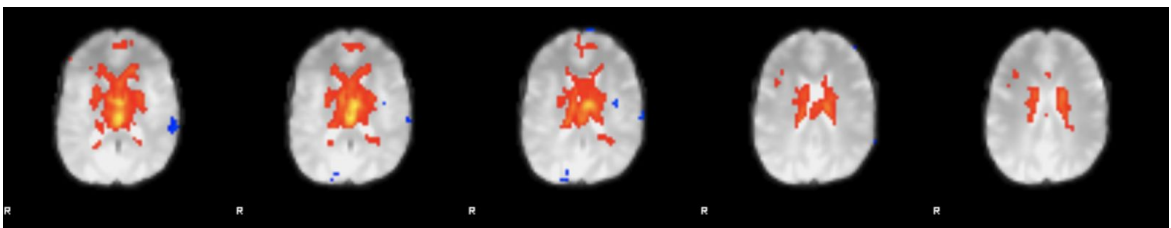
FEAT's Multivariate Exploratory Linear Optimized Decomposition into Independent Components (MELODIC) tool decomposes an image into independent spatial maps, and a set of corresponding temporal components. Based on a visual assessment, those deemed artefact-related may then be removed - the data denoised - through *fsl\_regfilt*. MELODIC ICA can either be performed as part of FEAT preprocessing, if intended for exploratory purposes, or through a separate GUI. Having first done the latter, we attempted to identify artefact-related components that ought to be removed. Rough guidelines for identifying structured noise are available online, as well as in scientific literature. See Figure 2.5 for examples of components that present various motion-related artefacts, with interpretations based on Poldrack et al. (2011). Occurrences of strong artefacts between slices, coherent signal around the edges of the brain or the ventricles, or a time course that shows a

significant spike, can generally be considered noise (ibid.). Whilst an experienced researcher might be able to distinguish such components with enough confidence, we opted instead for one of the more robust ways of doing so.

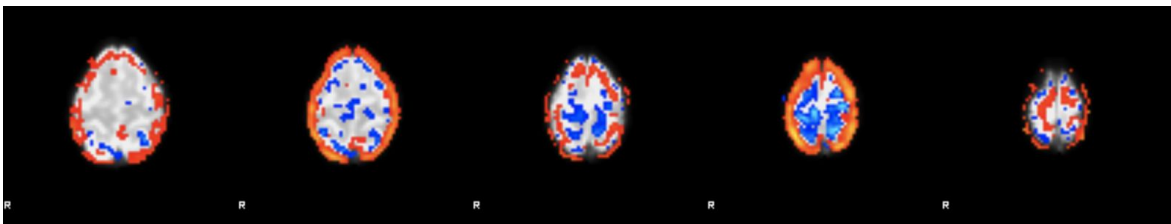
a)



b)



c)



d)

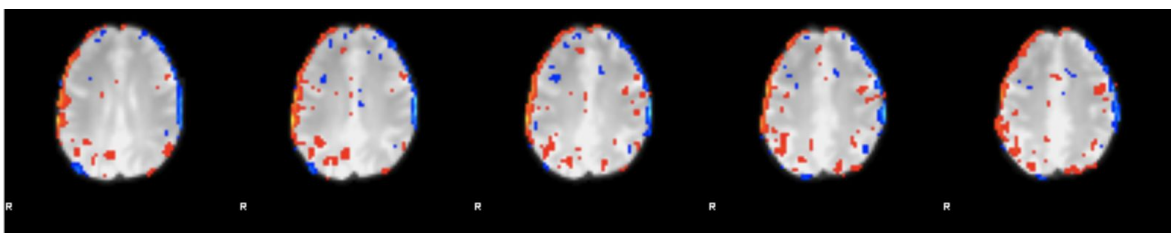


**Figure 2.5:** Selection of components classified motion by ICA-AROMA. a) large regions of positive and/or negative activation in the orbitofrontal cortex (rotation along the left-right axis); b) cardiac motion; c) a coherent ring of activation around the edges of the brain (bulk motion); d) positive activation on one side of the brain, negative on the other (movement along the left-right axis).

In order to avoid biased, manual labeling, we decided to rely on ICA-AROMA (ICA-based Automatic Removal of Motion Artefacts) v0.3-beta, a method that ‘automatically identifies and subsequently removes data-driven derived components that represent motion-related artifacts’ with high accuracy, while preserving signal of interest, and the temporal characteristics of the fMRI data (Mennes, 2017; Pruim et al., 2015a). It relies on a set of four theoretically motivated temporal and spatial features and, unlike other, similar algorithms, does not require classifier retraining (Pruim et al., 2015b; Salimi-Khorshidi et al., 2014). The freely-available software package is conveniently optimised for usage after fMRI data preprocessing with FSL FEAT, assuming that spatial smoothing and registration to the standard MNI152 template have been run, and temporal filtering has not. As explained by Pruim et al. (2015a), ‘applying secondary motion artifact removal prior to temporal filtering not only prevents ringing artifacts, but additionally prevents removal of low-frequency motion-related signal variance which can aid in identification of motion artifacts’. The decision to incorporate ICA-AROMA into our preprocessing pipeline informed some of the choices below, such as not running MELODIC as part of preprocessing within FSL FEAT, since ICA-AROMA includes it and runs it with optimal settings.

### Slice-timing correction

Slice-timing correction addresses the fact that slices in the plane of fMRI acquisition are temporally misaligned. Each slice of an fMRI volume is acquired at a different time. However, later processing assumes that all slices were acquired at exactly the same time. Since timing is essential for fMRI analysis, slice-timing correction attempts to shift the data, and is commonly applied by choosing a reference slice to which the remaining slices are interpolated (Poldrack et al., 2011). The further away a slice is from the reference slice, the more temporal interpolation it requires, thus increasing the risk of introducing interpolation errors. Moreover, interpolating slices of the data can also result in an interpolation of artefacts. Poldrack et al. (2011: 42) argue that interleaved acquisition, illustrated by Figure 2.6, with short repetition times ( $TR \leq 2$  seconds), particularly if

followed by spatial smoothing and the use of statistical models that include temporal derivatives, ‘is relatively robust to slice timing problems’.

Nevertheless, despite the ongoing debate about the effectiveness of this method, there is a general consensus that slice-timing correction should be included in the preprocessing pipeline - after motion correction and prior to any other spatial interpolations on the data - in order to reduce estimation bias and increase robustness of the data analysis (Sladky et al., 2011). Our images were acquired in interleaved fashion, with TR = 2.5 seconds. Although our preprocessing steps also include spatial smoothing and an addition of temporal derivatives to the statistical model, we decided to also incorporate slice-timing correction using Fourier-space time-series phase-shifting.

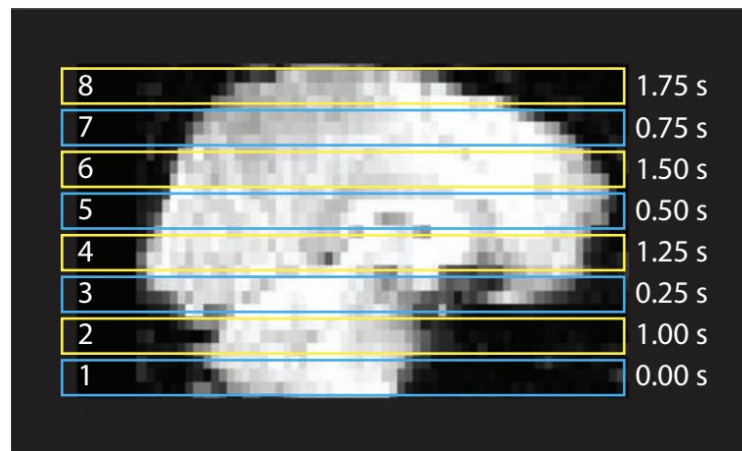


**Figure 2.6:** An illustration of slice timing in an interleaved fMRI acquisition, assuming TR = 2 seconds, with the relative time at which a given slice started being acquired depicted on the right. The odd slices are acquired first (sequentially), followed by the even slices (Poldrack et al., 2011: 41).

### Spatial smoothing

Having put a great amount of effort into obtaining data with the highest possible resolution, deliberately blurring it might seem highly counterintuitive. However, removing

high-frequency information by averaging part of the intensities of neighbouring voxels, especially considering that most of the noise in fMRI data is Gaussian, does, in fact, improve the signal-to-noise ratio. Since ‘most activations in fMRI studies extend across many voxels, the benefits of gain in signal for larger features may outweigh the costs of losing smaller features’, and also help reduce the spatial variability across individuals’ brains (Poldrack, 2011:50-51). Spatial smoothing is therefore commonly applied in fMRI analysis in order to increase statistical power, with the most common method being the convolution of the structural image with a Gaussian kernel. The extent of the smoothing performed on each volume of the data is described by the full width at half maximum (FWHM), in mm. No exact guidelines on how to decide on the extent of the smoothing exist. Less is generally more, especially if the activation signals one wants to detect are rather small. However, since the extent of the activation one expects to find is not generally known in advance, the decision is somewhat arbitrary. Poldrack (2011:52) recommends using twice the voxel size. We therefore applied spatial smoothing using a Gaussian kernel of FWHM 6.0mm.

#### Intensity normalisation

FEAT offers - but discourages - the option to calculate the mean intensity of each volume and scale it across the volume, thus making it constant. This could introduce a level of bias, and artificially deflate the amount of variance observed in the data. Since the option is explicitly discouraged, and the setting turned off by default, we decided not to apply it, and to instead apply the default grand-mean intensity normalisation of the entire four-dimensional dataset by a single multiplicative factor, so that higher-level analysis remains valid (Webster, 2017a).

#### High-pass temporal filtering

High-pass temporal filtering removes low-frequency signal, including a linear trend, such as the slow drift in fMRI data, and is therefore a rather standard part of fMRI preprocessing. For a blocked design, the length of the temporal period that one will allow

(as opposed to what will be cut off) should be at least as long as the entire cycle of all the blocks (Webster, 2017a). FEAT offers the option to estimate a reasonable cutoff frequency after the general linear model has been set up, and a way to make sure that the model will not be affected by it. Whilst we would normally perform high-pass filtering in FEAT, we did not, in order not to run it before running ICA-AROMA. We did, however, set up our model to get an idea of an appropriate length to be applied later in the analysis. For our model, FEAT suggested using a cutoff frequency of 90 s.

## Registration

In order to be able to perform group analysis and make generalisations, the images of the highly variable individual brains first need to be transformed and aligned from the ‘native space’ (the coordinates system as they were acquired) to a common spatial framework. This process is called intersubject registration, spatial normalisation, or co-registration when it concerns aligning different images of the same individual. A common coordinate frame of the data is called an atlas. A template is ‘an image that is representative of the atlas and provides a target to which individual images can be aligned’ (Poldrack et al., 2011: 55). The MNI templates are currently the most popular, and were also used by us. Unlike earlier methods that required the identification of anatomical landmarks, MNI templates allow for automated registration. FSL's MNI Avg152, T1 2×2×2 mm (i.e. the 152 nonlinear 6th generation of the MNI atlas) atlas that we used is derived from 152 structural images, averaged together after high-dimensional nonlinear registration into the common MNI152 coordinate system (Grabner et al., 2006). Given that our structural images had been brain-extracted, we chose the brain-extracted version of the template (MNI152\_T1\_2mm\_brain). Since our structural and 4D images were not oriented in the same way, we opted for the Full search - a better fit at the cost of more computation time.

A multi step registration was carried out, with the low resolution functional image first aligned to the corresponding high resolution structural images with FLIRT (Jenkinson and Smith, 2001; Jenkinson, 2002). The recommended Boundary-Based Registration (BBR)

method was used to achieve optimal results (Greve and Fischl, 2009). Second, the high resolution images were also registered to standard space images, using an affine transformation with 12 degrees of freedom (DOF). This step was further refined using FNIRT nonlinear registration with the default 10 mm warp resolution (spacing between the warp field control points), a computational anatomy method that permits local deformations and uses models based on physical phenomena, thus offering more flexibility and accuracy (Andersson et al., 2007a; Andersson et al., 2007b). In FEAT, the relevant registration information is saved, preprocessing and statistical analysis is performed on the data in native space, and registration is applied when group statistics are carried out.

## Output

It is important to assess the quality of the output of every stage before proceeding to the next. For every participant, FEAT creates a folder with a number of images and associated files, and provides an .html summary. We checked each to make sure it contained no errors or warnings that would signal an issue with the preprocessing. The time series output by MCFLIRT should normally cause concern if showing any sudden motion, especially high relative mean displacement of more than half a voxel size, which, in our case, they occasionally did. However, knowing that we had not yet run ICA-based denoising or applied temporal filtering, we disregarded this fact. We paid particular attention to the quality of the registration across the various spaces. As demonstrated by the example in Figure 2.7, the registration appeared to have been successful, with the red lines outlining the estimated boundaries between grey and white matter, as well as internal structures, such as the ventricles, rather accurately.

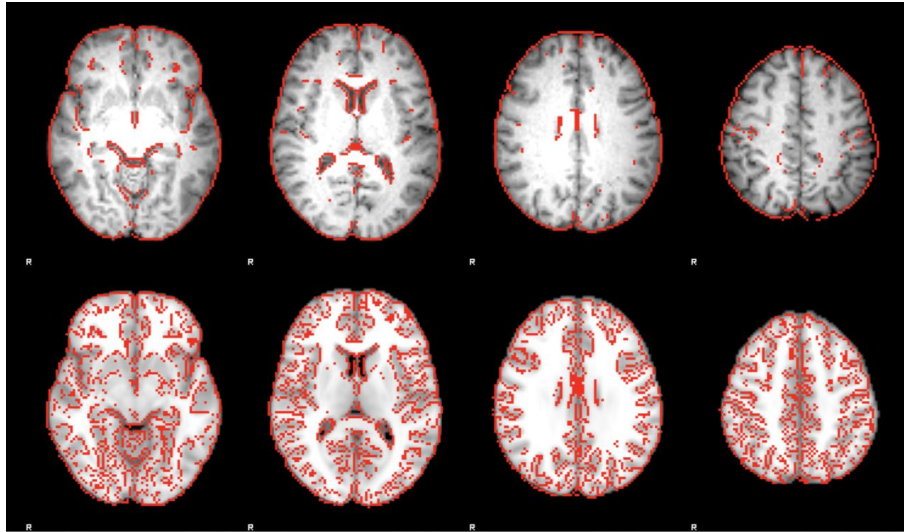


**Figure 2.7:** A successful registration of the high resolution image to standard space.

#### ICA-AROMA and high-pass temporal filtering

Finally, we ran ICA-AROMA followed by high-pass temporal filtering, through simple commands. For ICA-AROMA, we opted for the default, ‘non-aggressive’ version (partial component regression), in order not to remove a portion of the variance we were, in fact, interested in. Analysis was carried out using Probabilistic Independent Component Analysis, as implemented in MELODIC Version 3.14 (Beckmann and Smith, 2004). Masking of non-brain voxels, voxel-wise de-meaning of the data, and normalisation of the voxel-wise variance was applied to the input functional image. Pre-processed data were whitened and projected into a multidimensional subspace using probabilistic Principal Component Analysis (PCA) where the number of dimensions was estimated using the Laplace approximation to the Bayesian evidence of the model order (Minka, 2000). The whitened observations were decomposed into sets of vectors which describe signal variation across the temporal domain (time courses), and across the spatial domain (maps) by optimising for non-Gaussian spatial source distributions using a fixed-point iteration technique (Hyvärinen, 1999). Estimated Component maps were divided by the standard deviation of the residual noise and thresholded by fitting a mixture model to the histogram of intensity values (Beckmann and Smith, 2004).

For the high-pass temporal filtering, we used the cutoff frequency that FEAT had estimated for the corresponding statistical model, converted to sigma. When assessed visually, the components classified as motion by ICA-AROMA, and removed, appeared to, indeed, present noise. The video of the resulting denoised image, when previewed in FSLEyes, appeared significantly more stable than that of the original functional image. We therefore concluded that the operation had been successful. We also compared the time series and the level of noise, as estimated by FEAT, for each of the images - the initial 4D image, the denoised one, and the final, high-pass filtered image. Whilst the variance in the time series was similar for all three, for the latter, the signal strength was centered around 0, and the estimated level of noise was also null. This appeared to cause issues with later stages of the analysis. Calculating the mean of the denoised data and adding it to the high-pass filtered image made further analysis possible. Indeed, the FEAT wiki states that the 4D image after all filtering has been carried out is not normally zero mean, ‘the mean value for each voxel’s time course has been added back in for various practical reasons. When FILM begins the linear modelling, it starts by removing this mean’ (Webster, 2017a).

## **First-level analysis**

Further processing was also carried out using FEAT Version 6.00. For first-level statistical analysis, FEAT uses FMRIB’s Improved Linear Model (FILM), a method based on general linear modelling, or multiple regression. One assumption of the GLM is that the data are not temporally autocorrelated. However, even following high-pass filtering, fMRI data typically exhibit strong autocorrelation, which increases ‘as the temporal proximity of two data points increases’ (Poldrack et al., 2011:90). Since violating this assumption would lead to biased inferences and elevated false positive rates, prior to GLM estimation, FILM prewhitening was applied to account for any autocorrelation. FILM uses ‘a robust and accurate nonparametric estimation of time series autocorrelation to prewhiten each voxel’s time series’ (Webster, 2017a). It smoothes the correlation estimate spatially, thus removing low-frequency drift, and making the statistics valid and maximally efficient

## General linear model

The general linear model relates a single continuous dependent variable to one or more independent variables, also known as predictors, explanatory variables (EVs), or regressors. For fMRI analysis, the expected BOLD stimulus time course predicts the actual BOLD series. FILM uses a mass univariate GLM, meaning a voxel-by-voxel approach where the BOLD signal is modeled for every single voxel separately, before being combined across subjects. The GLM estimates the so-called parameter estimate (PE) for each EV - the number by which it needs to be multiplied so that a linear combination of all EVs best fits the data. A good fit between the data and the statistical model suggests that the voxel under consideration was, indeed, activated by the task or stimulus. For each voxel, a statistical test is performed to determine whether task-related activation is present in it. The statistic corresponding to that test results in a statistical image over all voxels. An appropriate statistical threshold, providing a balance between sensitivity and specificity, is necessary in order to determine where the activation was, in fact, statistically significant.

Given that our experimental design involved several stimuli with irregular timing, and was counterbalanced between subjects, a custom basic shape was necessary to describe it. For each EV of each participant, a .txt file indicating the onset times and durations of the corresponding blocks was selected. In order to match the difference between the stimulus function and the measured BOLD fMRI hemodynamic response, a convolution with a HRF was applied to the basic waveform. The mathematical operation of convolution blends two functions in a linearly-time invariant fashion - at each timepoint, their overlap is added up to arrive at the resulting time series. As emphasised by Poldrack et al. (2011: 74), ‘choosing an appropriate HRF function is key in capturing the shape as best as possible and will ensure a good fit of the GLM regressors to the BOLD time series when signal is present.’

Whilst the Gamma function is commonly used for this purpose, the canonical Double-Gamma HRF, which consists of a standard positive function at normal lag, and a

small, delayed, inverted Gamma, is, arguably, more suitable, as it also attempts to model the undershoot typical of the BOLD signal. Another option is to use a set of basis functions, rather than a single function. This offers more flexibility by allowing for the variability of the BOLD response in different brain areas. Having tried the FSL preset versions of all three approaches on one participant, and compared the results paying special attention to the peristimulus time averages, we opted for the Double-Gamma HRF, as it appeared to model the data better than the other two. In addition, temporal derivatives of the waveform - the latter, shifted slightly in time - were added to the model to achieve a slightly better fit to the data, reduce unexplained noise, and increase resulting statistical significance. The ‘canonical HRF plus derivatives’ approach we used, indeed, appears to be the most commonly used in fMRI analysis (Friston, 1998).

In addition to seeing how strongly each voxel is related to each EV, we were also interested in comparing various parameter estimates to see whether one EV is more relevant to the data than another - i.e. whether a linear combination of the parameter estimates is significant. ‘Contrasting’ the EVs, and creating a contrast matrix consisting of several contrast vectors, allowed us to test several contrasts simultaneously, with each reflecting a different statistical question, and resulting in a separate statistical map. In addition to hypothesis testing using single contrasts using a t-statistic, F-tests enable posing “OR” questions by simultaneous testing of multiple contrasts, to see whether any (combination) of them is statistically non-zero, and compare the contribution of each to the model. A number of t-contrasts and F-tests were carefully set up to reflect our research questions. (For a screenshot of the final design matrix, see Appendix A.) Whilst similar studies usually compare the conditions of interest with either a fixation, neutral emotional faces, or moving geometric shapes, we used both of the latter in order to control, simultaneously, for the effect of movement, and that of facial expressions per se (van der Gaag et al., 2007; Schraa-Tam et al., 2012). For simplicity, all contrasts compare the *mean* of the control conditions with (the mean of) the condition(s) of interest. As already mentioned, neither the motion parameters estimated by MCFLIRT, nor those computed using *fsl\_motion\_outliers* were added to the model as confound EVs because motion had already been addressed by ICA-AROMA. Since the model is designed to look like the data

prior to temporal filtering, the same amount of filtering that had been applied to the data, was also applied to the model.

Once the full model has been set up, clicking on the *Efficiency* button provides a graphical representation of the covariance of the design matrix, and the efficiency of the contrasts. The latter allowed us to verify that our model was set up properly. First, the matrix showing the absolute value of the normalised correlation of each EV with each EV should, for a design that is not rank-deficient, consist of white squares on the diagonal and significantly darker squares everywhere else. According to FSL's wiki page, in the second matrix, showing similar results but after the design matrix has been run through singular value decomposition (SVD), none of the diagonal squares should be completely black (Webster, 2017a). Lastly, the lower, most important, part of the window gave us an estimate of the efficiency of our model. The 'effect required', reflects the strength of the signal, expressed in % signal change, necessary to detect a statistically significant signal for a particular contrast, given the specified threshold. The lower the effect required, the more easily estimable that contrast would be. Both the matrices, and the effect required, which was around 1% for each of our contrasts, appeared reasonable. Upon clicking on Done, one last graphical representation of the entire model appears. Here, it is useful to verify that the period of the longest temporal cycle passed by the high-pass temporal filter, indicated by the red bar on the left, is longer than the total cycle time of the experiment. In our case, the high-pass filter had been estimated from the model and did, indeed, appear to be suitable for it.

## Statistical inference

The so-called multiple comparisons problem is a critical issue to fMRI analysis. Standard hypothesis tests are not designed to be used repetitively, for a set of related tests, such as statistic images consisting of, in our case, around 250 000 voxels. With the number of inferences being made, the number of those likely to be erroneous also increases. To account for this multiplicity when making estimations of the statistical significance of the results, it is important to choose a measure of the risk of false positives across the entire

image. At first level, the FEAT settings were left at default, meaning that  $Z$  (Gaussianised T/F) statistic images were thresholded using clusters determined by  $Z > 2.3$ , and the estimated significance level of each contiguous cluster was compared against a corrected cluster significance threshold of  $p < .05$  (Worsley, 2001). FSL uses 26-connectivity, meaning that voxels that share faces, edges, as well as corners are considered contiguous.

Whilst voxel-based correction would allow us to make very specific inferences, it does not take the fact that fMRI signals are likely to be spatially extended, and activated voxels clustered together, into account. Cluster-level correction is therefore more common, since it is more sensitive to activation, and better at detecting signal that is larger in scale than the smoothness of the data (a combination of its intrinsic smoothness, and the smoothing applied to it with the Gaussian kernel). It is a two-step procedure that takes spatial information available in the image into account. First, a primary *cluster-forming* threshold is applied to the data. Second, the significance of each cluster is determined by measuring its size, or mass (the sum of all voxel-level statistic values in a cluster), and comparing it to a *cluster-extent* threshold measured in units of contiguous voxels (Poldrack et al., 2011). Whilst cluster-level inference, too, has its drawbacks, such as the primary threshold being arbitrary, and the lack of spatial specificity in comparison to voxel-level inference, which becomes an issue for clusters that are too large, it remains commonly used, and the default method in FSL FEAT.

One way of reducing the number of multiple comparisons and increasing statistical power would be to reduce the search space by focusing on a specific region, based on a prior hypothesis about where activation is likely to occur. We did not, however, choose to constrain the search, and pre-threshold masking was therefore not applied. The active clusters were rendered as transparent blobs that can be overlaid onto the individual's anatomical image coregistered to the functional image. Time series plots of peak voxels were also output and later compared to the actual model plot.

Importantly, before running Statistics, the differential contrasts that had been set up and described above were masked with contrasts for the individual EVs, where appropriate. Whilst a simple differential contrast would merely reveal a difference between the conditions being compared, and would also provide significantly positive results if all of them were negative, we were only interested in results where the stimulus of interest not only activated a given brain region more than the control condition but was also positive at the same time. Fully understanding the results sometimes requires combining the individual statistic images in various ways. The contrast masking feature allowed us to achieve this.

## Output

Before proceeding to group-level analysis, we reviewed the output of the first-level analysis, making sure the summary reports contained no errors or warnings, briefly examined the thresholded activation maps for the different contrasts, and verified that there was a reasonable match between our model and the actual time series for the peak voxel for the given contrast.

## Group-level analysis

For modelling data across multiple participants, FEAT uses FMRIB's Local Analysis of Mixed Effects (FLAME). The single- and multi-level GLM are equivalent if the (co)variance structure is modified appropriately. The group analysis then 'only requires values of the parameter estimates and their (co)variance from the first level, generalising the well established 'summary statistics' approach in fMRI' and allowing for 'different pre-whitening and different first-level regressors to be used for each subject'' (Beckmann et al., 2003; Woolrich et al., 2004). Upon selecting the relevant lower-level FEAT directories, provided that all files adhere to the standard naming, FEAT finds all the files that are necessary for higher-level analysis. The higher-level model will be applied to each contrast, and create a separate directory for each.

FEAT offers both mixed-effects (ME) and fixed-effects (FE) modelling. The latter corresponds to the within-session time variances estimated in first-level analyses, and is more sensitive to activation. However, the conclusions that can be made from it are restricted since FE modelling ignores cross-subject variance and therefore does not allow for generalisations about the population from which the subjects were drawn. In contrast, ME modelling, a combination of FE variance and random-effects variance (the "true" cross-session variances of first-level parameter estimates), whilst being more conservative, allows for generalisations, and was also applied to our data (Webster, 2017a).

In addition to FLAME, FEAT also offers the option to use ordinary least squares (OLS) modelling as a fast but less accurate version of ME. FLAME itself is a two-stage process, with the first stage being a fast approximation that is significantly more accurate than - and almost as fast as - OLS. The second stage, then, further refines the accuracy of the results by applying implicit estimation of ME variance using Metropolis-Hastings Markov Chain Monte Carlo (MH MCMC) sampling at voxels demonstrated to be near threshold. Whilst the accuracy of the second stage comes at the cost of significantly more computation time, it is useful, particularly for a small number of subjects. The option to use automatic outlier deweighting, available for ME, detects outliers by comparing each participant's data to all the others', at each voxel, and deweighs them in group-level statistics (Woolrich, 2008). Understandably, this option, too, leads to a considerable increase in computation time. Having tried and compared all of the above methods on a small subset of the participants, we ultimately decided to simply use FLAME1. With our resources, running FLAME1+2 with automatic outlier deweighting on three participants took almost a day. Nevertheless, the results of FLAME1 appeared to provide virtually the same results.

Our goal was to find group means of lower level copes (the contrast of PE iamgea). This, in the GLM setup, translates to a single EV with the value set to 1 for each input (participant). However, given that we also had information about the age, sex, and handedness of the participants, we decided to take these into account. Research suggests that both gender and age might have an impact on empathy (Bailey and Henry, 2008;

Beadle et al., 2013; O'Brien et al., 2012; Toussaint and Webb, 2005). Whilst the MNS appears to exhibit a gender difference, its activity has been shown to be age-independent (Cheng et al., 2008; Nedelko et al., 2010). Rather than looking for correlations, we were interested in controlling for these extra variables, and added them as covariates (nuisance variables) to the model. All of them were first translated to numeric values and demeaned in order to make them independent of the other variables, and since they were not likely to be correlated, all of them were entered to the model simultaneously. Here, the only contrast we were interested in, then, was the one that took the group mean into account, while ignoring the nuisance variables. At group level, multiple comparisons were initially addressed in the same way that had been applied at first level - through cluster-level correction. Having reviewed hundreds of fMRI studies, Woo et al. (2014) found that the choice of a primary cluster-forming threshold is largely determined by the default option within the software used to perform the analysis. They argue that the latter are often too liberal, thus amplifying the disadvantages of cluster-level inference by resulting in clusters that cross anatomical boundaries, and make it 'impossible to reliably infer which anatomical regions show true effects' (ibid.). The default primary cluster-forming threshold (of  $p < .01$ ) in FSL is, indeed, too liberal. Rather than following the trend that Woo et al. (2014:413) called 'both endemic and detrimental to the neuroimaging field', we followed their recommendation and opted for a more stringent initial cluster-forming threshold of  $p < .001$  ( $Z > 3.1$ ), and a corrected cluster-extent threshold of  $p < .05$  (Worsley, 2001).

## Output

In the summary report, the sum of all input masks after transformation to standard space, shown in Figure 2.8, and the image showing voxels where only one mask was missing, suggested that the masks overlapped relatively well. The fact that the functional image of the averaged brain looked blurry, and the outlines of the individual brains were not visible, confirmed that spatial normalisation had been successful (Poldrack et al., 2011).

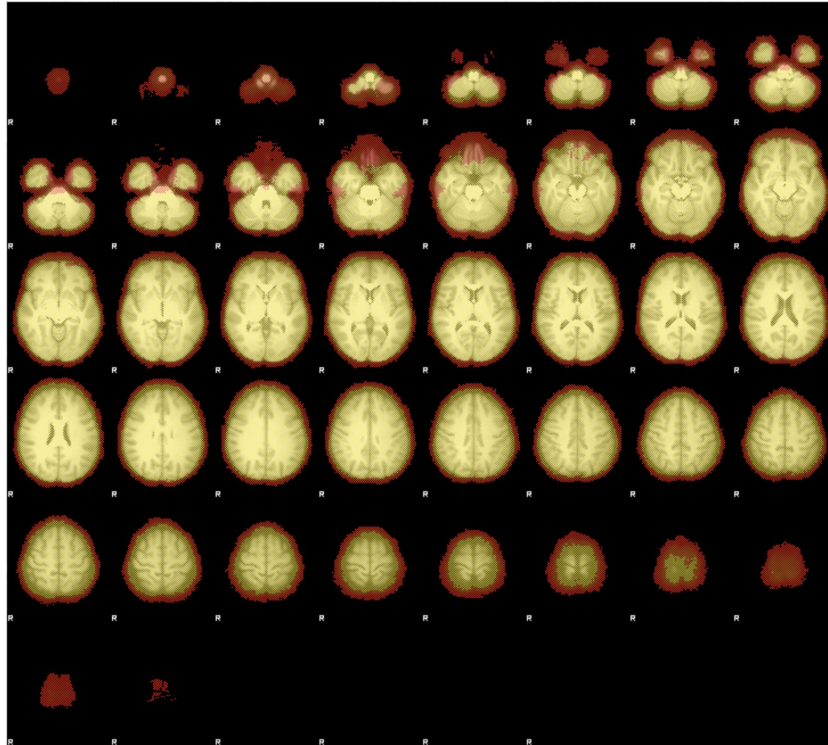


**Figure 2.8:** The sum of all input masks after transformation to standard space.



### Statistical inference

As already discussed, the amount of data in an fMRI dataset makes the choice of an approach for accounting for uncertainty in the data particularly important - and challenging. At group level, the choice becomes crucial, as it can have substantial impact on the conclusions drawn from the analysis. Therefore, whilst at first level the default FSL settings for statistical inference were used, at group level, measures of correcting for multiple comparisons were reconsidered after analysis within FEAT, and an alternative method to the initially used cluster-level correction was, ultimately, adopted.

Two main measures - false discovery rate (FDR) and familywise error rate (FWE) - were considered. Whilst FDR offers greater sensitivity, the latter comes at the cost of a higher risk of false positives. Moreover, similarly to cluster inference, it lacks spatial specificity. We therefore turned to FWE - the probability of one or more false positives in the image

being false positives - instead. Various parametric and nonparametric procedures providing corrected P-values exist (Poldrack et al., 2011).

Having dismissed voxel-level corrections, such as the Bonferroni correction, and corrections based on random field theory (RFT), as overly conservative and insufficiently sensitive for the present sample size, we ultimately opted for a nonparametric approach. Unlike parametric approaches, the latter make no assumptions about the probability distribution for the voxel values in the statistic image (Nichols and Holmes, 2002). Since the noise in fMRI data does not follow a simple distribution, the null distribution is, here, unknown, and the assumptions of parametric methods often violated. Eklund et al. (2016) have argued against the use of parametric methods for fMRI analysis, demonstrating that a considerable portion of fMRI studies present weakly significant results with inflated false positive rates, questioning their validity, and arguing that ‘the principal cause of the invalid cluster inferences is spatial autocorrelation functions that do not follow the assumed Gaussian shape’. Permutation, also called randomisation, methods that use the data themselves to obtain empirical null distributions of the test statistics of interest, such as the permutation test initially proposed by Holmes et al. (1996), therefore appear to be more appropriate for inference on fMRI data. The absence of distributional assumptions make the permutation test an approach that relies on minimal assumptions about the design of the experiment, allows for exact control, and is generally recommended as a robust and accurate, albeit computationally intensive, method of obtaining FWE-corrected results (Hayasaka and Nichols, 2003; Poldrack et al., 2011).

Permutation was performed using *randomise*, FSL’s own tool for nonparametric permutation inference on neuroimaging data (Winkler et al., 2014). The 16 contrasts that had been specified at first level resulted in 16 cope directories (the group mean for each) at group level, each containing a mean functional image. Each of the latter was selected as input for a separate run of *randomise*. Since permutation is not possible for a single-group mean (consisting only of 1s), in this case, *randomise* generates random samples by inverting the sign of the 1s instead. For more complex designs, the design matrix and the

contrast matrix need to be specified in the command line. Whilst we were investigating a group mean, our matrices also included the demeaned values of the confound variables. The latest version of *randomise* no longer requires these to be processed separately (Winkler, 2016). Together with the group brain mask image, we thus also specified the design and contrast matrices. *Randomise* appeared to have correctly identified the nature of the contrast and ‘flipped’ it, rather than attempting to permute it. Aiming for accurate results, notwithstanding the computation time required to arrive at them, we chose to generate 5000 flips when building up the null distribution to test against, for each image. The -D option for demeaning was not used, since the data had already been demeaned.

*Randomise* can output voxel-based, cluster-based, as well as other tests. The desire to take the spatial information available in the data into account led us to dismiss voxel-level inference. Cluster-level inference is, itself, not without drawbacks - namely, the arbitrariness of the initial cluster-forming threshold, and the lack of spatial specificity. We thus opted for an alternative test statistic called the Threshold-Free Cluster Enhancement (TFCE) instead (Smith and Nichols, 2009). As the name suggests, TFCE, a relatively recent method, addresses the above-mentioned drawbacks by not using an arbitrary threshold. Instead, it uses all possible cluster-forming thresholds and integrates over them to provide a voxel-level map that indicates cluster-level significance. With TFCE, ‘cluster-like structures are enhanced but the image remains fundamentally voxel-wise’ (Webster, 2017b). It thus finds clusters without the need for the latter to be defined in an inaccurate, binary way. Its authors argue that the method ‘gives generally better sensitivity than other methods over a wide range of test signal shapes and SNR values’, and ‘does indeed provide not just improved sensitivity, but richer and more interpretable output than cluster-based thresholding’ (ibid.).

The output of *randomise* consists of a test statistic image and a FWE-corrected P-value image. To get information about clusters and peaks, the former was first masked with the latter, thresholded at  $p < .05$  (translated to *-thr 0.95* in the command, since the FWE-corrected P-value images are stored as 1-P, for convenient display). Next, *cluster*

was run, resulting in several different outputs summarising the clusters and local maxima. Since the data had already been in MNI space, we chose to display the results in MNI (mm). For each cluster, a binarised mask was created.

Probabilistic atlases were interrogated with *atlasquery* in order to identify the brain areas corresponding to each cluster. The Harvard-Oxford structural atlases provided anatomical labels (Desikan et al., 2006). Based on the assumption that Brodmann areas reflect functionally important boundaries, the Jülich histological atlas was used to report functional areas, where available (Eickhoff et al., 2007). The results were also previewed in FSLEyes, with the min/max display range set at 0.95/1, and the mean high-resolution image, representative of the entire group and its anatomical variability, used as the most suitable background image. For a summary of the results - both for the comparison of specific emotions to the control conditions and, crucially, the mean of all emotions compared to the latter - see the tables and figures presented in Appendix B. Since minimum cluster size is not relevant with TFCE, even the smallest clusters are included.

## Results

The key results, as summarised in *Table B.5*, span over 19 clusters. Due to the probabilistic nature of the atlases we used, each cluster is assigned several brain areas, of which we decided to include all, as well as the probability with which the cluster is believed to belong to them. The resulting length of the table makes it somewhat difficult to summarise the results in a succinct way. Since different studies use different atlases, a comparison of the areas across studies is therefore also not trivial.

However, we see that our results do contain, or overlap with, the key brain regions of which the MNS is believed to consist. Area F5, where mirror neurons were first discovered

in the macaque brain, i.e. the rostral part of the premotor ventral cortex, is part of Brodmann area 6. Whilst the motor cortex of the macaque brain is relatively well mapped, ‘our knowledge of the human motor cortex is much less precise since a map as detailed as in the macaque is not yet available’ (Geyer et al., 2012). From a cytoarchitectonic point of view, however, the frontal premotor area F5 in monkeys appears to correspond to Broca’s area, i.e. Brodmann areas 44 and 45, in the inferior frontal opercular part of the human brain. More specifically, BA44 has been proposed to be the homolog of F5 (Rizzolatti and Craighero, 2004). Both BA6 and BA44 are among the areas of activation for the condition comparing the mean of all emotional stimuli to the control conditions. BA44 also appears to have been activated by individual emotional facial expressions, with the exception of the happy one.

In addition, various parts of the inferior parietal lobule, also an integral part of the MNS, appear to have been significantly activated both by each individual emotional stimulus, and their mean, as compared to the control conditions. Moreover, the insula, the amygdala, and the inferior frontal gyrus, identified as key regions in studies of emotional resonance, also appear to have been activated by all conditions, again, with the exception of the happy one, for the latter two. These exceptions appear to be in line with Fernández et al. (2012) finding that emotions with higher subjective arousal, such as anger or fear, are more easily induced by films designed to elicit emotions.

## Conclusion

We have identified areas of activation specific - and common - to four distinct emotional stimuli, some of which would likely also be activated if the participants were actually experiencing, not observing, the corresponding emotional states. As explained at the beginning, the areas found to be significantly activated do not necessarily present areas of the mirror neuron system, although they are potentially part of it. In order to distinguish the MNS from other systems common to emotional facial expression processing, a control

experiment measuring the latter is required. However, similar studies that did include the latter, as well as studies of the MNS generally, identified some of the same regions, thus further confirming our intuition (Bastiaansen et al., 2011; van der Gaag et al., 2007). Future steps include, first and foremost, replicating the study while also including a task that makes participants experience the emotional states under question.

We make no assumptions about the function or significance of the mirror neuron system. The present work is, nevertheless, based on a number of assumptions that have been alluded to above. Firstly, we assume that the facial expressions in the video clips we used as stimuli were reflective of the emotions we believe them to represent, and successful at eliciting those in the participants. The latter could, admittedly, have been assessed using an appropriate indicator, such as commonly used emotion self-reports or, to an extent, by simultaneous acquisition of additional physiological measures. Second, we assume that conclusions about neuronal activity triggered by our stimuli can be reached using BOLD fMRI. Due to the hemodynamic response being an indirect measure of neural activity, and the coarse spatial resolution of fMRI, with each measurement voxel covering thousands of neurons, metabolic activity comparable to that found by other studies might, in fact, reflect different neural processes.

Stemming from a deep belief in the importance of replication for science, the present work aimed, to an extent, to replicate existing results within the field. It partly confirmed some of the findings, while refraining from making far-reaching, bold claims about their significance. In addition to identifying the relevant brain areas, its significance thus also lies in its implicit advocacy of replication, and caution, in science. Moreover, the detailed description of the process of learning to analyse fMRI data using FSL, including the thought process behind many of the decisions, also make it potentially useful as an fMRI analysis tutorial for beginners.

## Personal reflection

Similarly to many, including the countless researchers studying the topic, I am fascinated by the concept of empathy and was, initially, equally fascinated by the potential existence of a mirror neuron system. This fascination drove me to the decision to work on these topics within my master thesis. I was lucky to find a supervisor who happened to have relevant fMRI data that they were willing to share with me for this purpose. Eager to gain experience with fMRI analysis, I gladly accepted the opportunity and started analysing the data while, at the same time, studying the surrounding theory in more depth.

The research question first instinctively appeared rather basic to me. Surely, given how much had been written about the MNS, and how popular the concept is, even outside scientific literature, questions about its location would long have been answered. Nevertheless, I found that, considering the attention mirror neurons have been receiving, it is surprisingly difficult to find a straightforward answer to where exactly they are located. Whilst a number of different regions have been recognised as being part of the MNS, it appears that researchers are willing to accept any neuron that exhibits the ‘mirroring’ properties as a mirror neuron. Despite having read a lot, the seemingly basic question of whether mirror neurons are separate neurons whose sole purpose is to mirror, or whether some neurons take on the mirror role under some circumstances, was still not clear to me. The fact that mirror neurons appear to be these mythical neurons dispersed throughout the brain further highlights the notion that researchers are not clear on *what* they are in the first place. The deeper I delved into existing research, the more controversial the concept of mirror neurons appeared to me, and the more doubts I started having about its validity.

I started wondering about the extent to which the research is being driven by wishful thinking, more than facts. Gradually, existing evidence and theories started to appear more and more fluffy, and mirror neurons - or what some argue them to be - too good to be true.

The more I read, and thought, about the topic, the more interested I became not in the concept itself, but in the story surrounding it. Rather than doubting others, I tried to reflect on the extent to which I, personally, merely *wanted to* believe in mirror neurons, and was perhaps unconsciously willing to potentially overlook or misinterpret hard evidence. I made a conscious decision not to contribute to the inflated literature on the topic - to think critically, to not take the subject 'personally', and to try and free myself of the unconscious tendency to confirm the theory at all costs. I strived, first and foremost, to do my best at analysing the data I was given, whilst holding my motivations and the biases involved up to scrutiny throughout the process.

Although arguably 'the best procedure yet discovered for exposing fundamental truths', science is a messy affair, and the practice is not always as pure as the theory behind it (Atkins, 1995). Given that science is a field of human endeavour, the ego (meaning a person's sense of self-importance) inevitably plays an important role in it, and may steer it in undesirable directions. Conversely, it can be argued that without ego, a significant portion of the motivation to do science would disappear, and there would perhaps be no science at all. Given the amount, and effect, of bias in science, I believe that self-reflection should be a significantly more explicit part of it, permeating the scientific process, and evident in scientific papers. Whilst scientists should continue to strive to be objective, I believe that they should, at the same time, admit that they never fully can be. They will, inevitably, have an opinion, a feeling, a hunch about the facts they work with. Whilst this might help them make new connections and discoveries, it can be harmful if they fail to minimise subjective tendencies when relating and communicating facts to others.

Whilst science is about facts, I would argue that the essence of it is storytelling. The facts need to be communicated in one way or another, and the choice of interpretation and context within which they are presented can alter the resulting message significantly. This fuzzy aspect of science is exactly where a lack of knowledge or awareness, and various biases, are free to enter. Whilst science, of course, has methods to fight against the latter, it is, in practice, not immune to it. I feel that constructing a story around raw facts, and

making a conclusion based on them, requires a tremendous amount of knowledge and/or confidence. When coupled with the effort to do one's best, the courage to openly admit to one's weakness, rather than masking insecurity or a lack of competence with excessive self-confidence is, ultimately, a great strength. I wished for my thesis to be a proof of concept and strived to scrutinise and expose my own beliefs and knowledge at every step.

The fact that the hypothesis had been set, and the experiment designed and conducted long before my involvement, and as part of a bigger study of which I have not been told the details, meant that I could not go back and alter it, though I might have wished to do so. I did, indeed, have certain issues with the hypothesis from the very beginning, and further reading helped reinforce those. I felt that the experimental design was not sufficient to answer the research question it had been designed to reflect, and was therefore not sure how to approach the work. Adjusting the hypothesis at such a late stage is, of course, not acceptable - although by no means unheard of - and was not an option for me. Even if it had been, adjusting it to reflect my convictions would have meant having to redesign the experiment and collect the data again, which was out of question, as I do not have the means for doing so.

Throughout the work, I thus struggled with issues with the research question as it had been handed to me - with proceeding to work on it and claiming that my dataset did, in fact, answer it when I, myself, was not convinced. I felt that a link - or a few - were missing between finding brain areas activated by observing emotional facial expressions and claiming that these are part of the MNS, and that existing research could not help fill this void. Extensive reading around the topic made me believe that such leaps and wishful thinking are common (not only) in studies of mirror neurons, and I did not want to contribute to the issue. I arrived at a stage where I was doubting my thesis, and the point of continuing to work on it. I wondered how, knowing very little about fMRI, statistics, or the mirror neuron system, I could contribute to existing research. It also drove me to wonder how anyone can ever find the courage to boldly make a conclusion based on what seemed to me like a vastness of facts that can be cherry-picked and interpreted in innumerable

ways. This experience, however, made me realise that, like excessive self-esteem, excessive self-doubt hinders progress. Having overcome the disillusionment, I finally decided to focus on simply analysing the dataset to my best knowledge, including the original hypothesis but making my own, albeit limited, conclusions, rather than more attractive, inflated conclusions that I did not fully stand behind.

Although I relied on FSL tutorials, fMRI analysis handbooks, and various scientific papers when doing my analysis, the above also gave me the impression that a lot of the choices are somewhat arbitrary, and led by rules of thumb, and experience. Whilst I did my best to study the available sources, and make responsible choices, I remained conscious of, and somewhat nervous about, the fact that I lack the latter. Furthermore, the process and some of the literature I have read, and mentioned earlier, made me think about the extent to which even experienced scientist who routinely analyse fMRI data truly know what they are doing. An examination of my own motivations thus made me contemplate biases surrounding my chosen topic, and think about science itself - how it works and how it should work.

Eklund et al. (2016) suggest that, 'as no analysis is perfect and new limitations will be certainly found in the future', authors should make their statistical results and, ideally, the full data, publicly available. Doing so provides 'enormous opportunities for methodologists, but also the ability to revisit results when methods improve years later' (ibid.). Given that I do not own the data and my supervisor has not granted me the permission to publish my thesis, I was not able to share them. I did, however, strive to describe the results, as well as the process and my reasoning behind it, in enough detail, and followed best practices, namely Poldrack's (2008) guidelines for reporting an fMRI study. fMRI analysis is complex and I believe it is important to be aware of, albeit not paralysed by this fact, and to strive for perfection while acknowledging the extent and limits of one's knowledge and skills. This, after all, applies to all scientific endeavour, and humility and openness about the process should be encouraged, rather than looked down upon.

Conversely, although it is important to remain aware of its limits, as illustrated by the examples of global warming, or vaccination, undue emphasis on the shortcomings of science to those who do not sufficiently understand its strengths and potential will only make them lose all faith in it, or consider such serious issues to be matters of opinion, or conspiracies, rather than scientifically proven facts. Excessive relativisation is therefore harmful, as it helps create an environment where some may feel that they cannot be sure of anything - a perfect breeding ground for fake news and dangerous ideologies. Whilst not quite there, science is as close to being perfect as it gets. It needs protecting and should be done - and communicated - responsibly.

Doing science - and doing it the right way - requires an enormous amount of self control. It means being able to set a hypothesis at the beginning and report the findings, regardless of how seemingly uninteresting they might be, without adjusting or embellishing it in the process. It means being open to (not) finding anything, rather than focusing on finding evidence that supports previously held beliefs. It also requires an enormous amount of knowledge - impossible to be had by a single, perhaps all, humans - and, where it is lacking, it requires caution and humility. Pretending to know is perhaps easier than admitting, or even realising, what one does not know, and an illusion of competence is, ultimately, infinitely harmful to scientific discovery. Doing science responsibly means being honest about the true significance of one's findings, and making appropriate, unexaggerated conclusions. Cognitive, publication, and institutional biases make it all the harder not to succumb, and certainly have a significant impact on the quality of science, published or not. One can, at best, be aware of - and open about - their limits, imperfections, and underlying assumptions, and strive to minimise the impact of these factors.

I tried to set an example by the way I approached my thesis, and envisage to continue doing so in all my future work. Rather than discouraging me from even trying, the experience was very instructive and inspired me to try my very best to move away from to the surface, and get to the bottom of things.

# Bibliography

- Aguirre, Geoffrey K. et al. (1997) 'Empirical Analyses of BOLD fMRI Statistics. II. Spatially Smoothed Data Collected under Null-Hypothesis and Experimental Conditions', *NeuroImage* 5: 199–212. Available at: <https://www.ncbi.nlm.nih.gov/pubmed/9345549> [accessed on 5 February 2017]
- Allanson, Jennifer and Fairclough, Stephen H. (2004) 'A Research Agenda for Physiological Computing', *Interacting with Computers* 16(5): 857-878.
- Andersson, Jesper L.R. et al. (2007a) 'Non-Linear Optimisation', *FMRIB Technical Report* TR07JA1. Available at: <http://www.fmrib.ox.ac.uk/datasets/techrep/#TR07JA1> [accessed on 7 June 2017]
- Andersson, Jesper L.R. et al. (2007b) 'Non-Linear Registration, aka Spatial Normalisation', *FMRIB Technical Report* TR07JA2. Available at: <http://www.fmrib.ox.ac.uk/datasets/techrep/#TR07JA2> [accessed on 7 June 2017]
- Atkins, Peter (1995) 'Science as Truth', *History of the Human Sciences* 8(2): 97-102.
- Avenanti, Alessio et al. (2009) 'The Pain of a Model in the Personality of an Onlooker: Influence of State-Reactivity and Personality Traits on Embodied Empathy for Pain', *NeuroImage* 44(1): 275–283.
- van Baaren, Rick B. et al. (2001) Being Imitated: Consequences of Nonconsciously Showing Empathy. In: Decety and Ickes (eds.), *The Social Neuroscience of Empathy*. Cambridge, MA: MIT Press.
- Bailey, Phoebe E. and Henry, Julie D. (2008) 'Growing Less Empathetic With Age: Disinhibition of the Self-Perspective', *The Journals of Gerontology, Series B: Psychological Sciences and Social Sciences* 63(4): 219-226. Available at: <https://academic.oup.com/psychsocgerontology/article/63/4/P219/581720> [accessed on 15 March 2017]
- Ball, Philip (2015) 'The Trouble With Scientists: How One Psychologist is Tackling Human Biases in Science', *Nautilus*, 14 May 2015. Available at: <http://nautil.us/issue/24/error/the-trouble-with-scientists> [accessed on 14 August 2017]
- Bastiaansen, Jojanneke et al. (2011) 'Age-Related Increase in Inferior Frontal Gyrus Activity and Social Functioning in Autism Spectrum Disorder', *Biological Psychiatry* 69:

832-838. Available at: <https://www.ncbi.nlm.nih.gov/pubmed/21310395> [accessed on 4 December 2016]

Beadle, Janelle N. et al. (2013) 'Aging, Empathy, and Prosociality', *The Journals of Gerontology, Series B: Psychological Sciences and Social Sciences* 70(2): 213-222. Available at: <https://academic.oup.com/psychsocgerontology/article/70/2/213/572414> [accessed on 15 March 2017]

Beckmann, Christian F. et al. (2003) 'General Multilevel Linear Modeling for Group Analysis in fMRI', *NeuroImage* 20(2): 1052-1063. Available at: <https://www.ncbi.nlm.nih.gov/pubmed/14568475> [accessed 13 July 2017]

Beckmann, Christian F. and Smith, Stephen M. (2004) 'Probabilistic Independent Component Analysis for Functional Magnetic Resonance Imaging', *IEEE Transactions on Medical Imaging* 23(2): 137-152. Available at: <https://www.ncbi.nlm.nih.gov/pubmed/14964560> [accessed on 11 October 2017]

Bethel, Cindy L. et al. (2007) 'Survey of Psychophysiology Measurements Applied to Human-Robot Interaction', *16th IEEE International Symposium on Robot & Human Interactive Communication*.

Blair, R.J.R. and Blair, Karina S. (2001) Empathy, Morality and Social Convention: Evidence from the Study of Psychopathy and Other Psychiatric Disorders. In: Decety and Ickes (eds.), *The Social Neuroscience of Empathy*. Cambridge, MA: MIT Press.

Boesen, Kristi et al. (2004) 'Quantitative Comparison of Four Brain Extraction Algorithms', *NeuroImage* 22: 1255-1261. Available at: <https://www.ncbi.nlm.nih.gov/pubmed/15219597> [accessed on 12 November 2016]

Botvinick, Matthew et al. (2005) 'Viewing Facial Expressions of Pain Engages Cortical Areas Involved in the Direct Experience of Pain', *NeuroImage* 25(1): 312-319.

Boucsein, Wolfram (2012) *Electrodermal Activity*. 2nd ed. Germany: Springer.

Bower, Gordon H. (1983) 'Affect and Cognition', *Philosophical Transactions of the Royal Society of London* 3028: 387-402.

Boynton, Geoffrey M. et al. (1996) 'Linear Systems Analysis of Functional Magnetic Resonance Imaging in Human V1', *Journal of Neuroscience* 16(13): 4207-4221. Available at: <https://www.ncbi.nlm.nih.gov/pubmed/8753882> [accessed on 13 December 2016]

Calvo, Manuel G. et al. (2013) ‘When Does the Brain Distinguish Between Genuine and Ambiguous Smiles? An ERP Study’, *Brain and Cognition* 81(2): 237-246.

Cannon, Walter B. (1927) ‘The James-Lange Theory of Emotions: A Critical Examination and an Alternative Theory’, *The American Journal of Psychology* 39(1/4): 106-124. Available at: <https://www.jstor.org/stable/1415404> [accessed on 7 June 2017]

Catmur, Caroline et al. (2007) ‘Sensorimotor Learning Configures the Human Mirror System’, *Current Biology* 17(17): 1527–1531.

Chartrand, Tanja L. and Bargh, John A. (1999) ‘The Chameleon-Effect: The Perception-Behavior Link and Social Interaction’, *Journal of Personality and Social Psychology* 76: 893-910.

Cheng, Yawei et al. (2008) ‘Gender Differences in the Mu Rhythm of the Human Mirror-Neuron System’, *PLoS ONE* 3(5): e2113. Available at: <https://www.ncbi.nlm.nih.gov/pmc/articles/PMC2361218/> [accessed on 15 March 2017]

Clark-Polner, Elizabeth et al. (2017) ‘Multivoxel Pattern Analysis Does not Provide Evidence to Support the Existence of Basic Emotions’, *Cerebral Cortex* 27(3): 1944-1948. Available at: <https://www.ncbi.nlm.nih.gov/pubmed/26931530> [accessed on 2 December 2017]

Cohen, Mark A. (2005) ‘Against Basic Emotions, and Toward a Comprehensive Theory’, *The Journal of Mind and Behaviour* 26(4): 229-254. Available at: <https://www.jstor.org/stable/43854066> [accessed on 24 October 2016]

Dale, Anders M. (1999) ‘Optimal Experimental Design for Event-Related fMRI’, *Human Brain Mapping* 8(2-3): 109-114. Available at: <https://www.ncbi.nlm.nih.gov/pubmed/10524601> [accessed on 13 December 2016]

Damasio, Antonio and Carvalho, Gil B. (2013) ‘The Nature of Feelings: Evolutionary and Neurobiological Origins’, *Nature Neuroscience* 14: 143-152. Available at: <https://www.nature.com/articles/nrn3403> [accessed on 10 October 2016]

Darwin, Charles et al. (1872) *The Expression of the Emotions in Man and Animals*. London: John Murray.

Decety, Jean and Jackson, Philip L. (2004) ‘The Functional Architecture of Human Empathy’, *Behavioral and Cognitive Neuroscience Reviews* 3(2): 71–100.

Decety, Jean and Lamm, Claus (2001) Empathy versus Personal Distress: Recent Evidence from Social Neuroscience. In: Decety and Ickes (eds.), *The Social Neuroscience of Empathy*. Cambridge, MA: MIT Press.

Decety, Jean and Meyer, Meghan (2008) 'From Emotion Resonance to Empathic Understanding: A Social Developmental Neuroscience Account', *Development and Psychopathology* 20(4): 1053–1080.

Desikan, Rahul S. et al. (2006) 'An Automated Labeling System for Subdividing the Human Cerebral Cortex on MRI Scans into Gyral Based Regions of Interest', *NeuroImage* 31(3): 968-980. Available at: <https://www.ncbi.nlm.nih.gov/pubmed/16530430> [accessed on 18 December 2017]

Dijksterhuis, Ap (2005) Why We Are Social Animals: The High Road to Imitation as Social Glue. In: Hurley and Chater (eds.), *Perspectives on Imitation: From Cognitive Neuroscience to Social Science: Vol.2. Imitation, Human Development and Culture*. Cambridge, MA: MIT Press.

Eickhoff, Simon B. (2007) 'Assignment of Functional Activations to Probabilistic Cytoarchitectonic Areas Revisited', *NeuroImage* 36(3): 511-521. Available at: <https://www.ncbi.nlm.nih.gov/pubmed/17499520> [accessed on 17 December 2017]

Eisenberg, Nancy and Eggum, Natalie D. (2001) Empathic Responding: Sympathy and Personal Distress. In: Decety and Ickes (eds.), *The Social Neuroscience of Empathy*. Cambridge, MA: MIT Press.

Eklund, Anders et al. (2016) 'Cluster Failure Why fMRI Inferences for Spatial Extent Have Inflated False Positive Rates', *Proceedings of the National Academy of Science, USA* 113(28): 7900-7905. Available at: <https://www.ncbi.nlm.nih.gov/pmc/articles/PMC4948312/> [accessed on 1 September 2017]

Ekman, Paul and Friesen, Wallace V. (1971) 'Constants Across Cultures in Face and Emotion', *Journal of Personality and Social Psychology* 17(2): 124-129. Available at: [http://www.communicationcache.com/uploads/1/0/8/8/10887248/constants\\_across\\_cultures\\_in\\_the\\_face\\_and\\_emotion.pdf](http://www.communicationcache.com/uploads/1/0/8/8/10887248/constants_across_cultures_in_the_face_and_emotion.pdf) [accessed on 10 October 2016]

Ekman, Paul (1999) Basic Emotions. In: Dalgleish and Power (eds.), *Handbook of Cognition and Emotion*. Sussex, UK: John Wiley & Sons.

Ekstrom, Arne (2010) 'How and When the BOLD fMRI Signal Relates to Underlying Neural Activity', *Brain Research Reviews* 62(2): 233-244. Available at: <https://www.ncbi.nlm.nih.gov/pubmed/20026191> [accessed on 6 January 2017]

- Fadiga, Luciano et al. (1995) 'Motor Facilitation During Action Observation: A Magnetic Stimulation Study', *Journal of Neurophysiology* 73(6): 2608–11.
- Férrandez, Clarissa et al. (2012) 'Physiological Responses Induced by Emotion-Eliciting Films', *Applied Psychophysiology and Biofeedback* 37(2): 73-79.
- Frijda, Nico H. (1994) Varieties of Affect: Emotions and Episodes, Moods, and Sentiments. In: Ekman and Davidson (eds.), *The Nature of Emotion: Fundamental Questions*. New York: Oxford University Press.
- Friston, Karl J. et al. (1998) 'Event-Related fMRI: Characterizing Differential Responses', *NeuroImage* 7: 30–40. Available at: <https://www.ncbi.nlm.nih.gov/pubmed/9500830> [accessed on 3 June 2017]
- Fusar-Poli, Paolo et al. (2009) 'Functional Atlas of Emotional Faces Processing: A Voxel-Based Meta-Analysis of 105 Functional Magnetic Resonance Imaging Studies', *Journal of Psychiatry & Neuroscience* 34(6): 418-432. Available at: <https://www.ncbi.nlm.nih.gov/pmc/articles/PMC2783433/> [accessed on 3 May 2017]
- van der Gaag et al. (2007) 'Facial Expressions: What the Mirror Neuron System Can and Cannot Tell Us', *Social Neuroscience* 2(3-4): 179-222. Available at: <https://www.ncbi.nlm.nih.gov/pubmed/18633816> [accessed on 4 February 2017]
- Gallese, Vittorio et al. (1996) 'Action Recognition in the Premotor Cortex', *Brain: A Journal of Neurology* 119(2) :593–609.
- Gallese, Vittorio (2013) 'Mirror Neurons, Embodied Simulation and a Second-Person Approach to Mindreading', *Cortex* 49(10): 2954–2956.
- Ganglbauer, Eva et al. (2009) 'Applying Psychophysiological Methods for Measuring User Experience: Possibilities, Challenges and Feasibility', *User Experience Evaluation Methods in Product Development (UXEM'09)*.
- Gendron, Maria et al. (2014) 'Perceptions of Emotion from Facial Expressions are not Culturally Universal: Evidence from a Remote Culture', *Emotion* 14(2): 251-262. Available at: <https://www.ncbi.nlm.nih.gov/pmc/articles/PMC4752367/> [accessed on 23 November 2016]
- Geyer, Stefan et al. (2012) Motor Cortex. In: Mai and Paxinos (eds.), *The Human Nervous System*, 3rd edition. New York: Elsevier.

- Glover, Gary H. (2011) ‘Overview of Functional Magnetic Resonance Imaging’, *Neurosurgery Clinics of North America* 22: 133-139. Available at: <https://www.ncbi.nlm.nih.gov/pubmed/21435566> [accessed on 12 November 2016]
- Gore, John C. (2003) ‘Principles and Practice of Functional MRI of the Human Brain’, *Journal of Clinical Investigation* 112(1): 4-9. Available at: <https://www.ncbi.nlm.nih.gov/pmc/articles/PMC162295/> [accessed on 2 December 2016]
- Grabner, Günther et al. (2006) ‘Symmetric Atlasing and Model Based Segmentation: An Application to the Hippocampus in Older Adults’, *Medical Image Computing and Computer-Assisted Intervention* 9(2): 58-66. Available at: <https://www.ncbi.nlm.nih.gov/pubmed/17354756> [accessed on 6 June 2017]
- Greve, Douglas N. and Fischl, Bruce (2009) ‘Accurate and Robust Brain Image Alignment Using Boundary-Based Registration’, *NeuroImage* 48(1): 63-72. Available at: <https://www.ncbi.nlm.nih.gov/pubmed/19573611> [accessed on 22 May 2017]
- Gross, James J. and Levenson, Robert W. (1995) ‘Emotion Elicitation Using Films’, *Cognition and Emotion* 9: 87-108.
- Gur, Ruben C. et al. (2002) ‘A Method for Obtaining 3-Dimensional Facial Expressions and Its Standardization for Use in Neurocognitive Studies’, *Journal of Neuroscience Methods* 115: 137-43.
- Hayasaka, Satoru and Nichols, Thomas E. (2003) ‘Validating Cluster Size Inference: Random Field and Permutation Methods’, *NeuroImage* 20: 2343-2356. Available at: <https://www.ncbi.nlm.nih.gov/pmc/articles/PMC4214144/> [accessed on 11 August 2017]
- Heyes, Cecilia (2014) ‘Tinbergen on Mirror Neurons’, *Philosophical Transactions of the Royal Society B* 369(April): 20130180.
- Hickock, Gregory (2014) *The Myth of Mirror Neurons: The Real Neuroscience of Communication and Cognition*. New York: W. W. Norton & Company.
- Holmes, Andrew P. et al. (1996) ‘Nonparametric Analysis of Statistic Images from Functional Mapping Experiments’, *Journal of Cerebral Blood Flow & Metabolism* 16(1): 7-22. Available at: <https://www.ncbi.nlm.nih.gov/pubmed/8530558> [accessed on 2 September 2017]
- Hoque, Mohammed E. et al. (2012) ‘Exploring Temporal Patterns in Classifying Frustrated and Delighted Smiles’, *IEEE Transactions on Affective Computing* 3(3). Available at:

<http://hoques.com/Publications/2012/12-TAC-Hoque-Mcduff-Picard-12.pdf> [accessed on 23 December 2017]

Horvat, Marko et al. (2015) ‘Comparing Affective Responses to Standardized Pictures and Videos: A Study Report’, *MIPRO, 2015 Proceedings of the 38th International Convention, IEEE*.

Huettel, Scott A. et al. (2009) *Functional Magnetic Resonance Imaging*, 2nd edition. Massachusetts: Sinauer.

Hyvärinen, Aapo (1999) ‘Fast and Robust Fixed-Point Algorithms for Independent Component Analysis’, *IEEE Transactions on Neural Networks* 10(3): 626-634. Available at: <http://ieeexplore.ieee.org/document/761722/> [accessed on 10 October 2017]

Iacoboni, Marco et al. (2005) ‘Grasping the Intentions of Others with One’s Own Mirror Neuron System’, *PLoS Biology* 3(3): 0529–0535.

Iacoboni, Marco (2009) *Mirroring People: The Science of Empathy and How We Connect with Others*. New York: Picador.

Ioannidis, John P.A. (2005) ‘Why Most Published Research Findings Are Wrong’, *PLoS Medicine*. Available at: <https://doi.org/10.1371/journal.pmed.0020124> [accessed on 10 August 2017]

Ioannidis, John P.A. (2014) ‘How to Make More Published Research True’, *PLoS Medicine*. Available at: <https://doi.org/10.1371/journal.pmed.1001747> [accessed on 10 August 2017]

Jack, Rachael E. et al. (2012) ‘Facial Expressions of Emotion Are not Culturally Universal’, *PNAS* 109(19): 7241-7244. Available at: <http://www.pnas.org/content/109/19/7241.long> [accessed on 17 November 2016]

James, William (1890) *The Principles of Psychology*. New York: Henry Holt and Company.

Jenkinson, Mark (2012) *FSLMotionOutliers*. Available at: <https://fsl.fmrib.ox.ac.uk/fsl/fslwiki/FSLMotionOutliers> [accessed on 3 October 2017]

Jenkinson, Mark et al. (2002) ‘Improved Optimisation for the Robust and Accurate Linear Registration and Motion Correction of Brain Images’, *NeuroImage* 17(2): 825-841. Available at: <https://www.ncbi.nlm.nih.gov/pubmed/12377157> [accessed on 5 October 2017]

Jenkinson, Mark and Smith, Stephen M. (2001) 'A Global Optimisation Method for Robust Affine Registration of Brain Images', *Medical Image Analysis* 5(2): 143-156. Available at: <https://www.ncbi.nlm.nih.gov/pubmed/11516708> [accessed on 5 October 2017]

Jooper, Ridha et al. (2012) 'Publication Bias: What Are the Challenges and Can They Be Overcome?', *Journal of Psychiatry & Neuroscience* 37(3): 149-152. Available at: <https://www.ncbi.nlm.nih.gov/pmc/articles/PMC3341407/> [accessed on 10 August 2017]

Kanwisher, Nancy et al. (1997) 'The Fusiform Face Area: A Module in Human Extrastriate Cortex Specialized for Face Perception', *Journal of Neuroscience* 17: 4302-4311. Available at: <https://www.ncbi.nlm.nih.gov/pubmed/9151747> [accessed on 6 May 2017]

Kennett, Jeanette (2002) 'Autism, Empathy and Moral Agency,' *The Philosophical Quarterly* 52(208): 340-357. Available at: <http://www.jstor.org/stable/3543050> [accessed on 23 November 2015]

Kivikangas, Matias J. et al. (2011) 'A Review of the Use of Psychophysiological Methods in Game Research', *Journal of Gaming and Virtual Worlds* 3(3): 181-199.

Kleinginna, Paul R. and Kleinginna, Anne M. (1981) 'A Categorized List of Emotion Definitions, with Suggestions for a Consensual Definition', *Motivation and Emotion* 5(4): 345-379. Available at: <https://link.springer.com/article/10.1007/BF00992553> [accessed on 2 February 2017]

Kriegeskorte, Nikolaus et al. (2009) 'Circular Analysis in Systems Neuroscience: The Dangers of Double Dipping', *Nature Neuroscience* 12(5): 535-540. Available at: <https://www.ncbi.nlm.nih.gov/pubmed/19396166> [accessed on 13 August 2017]

Lamm, Claus and Majdandžić, Jasminka (2015) 'The Role of Shared Neural Activations, Mirror Neurons, and Morality in Empathy - A Critical Comment', *Neuroscience Research* 90: 15-24. Available at: <https://www.sciencedirect.com/science/article/pii/S0168010214002314#!> [accessed on 24 December 2017]

Lang, Peter J. et al. (1993) 'Looking at Pictures: Evaluative, Facial, Visceral, and Behavioral Responses', *Psychophysiology* 30(3): 261-73.

Lang, Peter J. et al. (2008) ‘International Affective Picture System (IAPS): Affective Ratings of Pictures and Instruction Manual’, *Technical Report A-8*. Gainesville, FL: University of Florida.

LeDoux, Joseph E. and Hoffman, Stefan G. (2018) ‘The Subjective Experience of Emotion: A Fearful View’, *Current Opinion in Behavioural Sciences* 19: 67-72. Available at: <http://www.sciencedirect.com/science/article/pii/S2352154617300694> [accessed on 2 December 2017]

Lisetti, Christine L. and Nasoz, Fatma (2004) ‘Using Noninvasive Wearable Computers to Recognize Human Emotions from Physiological Signals’, *EURASIP Journal on Applied Signal Processing* 11: 1672–1687.

Logothetis, Nikos K. et al. (2001) ‘Neurophysiological Investigation of the Basis of the fMRI Signal’, *Nature* 412: 150-157. Available at: <https://www.nature.com/articles/35084005> [accessed on 10 December 2016]

Logothetis, Nikos K. (2008) ‘What We Can and Cannot Do with fMRI’, *Nature* 453: 869-878. Available at: <https://www.nature.com/articles/nature06976> [accessed on 15 December 2016]

McCabe, David P. and Castel, Alan D. (2008) ‘Seeing is Believing: The Effect of Brain Images on Judgments of Scientific Reasoning’, *Cognition* 107: 343-352. Available at: <https://www.ncbi.nlm.nih.gov/pubmed/17803985> [accessed on 11 November 2017]

Mehrabian, Albert (1972). *Nonverbal communication*. Chicago, Illinois: Aldine-Atherton.

Mennes, Maarten (2017) *ICA-AROMA*. Available at: <https://github.com/rhr-pruim/ICA-AROMA> [accessed on 10 October 2017]

Minka, Thomas P. (2000) ‘Automatic Choice of Dimensionality for PCA’, *MIT Media Laboratory Perceptual Computing Section Technical Report No. 514*. Available at: <http://vismod.media.mit.edu/tech-reports/TR-514.pdf> [accessed on 11 October 2017]

Mouras, Harold et al. (2008) ‘Activation of Mirror-Neuron System by Erotic Video Clips Predicts Degree of Induced Erection: An fMRI Study’, *NeuroImage* 42(3): 1142–1150. Available at: <https://www.ncbi.nlm.nih.gov/pubmed/18598769> [accessed on 22 December 2017]

Mukamel, Roy et al. (2010) 'Single-Neuron Responses in Humans during Execution and Observation of Actions' *Current Biology* 20(8): 750–756.

Nedelko, Violetta et al. (2010) 'Age-Independent Activation in Areas of the Mirror Neuron System During Action Observation and Action Imagery. A fMRI Study', *Restorative Neurology and Neuroscience* 28(6): 737-747. Available at: <https://www.ncbi.nlm.nih.gov/pubmed/21209489> [accessed on 15 March 2017]

Nichols, Thomas E. and Holmes, Andrew P. (2002) 'Nonparametric Permutation Tests for Functional Neuroimaging: A Primer with Examples', *Human Brain Mapping* 15(1): 1-25. Available at: <http://www.fil.ion.ucl.ac.uk/spm/doc/papers/NicholsHolmes.pdf> [accessed on 5 September 2017]

Nickerson, Raymond S. (1998) 'Confirmation Bias: A Ubiquitous Phenomenon in Many Guises', *Review of General Psychology* 2(2): 175-220. Available at: <http://psy2.ucsd.edu/~mckenzie/nickersonConfirmationBias.pdf> [accessed on 13 August 2017]

Nieuwenhuis, Sander et al. (2011) 'Erroneous Analyses of Interactions in Neuroscience: A Problem of Significance', *Nature Neuroscience* 14: 1105-1107. Available at: <https://www.nature.com/articles/nn.2886> [accessed on 15 August 2017]

Nuzzo, Regina (2015) 'How Scientists Fool Themselves - And How They Can Stop', *Nature News*, 7 October 2015. Available at: <http://www.nature.com/news/how-scientists-fool-themselves-and-how-they-can-stop-1.18517> [accessed on 12 August 2017]

O'Brien, Ed et al. (2012) 'Empathic Concern and Perspective Taking: Linear and Quadratic Effects of Age Across the Adult Life Span', *The Journals of Gerontology, Series B: Psychological Sciences and Social Sciences* 68(2): 168-175. Available at: <https://www.ncbi.nlm.nih.gov/pubmed/22865821> [accessed on 14 March 2017]

Ogawa, Seiji et al. (1990) 'Brain Magnetic Resonance Imaging with Contrast Dependent on Blood Oxygenation', *Proceedings of the National Academy of Sciences* 87(24): 9868-9872. Available at: <https://www.ncbi.nlm.nih.gov/pmc/articles/PMC55275/> [accessed on 10 December 2016]

Open Science Collaboration (2015) 'Estimating the Reproducibility of Psychological Science', *Science* 349(6251). Available at: <http://science.sciencemag.org/content/349/6251/aac4716> [accessed on 13 August 2017]

- Orgs, Guido et al. (2008) 'Expertise in Dance Modulates Alpha/Beta Event-Related Desynchronization During Action Observation', *European Journal of Neuroscience* 27(12): 3380–3384.
- Park, Byungho (2009) 'Psychophysiology as a Tool for HCI Research: Promises and Pitfalls', *Proceedings of the 13th international Conference on Human-Computer interaction*, San Diego, CA.
- Pascolo, Paolo B. et al. (2009) 'The Mirror-Neuron System Paradigm and its Consistency', *Gait & Posture* 30: S65.
- Pascolo, Paolo B. et al. (2013) 'Just How Consistent is the Mirror Neuron System Paradigm?', *Progress in Neuroscience* 1(12): 29–43.
- di Pellegrino, Giuseppe et al. (1992). 'Understanding Motor Events: A Neurophysiological Study', *Experimental Brain Research* 91(1):176–180.
- Pfeifer, Jennifer H. and Dapretto, Mirella (2001) 'Mirror, Mirror, in my Mind': Empathy, Interpersonal Competence, and the Mirror Neuron System. In: Decety and Ickes (eds.), *The Social Neuroscience of Empathy*. Cambridge, MA: MIT Press.
- Philippot, Pierre (1993) 'Inducing and Assessing Differentiated Emotion-Feeling States in the Laboratory', *Cognition and Emotion* 7(2): 171-193.
- Plutchik, Robert (1980) 'The Nature of Emotions' *American Scientist* 89(4): 344-350.
- Poldrack, Russell A. et al. (2008) 'Guidelines for Reporting an fMRI Study', *NeuroImage* 40(2): 409-414. Available at: <https://www.sciencedirect.com/science/article/pii/S1053811907011020#app1> [accessed on 1 October 2017]
- Poldrack, Russell A. et al. (2011) *Handbook of Functional MRI Data Analysis*. Cambridge: Cambridge University Press.
- Press, Clare et al. (2012) 'fMRI Evidence of 'Mirror' Responses to Geometric Shapes', *PLoS ONE* 7(12): e51934.
- Prinz, Wolfgang (1997) 'Perception and Action Planning', *European Journal of Cognitive Psychology* 9(2): 129–154.
- Pruim, Raimon H.R. et al. (2015a) 'ICA-AROMA: A Robust ICA-Based Strategy for Removing Motion Artifacts from fMRI Data', *NeuroImage* 112: 267-277. Available at:

<http://www.sciencedirect.com/science/article/pii/S1053811915001822> [accessed on 10 October 2017]

Pruim, Raimon H.R. et al. (2015b) 'Evaluation of ICA-AROMA and Alternative Strategies for Motion Artifact Removal in Resting State fMRI', *NeuroImage* 112: 278-287. Available at: <https://www.ncbi.nlm.nih.gov/pubmed/25770990> [accessed on 10 October 2017]

Reisenzein, Rainer et al. (2013) 'Coherence Between Emotion and Facial Expression: Evidence from Laboratory Experiments', *Emotion Overview* 5(1): 16-23.

Ramachandran, Vilayanur S. (2000) 'Mirror Neurons and Imitation Learning as the Driving Force Behind 'The Great Leap Forward' in Human Evolution', *Edge.org*. Available at: <https://www.edge.org/conversation/mirror-neurons-and-imitation-learning-as-the-driving-force-behind-the-great-leap-forward-in-human-evolution> [accessed on 12 August 2016]

Ramachandran, Vilayanur S. and Oberman, Lindsay M. (2006) 'Broken Mirrors: A Theory of Autism', *Scientific American* 295(5): 62–69.

Rameson, Lian T. and Lieberman, Matthew D. (2009) 'Empathy: A Social Cognitive Neuroscience Approach', *Personality Psychology Compass* 3(1): 94-100. Available at: [www.scn.ucla.edu/pdf/Rameson\(2009\).pdf](http://www.scn.ucla.edu/pdf/Rameson(2009).pdf) [accessed on 22 November 2015]

Rigoulot, Simon and Pell, Marc D. (2012) 'Seeing Emotion with Your Ears: Emotional Prosody Implicitly Guides Visual Attention to Faces', *PLoS One* 7(1). Available at: <http://journals.plos.org/plosone/article?id=10.1371/journal.pone.0030740> [accessed on 2 December 2017]

Rizzolatti, Giacomo et al. (1996) 'Premotor Cortex and the Recognition of Motor Actions', *Brain Research: Cognitive Brain Research* 3(2): 131–41.

Rizzolatti, Giacomo and Craighero, Laila (2004) 'The Mirror-Neuron System', *Annual Review of Neuroscience* 27: 169–192.

Rizzolatti, Giacomo and Fabbri-Destro, Maddalena (2008) 'The Mirror System and its Role in Social Cognition', *Current Opinion in Neurobiology* 18(2): 179–184.

Rizzolatti, Giacomo. and Fadiga, Luciano (1998) 'Grasping Objects and Grasping Action Meanings: The Dual Role of Monkey Rostroventral Premotor Cortex (Area F5)', *Novartis Foundation Symposium* 218: 81–103.

Rizzolatti, Giacomo and Sinigaglia, Corrado (2010) 'The Functional Role of the Parieto-Frontal Mirror Circuit: Interpretations and Misinterpretations', *Nature Reviews. Neuroscience* 11(4): 264–274.

Salimi-Khorshidi, Gholamreza et al. (2014) ‘Automatic Denoising of Functional MRI Data: Combining Independent Component Analysis and Hierarchical Fusion of Classifiers’, *NeuroImage* 90: 449-468. Available at: <https://www.ncbi.nlm.nih.gov/pubmed/24389422> [accessed on 9 October 2017]

Schachter, Stanley and Singer, Jerome (1962) ‘Cognitive, Social and Physiological Determinants of Emotional State’, *Psychological Review* 69(5): 379-399.

Schraa-Tam, Caroline K. L. et al. (2012) ‘fMRI Activities in the Emotional Cerebellum: A Preference for Negative Stimuli and Goal-Directed Behaviour’, *Cerebellum* 11: 233-245. Available at: <https://www.ncbi.nlm.nih.gov/pubmed/21761197> [accessed on 12 November 2016]

Segal, Elizabeth A. (2011) ‘Social Empathy: A Model Built on Empathy, Contextual Understanding, and Social Responsibility That Promotes Social Justice,’ *Journal of Social Service Research* 37(3): 266-277. Available at: <http://dx.doi.org/10.1080/01488376.2011.564040> [accessed on 23 November 2015]

Shamay-Tsoory, Simone G. (2001) Empathic Processing: Its Cognitive and Affective Dimensions and Neuroanatomical Basis. In Decety and Ickes (eds.), *The Social Neuroscience of Empathy*. Cambridge, MA: MIT Press.

Singer, Tania and Klimecki, Olga M. (2014) ‘Empathy and Compassion,’ *Current Biology* 24(18): 875-878. Available at: <http://dx.doi.org/10.1016/j.cub.2014.06.054> [accessed on 23 November 2015]

Sinigaglia, Corrado and Rizzolatti, Giacomo (2011) ‘Through the Looking Glass: Self and Others’, *Consciousness and Cognition* 20(1): 64–74.

Sladky, Ronald et al. (2011) ‘Slice-Timing Effects and Their Correction in Functional MRI’, *NeuroImage* 58: 588-594. Available at: <https://www.ncbi.nlm.nih.gov/pmc/articles/PMC3167249/> [accessed on 14 December 2016]

Solomon, Robert C. and Stone, Lori D. (2002) ‘On ‘Positive’ and ‘Negative’ Emotions’, *Journal for the Theory of Social Behaviour* 32(4): 0021-8308.

Smith, Anne M. et al. (1999) ‘Investigation of Low Frequency Drift in fMRI Signal’, *NeuroImage* 9: 526–33. Available at: <https://www.ncbi.nlm.nih.gov/pubmed/10329292> [accessed on 3 February 2017]

Smith, Stephen M. (2002) 'Fast Robust Automated Brain Extraction', *Human Brain Mapping* 17: 143-155. Available at: <https://www.ncbi.nlm.nih.gov/pubmed/12391568> [accessed on 12 October 2016]

Smith, Stephen M. et al. (2004) 'Advances in Functional and Structural MR Image Analysis and Implementation as FSL', *NeuroImage* 23(S1): 208-219. Available at: <https://www.ncbi.nlm.nih.gov/pubmed/15501092> [accessed on 13 November 2016]

Smith, Stephen M. and Nichols, Thomas E. (2009) 'Threshold-Free Cluster Enhancement: Addressing Problems of Smoothing, Threshold Dependence and Localisation in Cluster Inference', *NeuroImage* 44(1): 83-98. Available at: <https://www.ncbi.nlm.nih.gov/pubmed/18501637> [accessed on 7 September 2017]

Sutherland, Georgina et al. (1982) 'Experimental Investigations of the Relationship Between Mood and Intrusive Unwanted Cognitions', *British Journal of Medical Psychology* 55: 127-138.

Tkach, Dennis et al. (2007) 'Congruent Activity During Action and Action Observation in Motor Cortex', *The Journal of Neuroscience* 27(48): 13241–13250.

Toussaint, Loren and Webb, Jon R. (2005) 'Gender Differences in the Relationship Between Empathy and Forgiveness', *The Journal of Social Psychology* 145(6): 673-685. Available at: <https://www.ncbi.nlm.nih.gov/pmc/articles/PMC1963313/> [accessed on 14 March 2017]

Uhrig, Meike K. et al. (2016) 'Emotion Elicitation: A Comparison of Pictures and Films', *Frontiers in Psychology* 7: 180. Available at: <https://www.ncbi.nlm.nih.gov/pmc/articles/PMC4756121/> [accessed on 13 April 2017]

Uithol, Sebo et al. (2011) 'Understanding Motor Resonance', *Social Neuroscience* 6(4): 388–397.

Vanderwert, Ross E. et al. (2013) 'The Mirror Mechanism and Mu Rhythm in Social Development', *Neuroscience Letters* 540: 15–20.

Velten, Emmett (1968) 'A Laboratory Task For the Induction of Mood States', *Behaviour Research and Therapy* 6: 473-482.

Vul, Ed et al. (2009) 'Puzzlingly High Correlations in fMRI Studies of Emotion, Personality, and Social Cognition', *Perspectives on Psychological Science* 4(3): 274-290. Available at: <https://www.ncbi.nlm.nih.gov/pubmed/26158964> [accessed on 15 August 2017]

Watson, Jeanne C. and Greenberg, Leslie S. (2001) Empathic Resonance: A Neuroscience Perspective. In: Decety and Ickes (eds.), *The Social Neuroscience of Empathy*. Cambridge, MA: MIT Press.

Webster, Matthew (2015) *MCFLIRT*. Available at: <https://fsl.fmrib.ox.ac.uk/fsl/fslwiki/MCFLIRT> [accessed on 2 October 2017]

Webster, Matthew (2017a) *FEAT*. Available at: <https://fsl.fmrib.ox.ac.uk/fsl/fslwiki/FEAT> [accessed on 1 December 2016]

Webster, Matthew (2017b) *Randomise: User Guide*. Available at: <https://fsl.fmrib.ox.ac.uk/fsl/fslwiki/Randomise/UserGuide> [accessed on 3 September 2017]

Weisberg, Deena S. et al. (2008) 'The Seductive Allure of Neuroscience Explanations', *Journal of Cognitive Neuroscience* 20(3): 470-477. Available at: <https://www.ncbi.nlm.nih.gov/pmc/articles/PMC2778755/> [accessed on 11 November 2017]

Wicker, Bruno et al. (2003) 'Both of us Disgusted in My Insula: The Common Neural Basis of Seeing and Feeling Disgust', *Neuron* 40(3): 655-664.

Winkler, Anderson M. et al. (2014) 'Permutation Inference for the General Linear Model', *NeuroImage* 92: 381-397. Available at: <https://www.ncbi.nlm.nih.gov/pubmed/24530839> [accessed on 2 September 2017]

Winkler, Anderson M. (2016) *Randomise*. Available at: <https://fsl.fmrib.ox.ac.uk/fsl/fslwiki/Randomise> [accessed on 8 September 2017]

Woo, Choong-Wan et al. (2014) 'Cluster-Extent Based Thresholding in fMRI Analyses: Pitfalls and Recommendations', *NeuroImage* 91: 412-419. Available at: <https://www.ncbi.nlm.nih.gov/pmc/articles/PMC4214144/> [accessed on 17 August 2017]

Woolrich, Mark W. et al. (2004) 'Multilevel Linear Modeling for fMRI Group Analysis Using Bayesian Inference', *NeuroImage* 21(4): 1732-1747. Available at: <https://www.ncbi.nlm.nih.gov/pubmed/15050594> [accessed on 14 July 2017]

Woolrich, Mark W. (2008) 'Robust Group Analysis Using Outlier Inference', *NeuroImage* 41(2): 286-301. Available at: <https://www.ncbi.nlm.nih.gov/pubmed/18407525> [accessed on 15 July 2017]

Worsley, Keith J. (2001) Statistical Analysis of Activation Images. In: Jezzard, Matthews and Smith (eds.), *Functional MRI: An Introduction to Methods*. New York: Oxford University Press.

Zarahn, Eric et al. (1997) 'Empirical Analyses of BOLD fMRI Statistics. I. Spatially Unsmoothed Data Collected under Null-Hypothesis Conditions', *NeuroImage* 5: 179–97. Available at: <https://www.ncbi.nlm.nih.gov/pubmed/9345548> [accessed on 4 February 2017]

Zhou, Haotian et al. (2017) 'Inferring Perspective Versus Getting Perspective: Underestimating the Value of Being in Another Person's Shoes', *Psychological Science* 28(4): 482-493.

Zupan, Barbra and Babbage, Duncan R. (2017) 'Film Clips and Narrative Text as Subjective Emotion Elicitation Techniques', *The Journal of Social Psychology* 157: 194-210. Available at: <http://www.tandfonline.com/doi/abs/10.1080/00224545.2016.1208138?journalCode=vsoc2> [accessed on 2 February 2017]

# Appendix A

## FSL GUI settings and commands

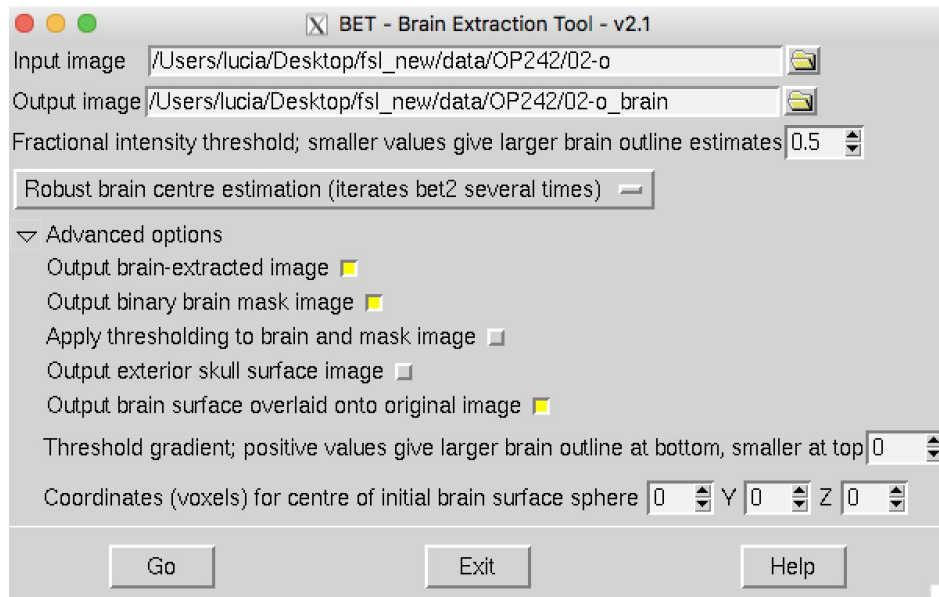


**Figure A.1: FSL's brain extraction tool - BET v2.1.** Prior to any preprocessing, both structural images were brain-extracted using BET. For the high-resolution image, a robust brain centre estimation with the fractional intensity threshold initially set to 0.5 was implemented. In addition to the brain-extracted image, a binary brain mask and an image of brain surface were also output by BET.

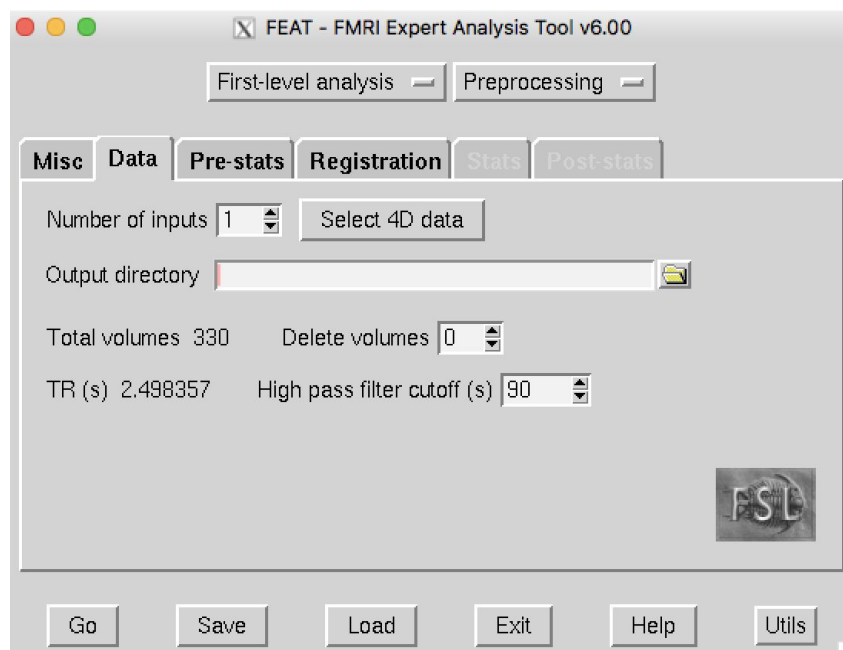


**Figure A.2: Preprocessing was carried out in FSL's FEAT Version 6.00.** Under the Data tab, a functional image was selected as input. FEAT automatically detects the number of total volumes in the image, and the TR with which they were acquired, from the metadata stored in the header of the image file. Since, in this case, no initial dummy volumes were saved, the number of volumes to delete was left at zero.

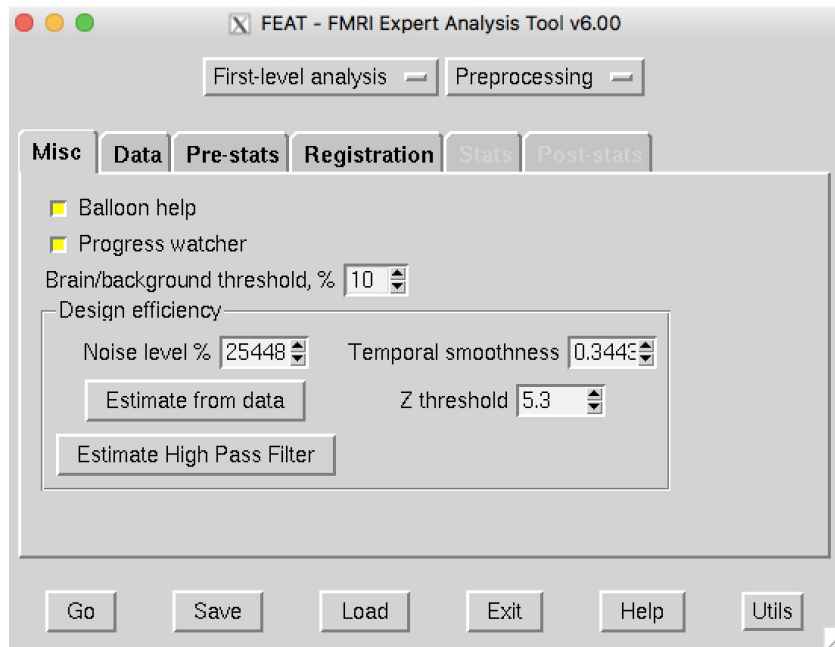


**Figure A.3: First-level analysis.** Under Design efficiency, the Misc tab offers the option to get an estimate of the noise characteristics that will be left in the data following preprocessing. In the case of the present experiment, the estimate noise level was quite high. This estimate, however, does not take motion correction into account. Provided that the statistical model has been set up under Stats, clicking on Estimate High Pass Filter will provide a corresponding high-pass filter cutoff, shown under the Data tab.

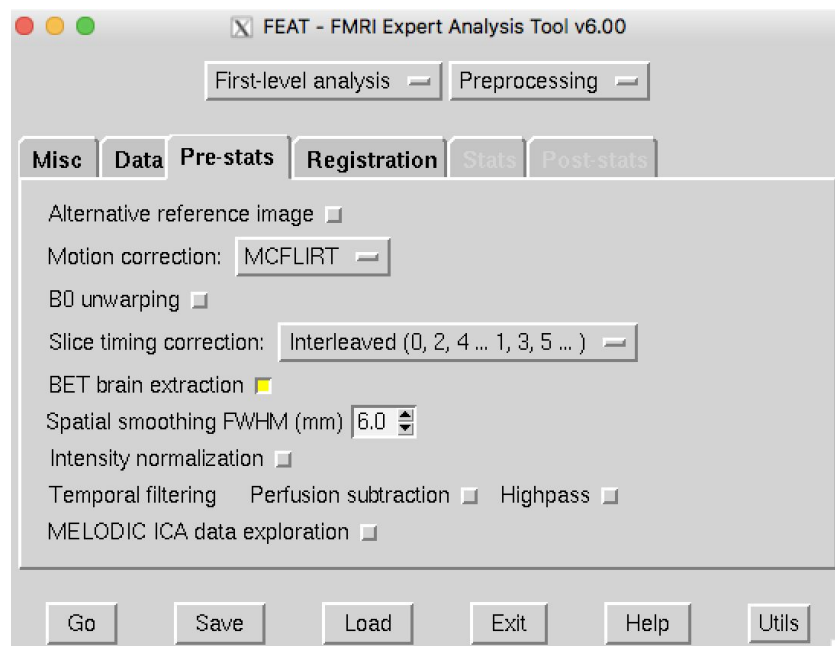


**Figure A.4: Pre-Stats.** Head motion parameters were estimated using MCFLIRT. The functional image was also brain extracted. Slice-timing correction was set to interleaved and the FWHM of spatial smoothing was adjusted to 6mm. Instead of intensity normalisation, the default grand-mean intensity normalisation of the entire 4D dataset by a single multiplicative factor was applied.

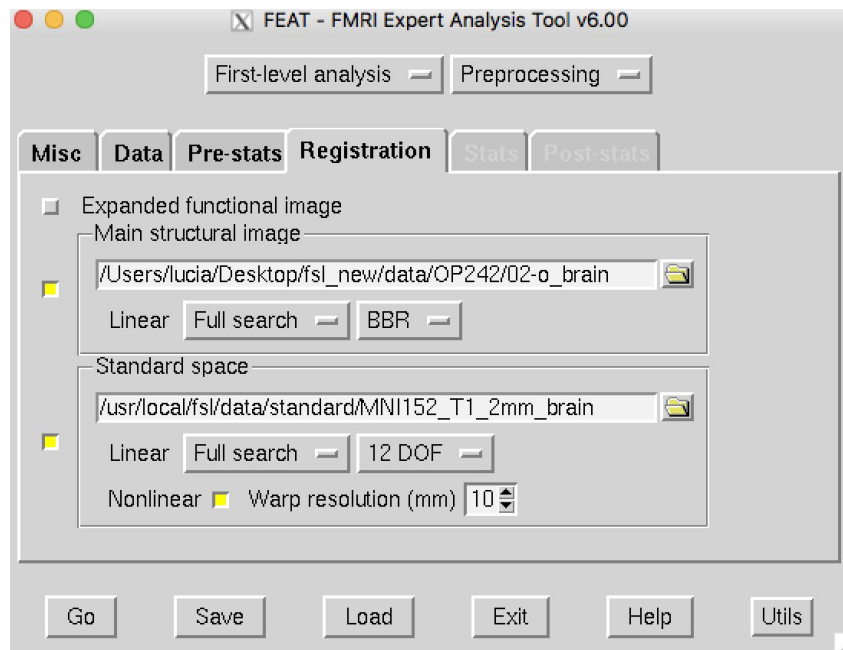


**Figure A.5: Registration.** Under registration, the low-resolution functional image to be co-registered to the functional image and subsequently registered to standard space (the brain-extracted version of the MNI152 template) was input. For optimal results, Full search and the BBR method were selected for co-registration. Registration to standard space was further refined by a non-linear registration with a warp resolution of 10 mm. Preprocessing was initiated by pressing the **Go** button.

The non-aggressive version of ICA-AROMA was run on the preprocessed data:

```
ICA_AROMA.py -feat /OP242/10.feats -out /OP242/10.feats/ICA_AROMA/
```

The output of ICA-AROMA was high-pass filtered, with a frequency cutoff of 90 s (translated to sigma):

```
fslmaths /OP242/10.feats/ICA_AROMA/denoised_func_data_nonaggr.nii.gz -bptf  
18.0101072722 -1 /OP242/10.feats/ICA_AROMA/temp_filtered.nii.gz
```

Mean variance of the denoised data was calculated and added to the high-pass filtered image to make further analysis possible:

```
fslmaths /OP242/10.feats/ICA_AROMA/denoised_func_data_nonaggr.nii.gz -Tmean  
/OP242/10.feats/ICA_AROMA/mean_denoised_func_data_nonaggr.nii.gz
```

```
fslmaths /OP242/10.feats/ICA_AROMA/temp_filtered.nii.gz -add  
/OP242/10.feats/ICA_AROMA/mean_denoised_func_data_nonaggr.nii.gz  
/OP242/10.feats/ICA_AROMA/temp_filtered_with_mean.nii.gz
```

The resulting temp\_filtered\_with\_mean image served as input for statistical analysis.

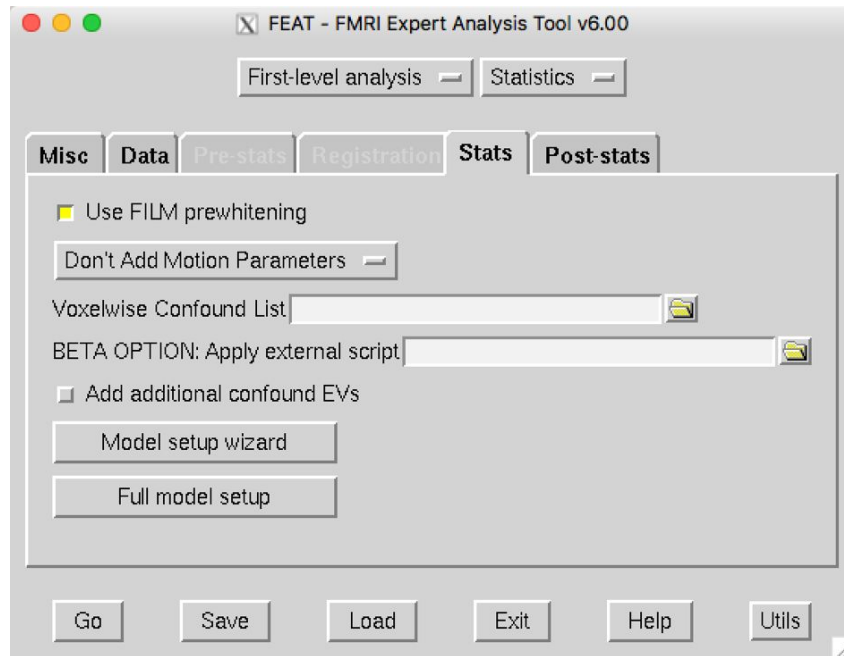


**Figure A.6: Stats.** Prior to GLM estimation, FILM prewhitening was applied to account for any autocorrelation. Since motion had already been addressed by ICA-AROMA, no additional motion parameters were added to the model as confound EVs.

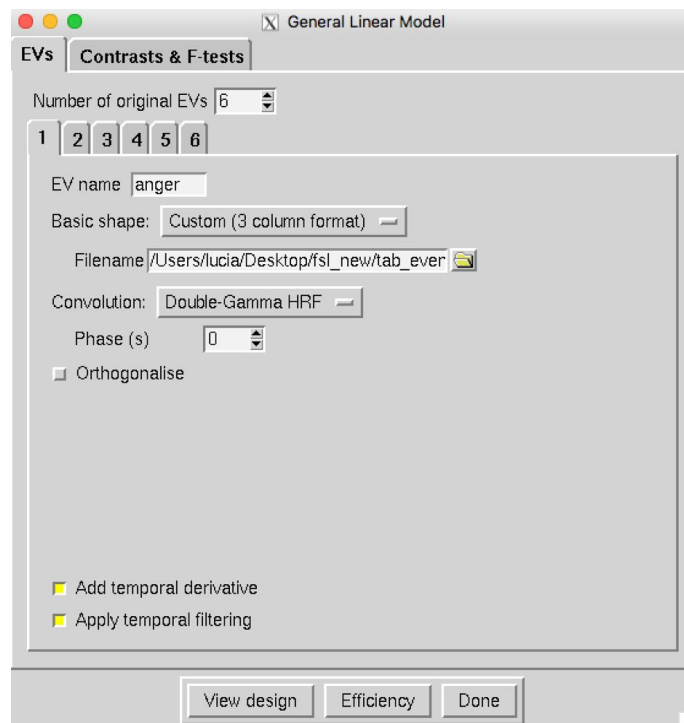


**Figure A.7: GLM - EVs.** A .txt file describing the custom basic shape for each stimulus was input and convolved with the canonical Double-Gamma HRF function. Temporal derivatives were added for a better fit. The same amount of filtering that had been applied to the data, was also applied to the model.

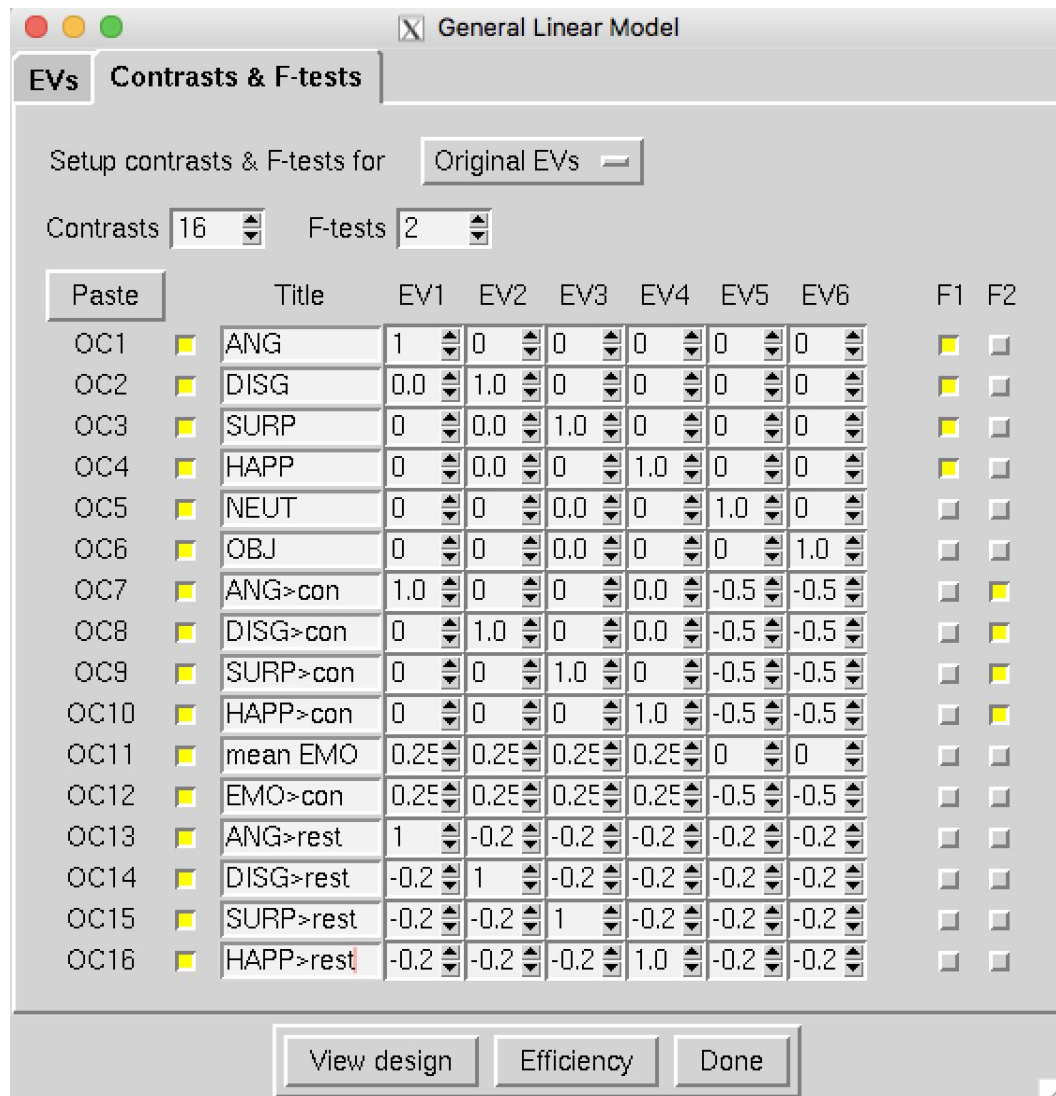


**Figure A.8: GLM - Contrasts and F-tests.** A number of t-contrasts and F-tests were set up to reflect our research questions. OC7-OC10 correspond to the difference between a particular emotional facial expression and the mean of the control conditions. F2 is asking an "or" question about all four - aims to identify areas where *at least one* of the emotional facial expression results in an activation that is significantly different to the mean of the control conditions. OC12 compares the mean of all emotional facial expressions to the mean of the control conditions. OC13-OC16 correspond to a comparison of a particular emotional facial expression to the mean of all other conditions.

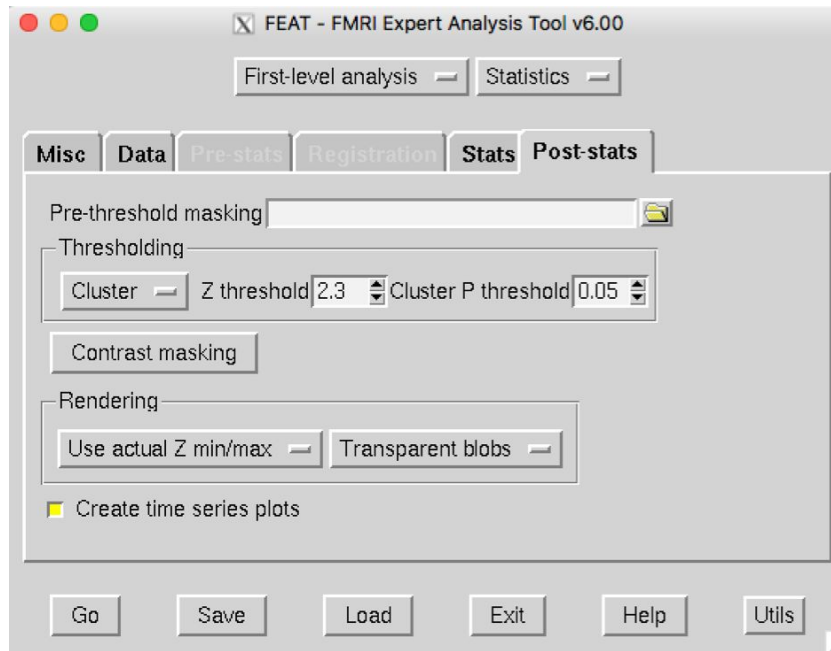


**Figure A.9: Post-stats.** At this stage, the default settings - cluster-based thresholding with a primary threshold of  $p < .05$  ( $Z > 2.3$ ) and a corrected cluster-extent threshold of  $p < .05$  - were used, with more attention being paid to statistical inference at group level.

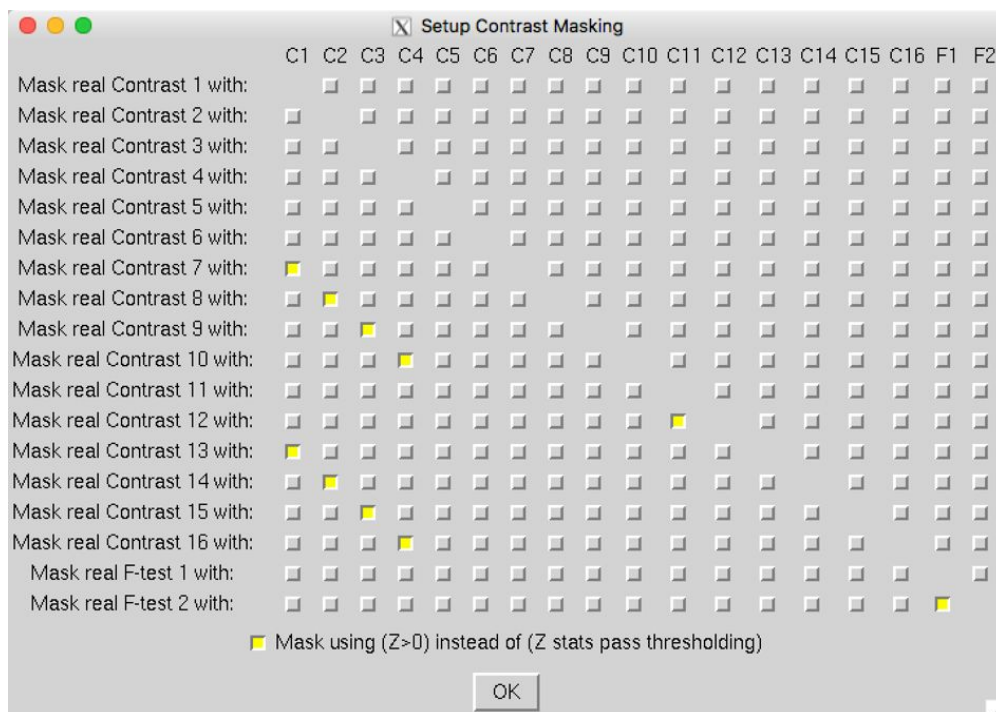


**Figure A.10: Contrast masking.** Since we were only interested in results where, in addition to activating a given brain region more than the control conditions, the stimulus of interest was also positive, differential contrasts were masked with contrasts for the individual EVs, where appropriate, using  $Z > 0$ .

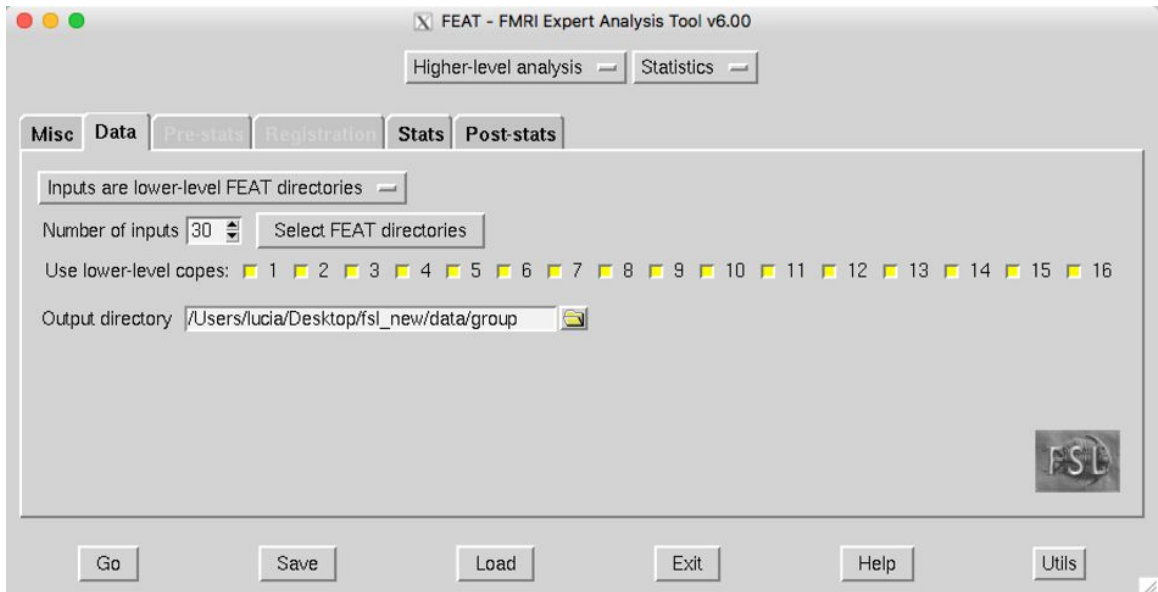


**Figure A.11: Higher-level analysis.** Upon selecting the relevant lower-level FEAT directories, FEAT finds all the files that are necessary for higher-level analysis. Although it was, arguably, not necessary, we used all lower-level copes. The higher-level model will thus be applied to each lower-level contrast, and create a separate directory for each.

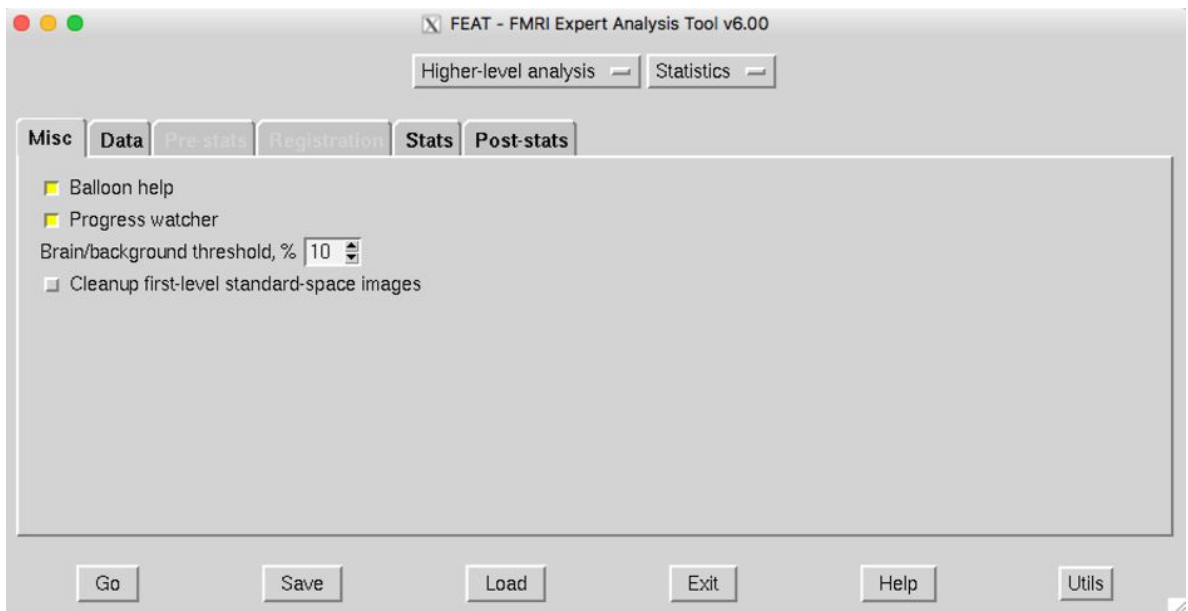


**Figure A.12: Misc.** At higher level, the settings under Misc were left unchanged.

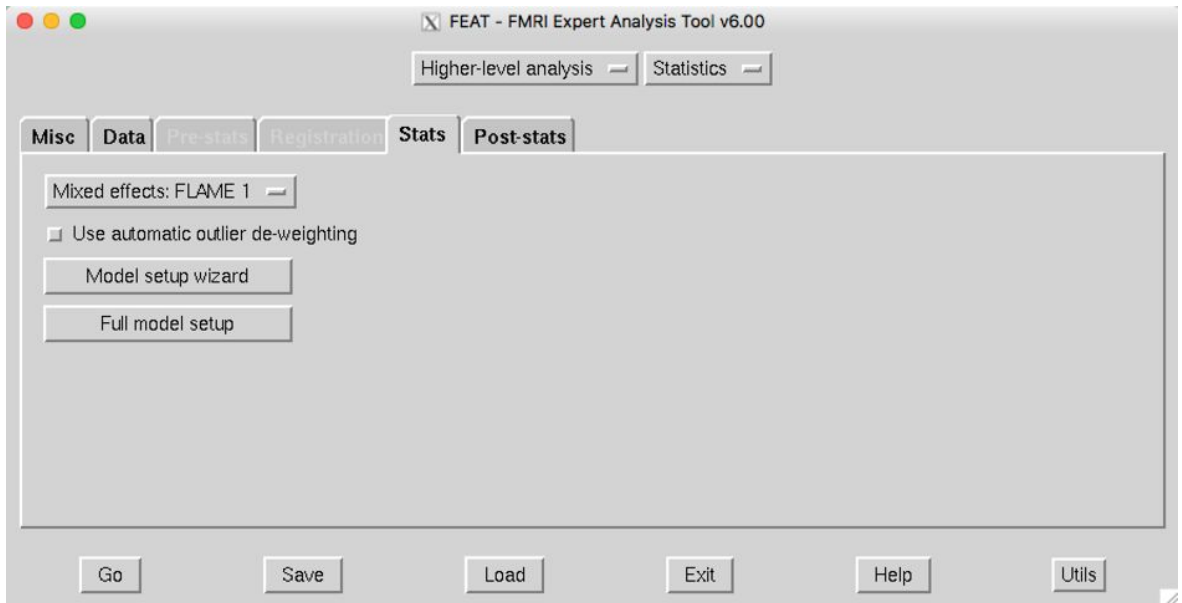


**Figure A.13: Stats.** FLAME Stage 1 fast approximation modelling was applied at group level. Neither Stage 2 nor automatic outlier deweighting was used, as the improvement in results did not appear to be proportional to the significantly higher computation time they require.

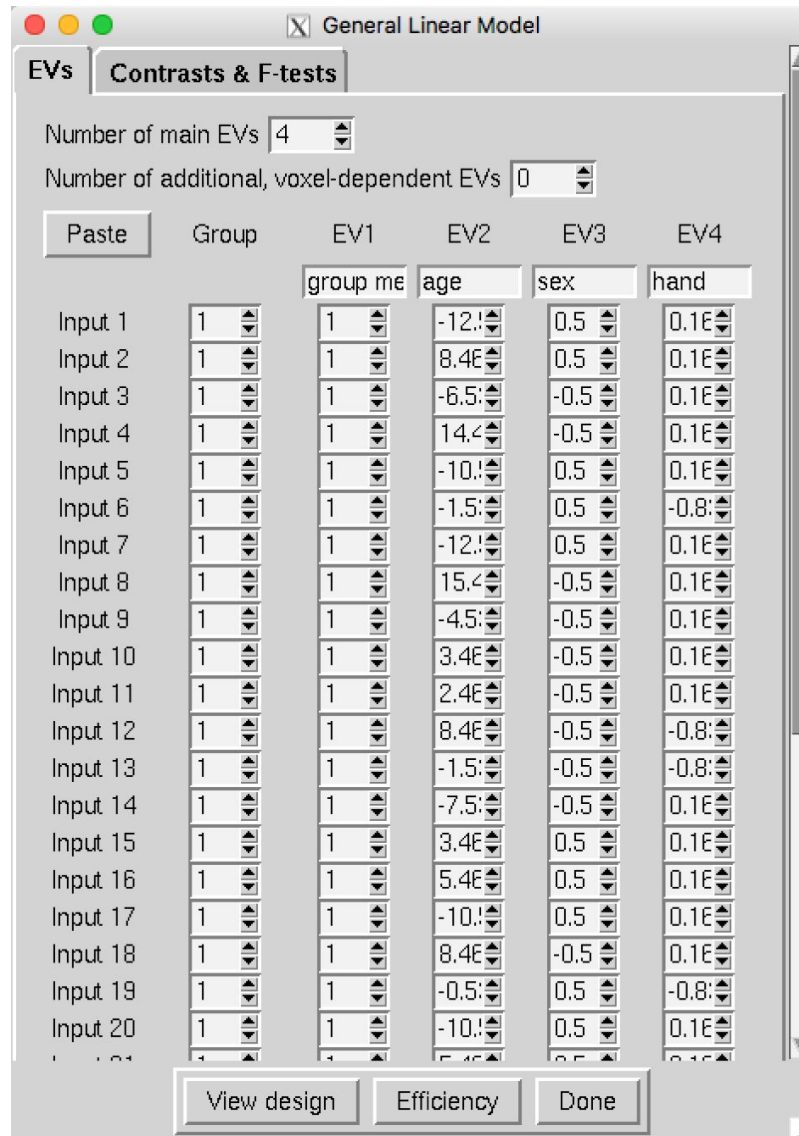


**Figure A.14: Higher-level GLM - EVs.** In addition to a column of 1s representing the group mean, demeaned (orthogonalised) values for three additional variables were entered as nuisance variables.

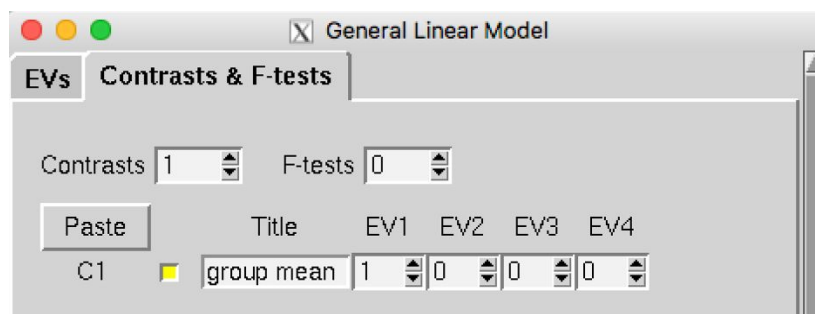


**Figure A.15: Higher-level GLM - Contrasts.** In order to test the data for non-zero mean after accounting for any unique variance due to the nuisance variables, only one contrast was necessary.

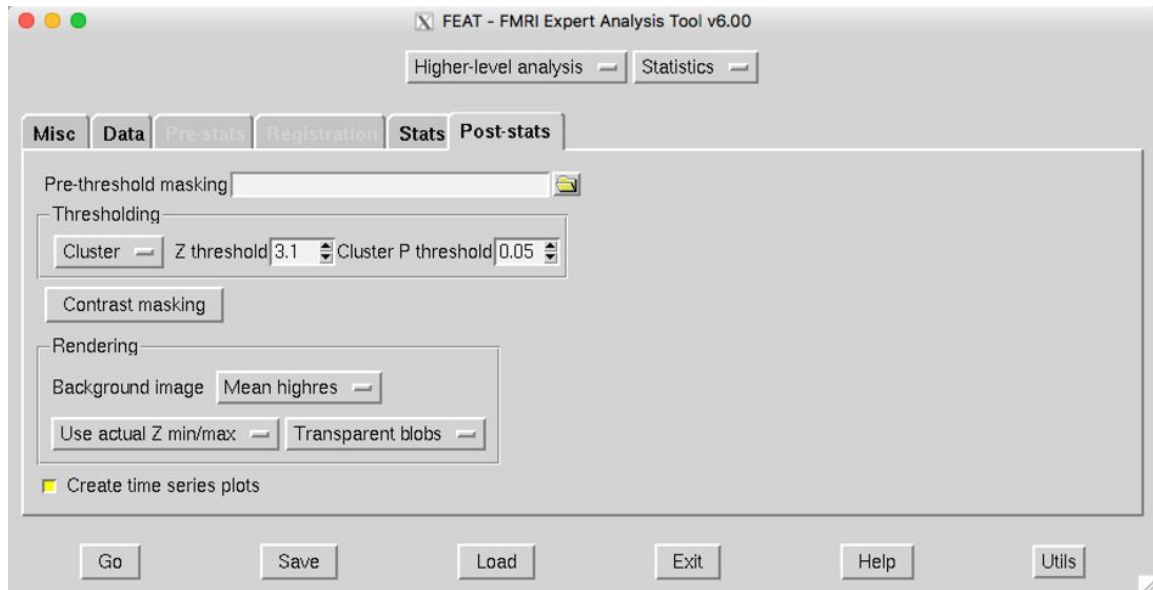


**Figure A.16: Post-stats.** At group level, cluster-based thresholding with a primary threshold of  $p < .001$  ( $Z > 3.1$ ) and a corrected cluster-extent threshold of  $p < .05$  were initially used.

Higher-level analysis resulted in a `.gfeat` directory with 16 `cope.feat` directories - one for each lower-level contrast - each of them containing a `filtered_func_data` image. The following *randomise* script, using the Threshold-Free Cluster Enhancement method, was run on the latter, generating 5000 permutations:

```
randomise -i /group.gfeat/cope12.feat/filtered_func_data.nii.gz -o  
/group.gfeat/cope12.feat/randomise -d /group.gfeat/cope12.feat/design.mat -t  
/group.gfeat/cope12.feat/design.con -m /group.gfeat/cope12.feat/mask -n 5000 -T
```

In order to extract mask and peak information from the *randomise* output, the raw test statistic image was first masked with the significant voxels from the FWE-corrected P-value image ( $p < .05$ ):

```
fslmaths /group.gfeat/cope12.feat/randomise_tfce_corr_p_tstat1.nii.gz -thr 0.95 -bin  
-mul /group.gfeat/cope12.feat/randomise_tstat1.nii.gz  
/group.gfeat/cope12.feat/randomise_thresh_tstat1.nii.gz
```

Next, *cluster* was run to extract clusters and local maxima, resulting in several different outputs, reporting the coordinates in MNI space (mm):

```
cluster --in=/group.gfeat/cope12.feat/randomise_thresh_tstat1.nii.gz --thresh=0.0001  
--oindex=/group.gfeat/cope12.feat/randomise_thresh_tstat1_cluster_index
```

```
--olmax=/group.gfeat/cope12.feat/randomise_thresh_tstat1_lmax.txt  
--osize=/group.gfeat/cope12.feat/randomise_thresh_tstat1_cluster_size --mm  
--scalarname="1-p" > /group.gfeat/cope12.feat/cluster_info.txt
```

For each cluster, a mask was created. For illustration, see the command for cluster #10:

```
fslmaths -dt int /group.gfeat/cope12.feat/randomise_thresh_tstat1_cluster_index  
-thr 10 -uthr 10 -bin /group.gfeat/cope12.feat/cluster_mask10
```

Various atlas images were interrogated with *atlasquery* in order to identify the corresponding anatomical and functional brain areas:

```
atlasquery -a "Harvard-Oxford Subcortical Structural Atlas" -m  
/group.gfeat/cope12.feat/cluster_mask10
```

For tables and figures summarising the results, see Appendix B.

# Appendix B

## Summary of results

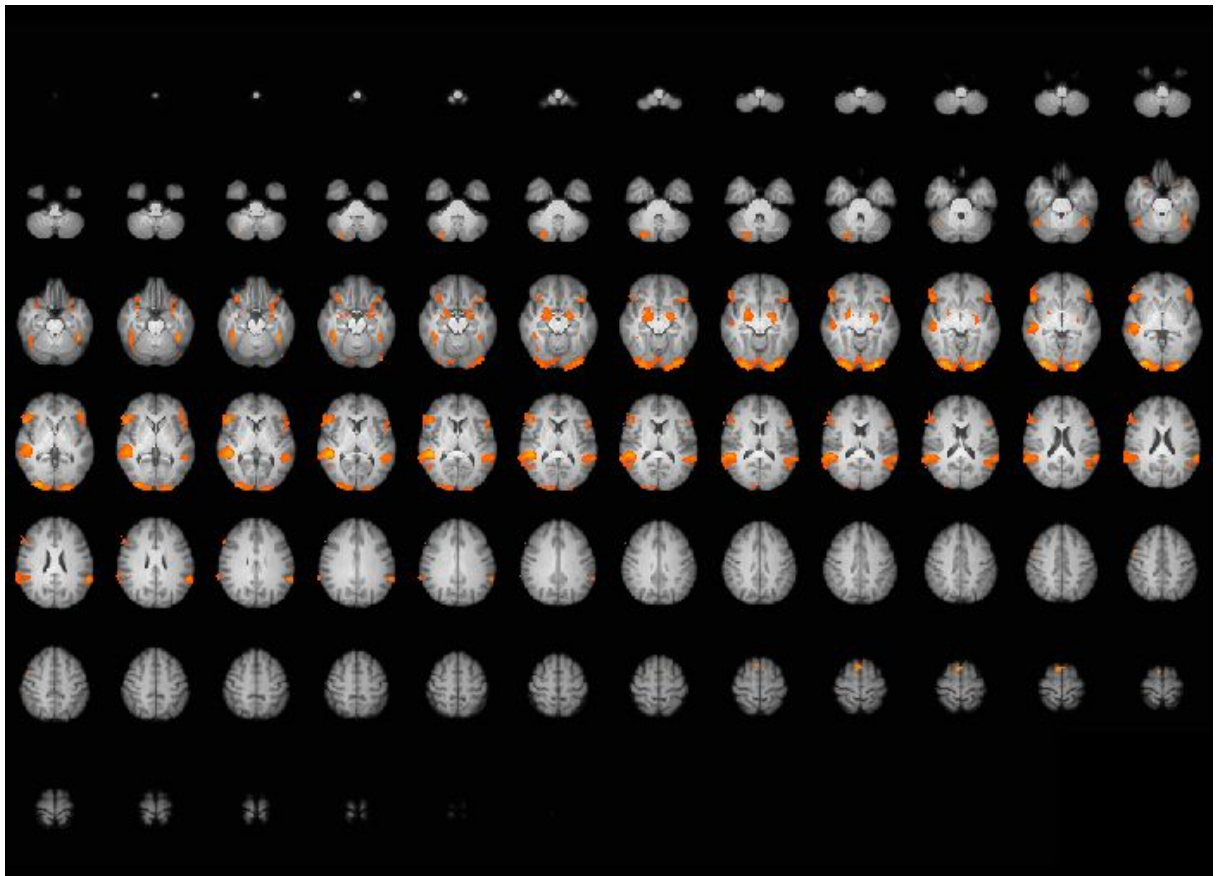


**Figure B.1: Clusters of activation - angry emotional facial expressions vs. neutral facial expressions and moving geometric shapes. TFCE  $t$ -statistic map masked with the FWE-corrected image thresholded at  $p < .05$ , overlaid on the mean high-resolution image.**

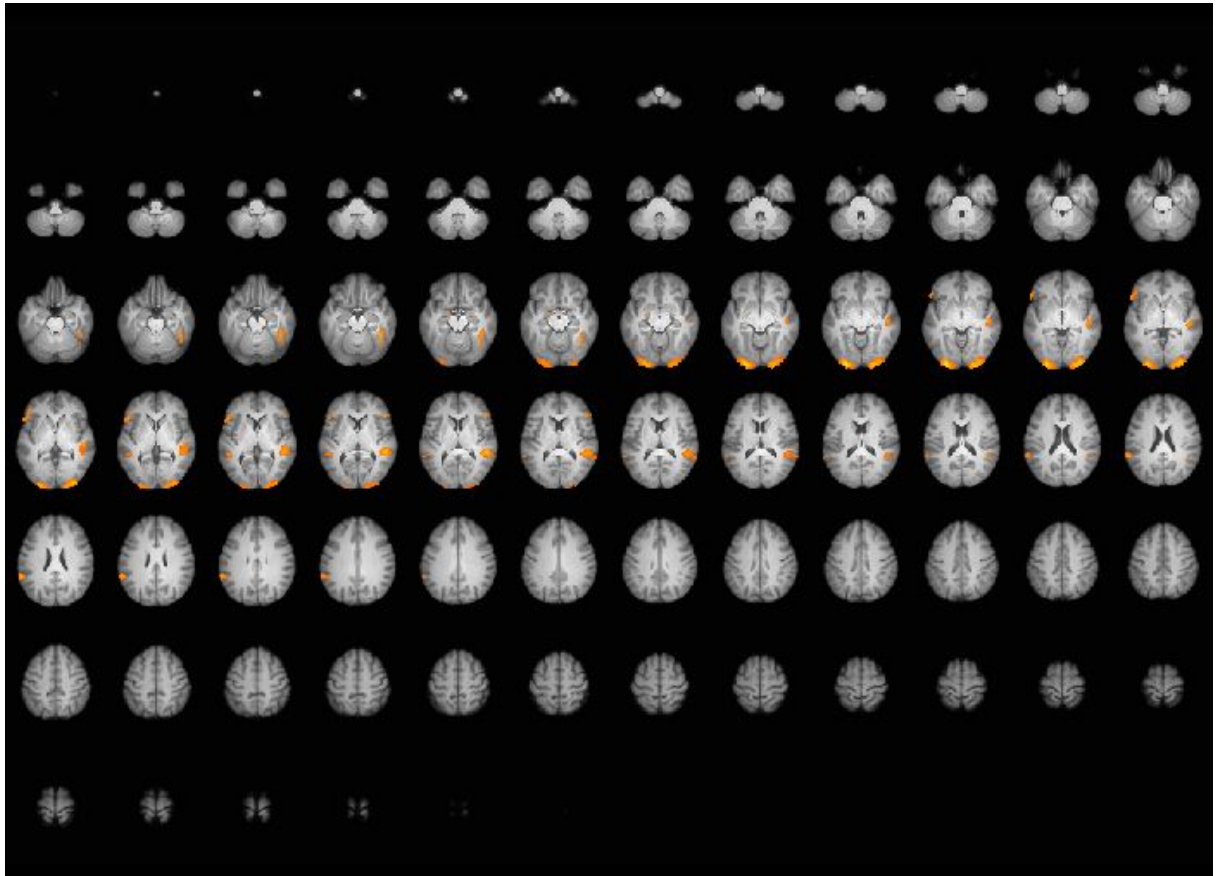


**Figure B.2: Clusters of activation - disgusted emotional facial expressions vs. neutral facial expressions and moving geometric shapes.** TFCE *t*-statistic map masked with the FWE-corrected image thresholded at  $p < .05$ , overlaid on the mean high-resolution image.

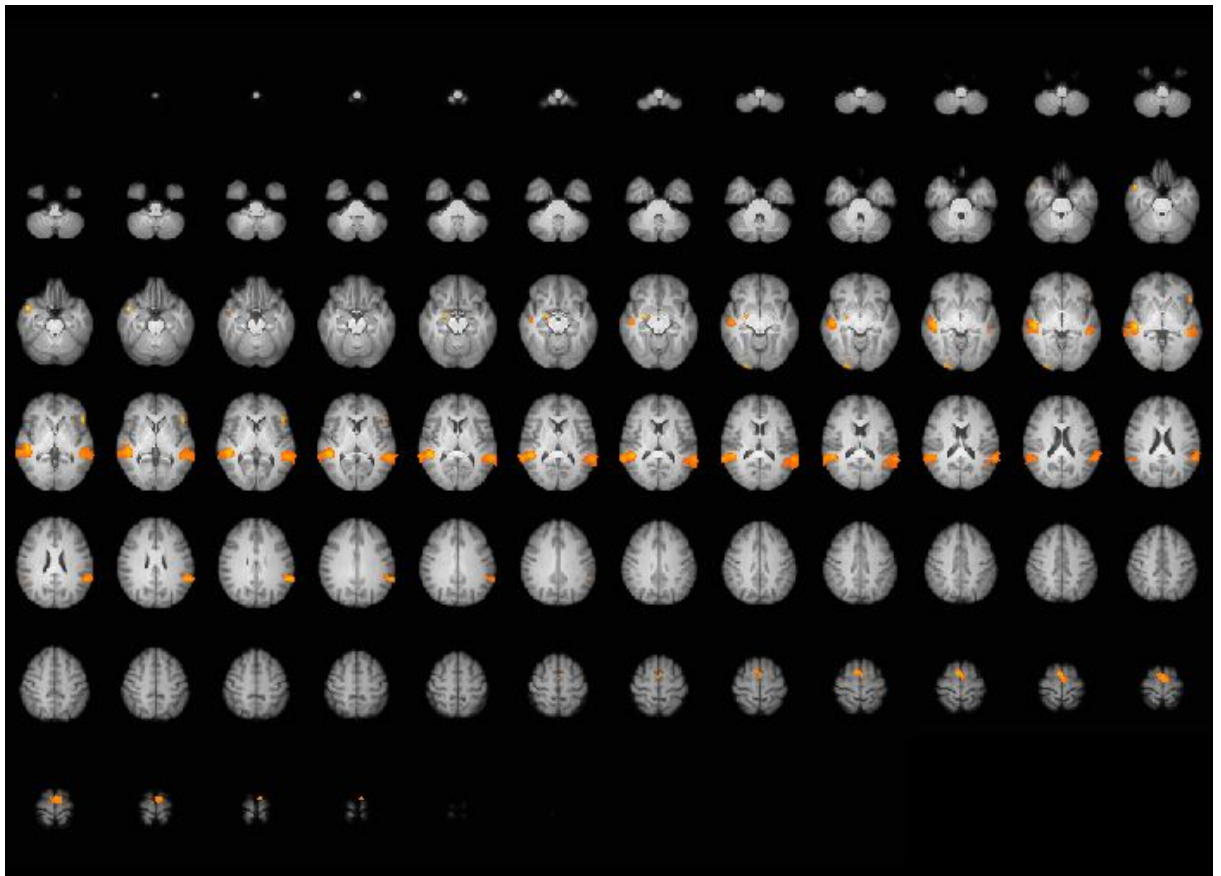


**Figure B.3: Clusters of activation - surprised emotional facial expressions vs. neutral facial expressions and moving geometric shapes.** TFCE *t*-statistic map masked with the FWE-corrected image thresholded at  $p < .05$ , overlaid on the mean high-resolution image.

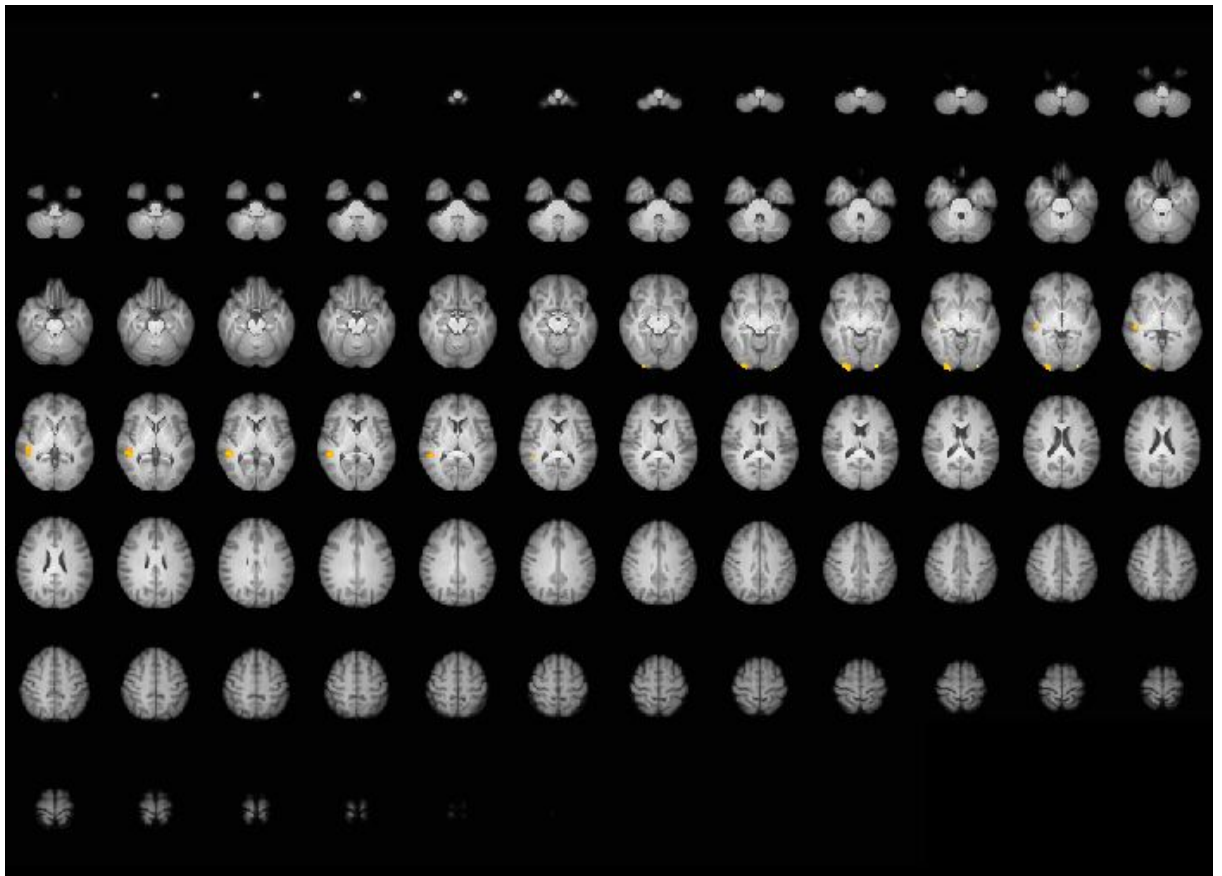


**Figure B.4: Clusters of activation - happy emotional facial expressions vs. neutral facial expressions and moving geometric shapes. TFCE  $t$ -statistic map masked with the FWE-corrected image thresholded at  $p < .05$ , overlaid on the mean high-resolution image.**

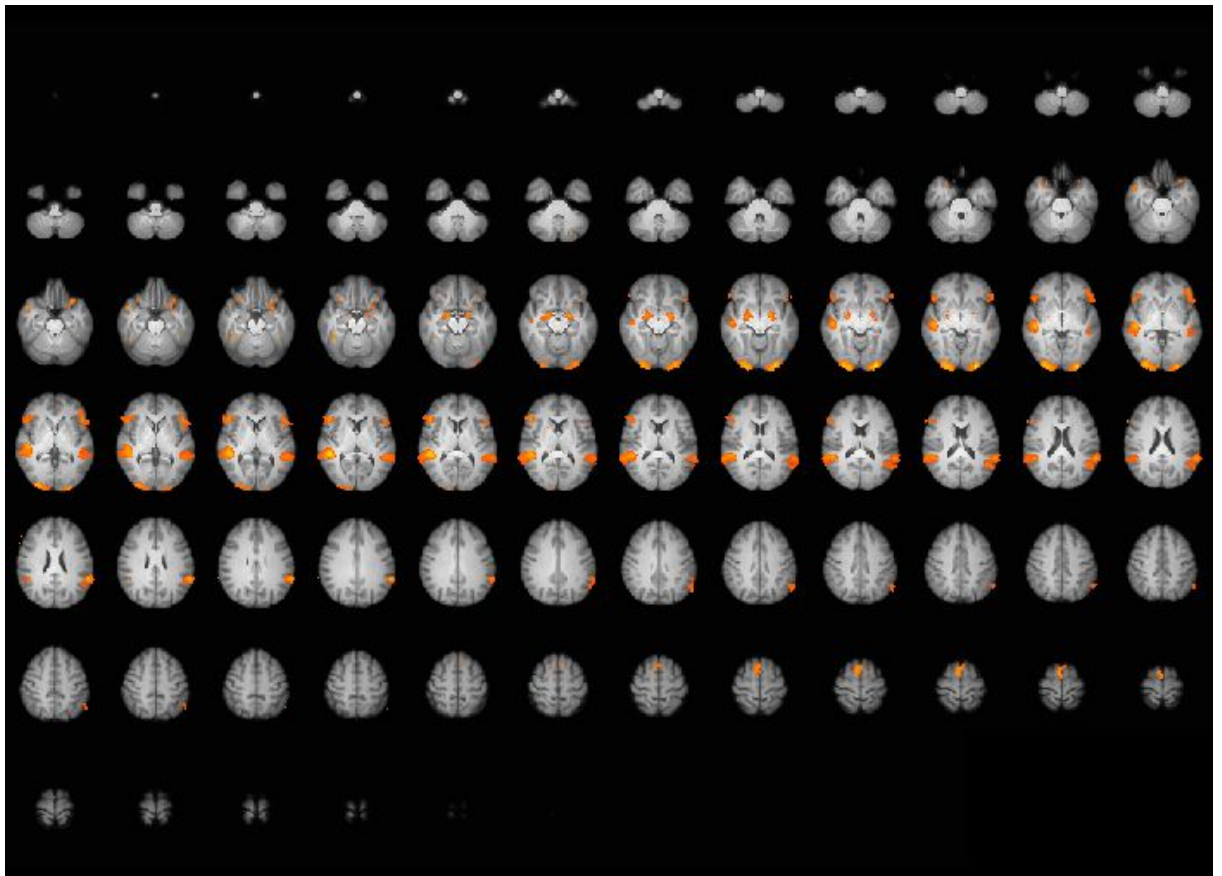


**Figure B.5: Clusters of activation - all emotional facial expressions vs. neutral facial expressions and moving geometric shapes.** TFCE *t*-statistic map masked with the FWE-corrected image thresholded at  $p < .05$ , overlaid on the mean high-resolution image.

**Table B.1: Angry emotional facial expressions vs. neutral facial expressions and moving geometric shapes.** Areas of activation with the cluster size (number of voxels), *T* value of the local maximum, MNI coordinates, the anatomical and functional areas within the cluster, and the probabilities of it being part of them, according to the relevant atlas.

**Angry emotional facial expressions vs. control conditions**

Size	<i>T</i> value	MNI coord. (mm)			Anatomic area	Side	Functional area	prob. (%)
		x	y	z				
2722	10.9	-28	-96	-6	Lateral Occipital Cortex, superior division		GM Visual cortex V1 BA17 L	11.33
					Lateral Occipital Cortex, inferior division		GM Visual cortex V1 BA17 R	19.43
					Intracalcarine Cortex		GM Visual cortex V2 BA18 L	12.59
					Cuneal Cortex		GM Visual cortex V2 BA18 R	15.30
					Lingual Gyrus		GM Visual cortex V3V L	9.25
					Occipital Fusiform Gyrus		GM Visual cortex V3V R	8.75
					Supracalcarine Cortex		GM Visual cortex V4 L	4.69
					Occipital Pole		GM Visual cortex V4 R	3.39
					<i>Cerebral White Matter</i>	L	WM Callosal body	0.01
					<i>Cerebral Cortex</i>	L	WM Optic radiation R	7.72
					<i>Cerebral White Matter</i>	R	WM Optic radiation L	6.11
					<i>Cerebral Cortex</i>	R		
					2078	9.61	48	-36
Superior Temporal Gyrus, posterior division		GM Inferior parietal lobule PF R	3.87					
Middle Temporal Gyrus, anterior division		GM Inferior parietal lobule PFcm R	0.40					
Middle Temporal Gyrus, posterior division		GM Inferior parietal lobule PFm R	4.96					
Middle Temporal Gyrus, temporooccipital part		GM Inferior parietal lobule Pga R	6.64					
Supramarginal Gyrus, anterior division		GM Inferior parietal lobule PGp R	0.62					
Supramarginal Gyrus, posterior division		GM Primary auditory cortex TE1.0 R	0.05					
Angular Gyrus		GM Primary auditory cortex TE1.1 R	0.12					
Lateral Occipital Cortex, superior division		GM Visual cortex V5 R	0.44					
Lateral Occipital Cortex, inferior division		WM Acoustic radiation R	0.11					
Parietal Operculum Cortex		WM Callosal body	0.01					
Planum Polare		WM Inferior occipito-frontal fascicle R	0.08					
Heschl's Gyrus (includes H1 and H2)		WM Optic radiation R	0.48					

					Planum Temporale	0.69		GM Insula Id1 R	0.61
					<i>Cerebral White Matter</i>	28.66	R	GM Insula Ig1 R	0.05
					<i>Cerebral Cortex</i>	59.92	R	GM Insula Ig2 R	0.07
1296	7.14	54	22	0	Frontal Pole	4.32		GM Broca's area BA44 R	8.10
					Insular Cortex	0.11		GM Broca's area BA45 R	33.34
					Middle Frontal Gyrus	0.58		GM Primary auditory cortex TE1.2 R	0.04
					Inferior Frontal Gyrus, pars triangularis	16.50		GM Secondary somatosensory cortex / OP4 R	0.00
					Inferior Frontal Gyrus, pars opercularis	7.58			
					Precentral Gyrus	0.57			
					Temporal Pole	1.51			
					Frontal Orbital Cortex	11.96			
					Parahippocampal Gyrus, anterior division	0.01			
					Frontal Operculum Cortex	3.38			
					Central Opercular Cortex	0.03			
					Planum Polare	0.00			
					<i>Cerebral White Matter</i>	15.74	R		
					<i>Cerebral Cortex</i>	54.43	R		
					<i>Amygdala</i>	0.01	R		
986	6.36	-60	-46	22	Superior Temporal Gyrus, posterior division	7.64		GM Inferior parietal lobule PF L	11.84
					Middle Temporal Gyrus, posterior division	1.90		GM Inferior parietal lobule PFcm L	1.41
					Middle Temporal Gyrus, temporooccipital part	8.95		GM Inferior parietal lobule PFm L	8.00
					Supramarginal Gyrus, anterior division	1.08		GM Inferior parietal lobule Pga L	4.27
					Supramarginal Gyrus, posterior division	23.54		GM Inferior parietal lobule PGp L	1.60
					Angular Gyrus	15.32		GM Visual cortex V5 L	0.04
					Lateral Occipital Cortex, superior division	2.89		WM Optic radiation L	0.03
					Lateral Occipital Cortex, inferior division	0.60			
					Parietal Operculum Cortex	1.56			
					Planum Temporale	1.81			
					<i>Cerebral White Matter</i>	27.20	L		
					<i>Cerebral Cortex</i>	68.81	L		
762	6.35	-40	22	-16	Frontal Pole	3.32		GM Amygdala_laterobasal group L	0.04
					Insular Cortex	0.76		GM Amygdala_superficial group L	0.12
					Middle Frontal Gyrus	0.44		GM Broca's area BA44 L	13.45
					Inferior Frontal Gyrus, pars triangularis	10.86		GM Broca's area BA45 L	15.24

					Inferior Frontal Gyrus, pars opercularis	13.33		GM Hippocampus entorhinal cortex L	0.07
					Precentral Gyrus	2.16		GM Primary somatosensory cortex BA3b L	0.00
					Temporal Pole	2.67		WM Inferior occipito-frontal fascicle L	0.23
					Frontal Orbital Cortex	23.16		WM Uncinate fascicle L	0.08
					Parahippocampal Gyrus, anterior division	0.31			
					Frontal Operculum Cortex	4.97			
					Central Opercular Cortex	1.19			
					Planum Polare	0.01			
					<i>Cerebral White Matter</i>	17.87	L		
					<i>Cerebral Cortex</i>	72.83	L		
					<i>Putamen</i>	0.04	L		
					<i>Amygdala</i>	0.61	L		
419	6.14	22	-2	-10	Insular Cortex	0.01		GM Amygdala_centromedial group R	10.54
					Temporal Pole	0.00		GM Amygdala_laterobasal group R	17.26
					Frontal Orbital Cortex	0.77		GM Amygdala_superficial group R	24.82
					Parahippocampal Gyrus, anterior division	0.13		GM Hippocampus cornu ammonis R	11.79
					<i>Cerebral White Matter</i>	27.51	R	GM Hippocampus entorhinal cortex R	2.00
					<i>Cerebral Cortex</i>	13.29	R	GM Hippocampus dentate gyrus R	3.33
					<i>Putamen</i>	7.57	R	GM Hippocampus hippocampal-amygdaloid transition area R	4.05
					<i>Pallidum</i>	4.35	R	GM Hippocampus subiculum R	4.09
					<i>Hippocampus</i>	4.18	R	WM Acoustic radiation R	0.67
					<i>Amygdala</i>	29.96	R	WM Corticospinal tract R	4.50
					<i>Accumbens</i>	0.00	R	WM Fornix	0.38
								WM Inferior occipito-frontal fascicle R	0.01
								GM Lateral geniculate body R	0.00
								GM Medial geniculate body R	0.02
								WM Optic radiation R	0.52
								WM Uncinate fascicle R	0.35
								GM Insula Id1 R	0.02
350	5.96	-18	-6	-14	Temporal Pole	0.01		GM Amygdala_centromedial group L	18.81
					Frontal Orbital Cortex	0.01		GM Amygdala_laterobasal group L	23.84
					Parahippocampal Gyrus, anterior division	0.20		GM Amygdala_superficial group L	28.14
					<i>Cerebral White Matter</i>	31.55	L	GM Hippocampus cornu ammonis L	13.43

					<i>Cerebral Cortex</i>	5.94	L	GM Hippocampus entorhinal cortex L	1.33
					<i>Putamen</i>	9.48	L	GM Hippocampus dentate gyrus L	3.29
					<i>Pallidum</i>	4.98	L	GM Hippocampus hippocampal-amygdaloid transition area L	3.56
					<i>Hippocampus</i>	4.04	L	GM Hippocampus subiculum L	3.49
					<i>Amygdala</i>	33.49	L	WM Corticospinal tract L	2.05
					<i>Accumbens</i>	0.00	L	WM Fornix	0.20
								WM Inferior occipito-frontal fascicle L	0.03
								GM Lateral geniculate body L	0.79
								WM Optic radiation L	4.64
								WM Uncinate fascicle L	0.42
								GM Insula Id1 L	0.05
318	6.1	40	-42	-16	Inferior Temporal Gyrus, posterior division	4.04		GM Visual cortex V4 R	0.32
					Inferior Temporal Gyrus, temporooccipital part	9.45		WM Callosal body	0.05
					Lateral Occipital Cortex, inferior division	0.62		WM Optic radiation R	2.09
					Temporal Fusiform Cortex, posterior division	4.53			
					Temporal Occipital Fusiform Cortex	28.29			
					Occipital Fusiform Gyrus	2.39			
					<i>Cerebral White Matter</i>	21.17	R		
					<i>Cerebral Cortex</i>	51.32	R		
233	6.63	-42	-44	-22	Inferior Temporal Gyrus, posterior division	4.77		WM Optic radiation L	0.37
					Inferior Temporal Gyrus, temporooccipital part	8.52			
					Lateral Occipital Cortex, inferior division	0.01			
					Temporal Fusiform Cortex, posterior division	16.09			
					Temporal Occipital Fusiform Cortex	20.28			
					Occipital Fusiform Gyrus	0.14			
					<i>Cerebral White Matter</i>	12.50	L		
					<i>Cerebral Cortex</i>	51.49	L		
205	5.24	32	-80	-42	<i>Cerebral Cortex</i>	0.00	R		
100	6.2	8	8	68	Superior Frontal Gyrus	36.43		GM Premotor cortex BA6 L	2.89
					Precentral Gyrus	0.03		GM Premotor cortex BA6 R	51.97
					Juxtapositional Lobule Cortex	15.11			
					Paracingulate Gyrus	0.02			
					<i>Cerebral White Matter</i>	0.12	L		

					<i>Cerebral Cortex</i>	7.00	L		
					<i>Cerebral White Matter</i>	17.87	R		
					<i>Cerebral Cortex</i>	61.03	R		
30	5.3	50	4	46	Middle Frontal Gyrus	14.73		GM Broca's area BA44 R	5.50
					Precentral Gyrus	54.13		GM Primary somatosensory cortex BA1 R	0.30
					Postcentral Gyrus	0.10		GM Primary somatosensory cortex BA3b R	1.27
					<i>Cerebral White Matter</i>	14.13	R	GM Premotor cortex BA6 R	38.47
					<i>Cerebral Cortex</i>	80.83	R	WM Corticospinal tract R	0.13
14	4.78	-40	-2	-16	Insular Cortex	21.64		AWM Inferior occipito-frontal fascicle L	7.07
					Temporal Pole	0.36		WM Optic radiation L	0.29
					Planum Polare	27.00		WM Uncinate fascicle L	0.50
					<i>Cerebral White Matter</i>	25.92	L	GM Insula Id1 L	2.21
					<i>Cerebral Cortex</i>	71.09	L		

**Table B.2: Disgusted emotional facial expressions vs. neutral facial expressions and moving geometric shapes.** Areas of activation with the cluster size (number of voxels), *T* value of the local maximum, MNI coordinates, the anatomical and functional areas within the cluster, and the probabilities of it being part of them, according to the relevant atlas.

**Disgusted emotional facial expressions vs. control conditions**

Size	<i>T</i> value	MNI coord. (mm)			Anatomic area	Side	Functional area	
		x	y	z			cortical/subcortical	prob. (%)
868	8.1	34	-94	-2	Lateral Occipital Cortex, superior division		GM Visual cortex V1 BA17 R	35.49
					Lateral Occipital Cortex, inferior division		GM Visual cortex V2 BA18 R	34.02
					Intracalcarine Cortex		GM Visual cortex V3V R	22.67
					Lingual Gyrus		GM Visual cortex V4 R	7.25
					Occipital Fusiform Gyrus		WM Callosal body	0.00
					Occipital Pole		WM Optic radiation R	17.27
					<i>Cerebral White Matter</i>	R		
					<i>Cerebral Cortex</i>	R		
827	7.73	52	-38	6	Superior Temporal Gyrus, anterior division		GM Inferior parietal lobule PF R	0.27
					Superior Temporal Gyrus, posterior division		GM Inferior parietal lobule PFcm R	0.02
					Middle Temporal Gyrus, anterior division		GM Inferior parietal lobule PFm R	1.91
					Middle Temporal Gyrus, posterior division		GM Inferior parietal lobule Pga R	3.09
					Middle Temporal Gyrus, temporooccipital part		GM Inferior parietal lobule PGp R	0.04
					Supramarginal Gyrus, posterior division		GM Primary auditory cortex TE1.0 R	0.12
					Angular Gyrus		GM Primary auditory cortex TE1.1 R	0.21
					Lateral Occipital Cortex, superior division		WM Acoustic radiation R	0.31
					Parietal Operculum Cortex		WM Callosal body	0.07
					Planum Polare		WM Inferior occipito-frontal fascicle R	0.20
					Heschl's Gyrus (includes H1 and H2)		WM Optic radiation R	0.87
					Planum Temporale		GM Insula Id1 R	1.61
					<i>Cerebral White Matter</i>	R	GM Insula Ig1 R	0.08
					<i>Cerebral Cortex</i>	R	GM Insula Ig2 R	0.15
					703	9.52	-26	-98
Lateral Occipital Cortex, inferior division		GM Visual cortex V2 BA18 L	28.64					

					Intracalcarine Cortex	0.00		GM Visual cortex V3V L	27.14
					Lingual Gyrus	0.09		GM Visual cortex V4 L	12.49
					Occipital Fusiform Gyrus	2.41		WM Optic radiation L	10.03
					Occipital Pole	46.64			
					<i>Cerebral White Matter</i>	23.14	L		
					<i>Cerebral Cortex</i>	59.78	L		
283	6.6	-62	-44	24	Superior Temporal Gyrus, posterior division	9.01		GM Inferior parietal lobule PF L	29.44
					Middle Temporal Gyrus, posterior division	2.83		GM Inferior parietal lobule PFcm L	4.31
					Middle Temporal Gyrus, temporooccipital part	4.33		GM Inferior parietal lobule PFm L	15.52
					Supramarginal Gyrus, anterior division	3.87		GM Inferior parietal lobule Pga L	3.05
					Supramarginal Gyrus, posterior division	33.50			
					Angular Gyrus	8.66			
					Lateral Occipital Cortex, superior division	0.02			
					Parietal Operculum Cortex	4.86			
					Planum Temporale	3.38			
					<i>Cerebral White Matter</i>	20.03	L		
					<i>Cerebral Cortex</i>	74.44	L		
226	6.46	42	-44	-18	Inferior Temporal Gyrus, posterior division	4.03		GM Visual cortex V4 R	0.17
					Inferior Temporal Gyrus, temporooccipital part	14.91		WM Callosal body	0.02
					Lateral Occipital Cortex, inferior division	0.93		WM Optic radiation R	1.62
					Temporal Fusiform Cortex, posterior division	4.84			
					Temporal Occipital Fusiform Cortex	37.99			
					Occipital Fusiform Gyrus	3.53			
					<i>Cerebral White Matter</i>	27.18	R		
					<i>Cerebral Cortex</i>	68.58	R		
195	5.61	-56	24	-4	Frontal Pole	6.54		GM Broca's area BA44 L	13.48
					Inferior Frontal Gyrus, pars triangularis	28.48		GM Broca's area BA45 L	26.92
					Inferior Frontal Gyrus, pars opercularis	9.93			
					Precentral Gyrus	0.15			
					Frontal Orbital Cortex	4.57			
					Frontal Operculum Cortex	3.86			
					<i>Cerebral White Matter</i>	13.90	L		
					<i>Cerebral Cortex</i>	62.18	L		
44	5.83	50	26	8	Frontal Pole	0.70		GM Broca's area BA44 R	1.41

				Inferior Frontal Gyrus, pars triangularis	33.02		GM Broca's area BA45 R	54.30
				Inferior Frontal Gyrus, pars opercularis	8.84			
				Precentral Gyrus	0.16			
				Frontal Orbital Cortex	0.84			
				Frontal Operculum Cortex	3.57			
				<i>Cerebral White Matter</i>	39.95	R		
				<i>Cerebral Cortex</i>	57.13	R		
24	5.85	-18	-4	-16	Parahippocampal Gyrus, anterior division	0.08	GM Amygdala_centromedial group L	34.54
					<i>Cerebral White Matter</i>	15.04	L GM Amygdala_laterobasal group L	32.17
					<i>Cerebral Cortex</i>	6.51	L GM Amygdala_superficial group L	80.33
					<i>Pallidum</i>	1.88	L GM Hippocampus cornu ammonis L	2.25
					<i>Hippocampus</i>	0.23	L GM Hippocampus entorhinal cortex L	0.46
					<i>Amygdala</i>	69.65	L GM Hippocampus hippocampal-amygdaloid transition area L	2.92
							GM Hippocampus subiculum L	2.04

**Table B.3: Surprised emotional facial expressions vs. neutral facial expressions and moving geometric shapes.** Areas of activation with the cluster size (number of voxels), *T* value of the local maximum, MNI coordinates, the anatomical and functional areas within the cluster, and the probabilities of it being part of them, according to the relevant atlas.

**Surprised emotional facial expressions vs. control conditions**

Size	<i>T</i> value	MNI coord. (mm)			Anatomic area	Side	Functional area	prob. (%)						
		x	y	z					cortical/subcortical	prob. (%)				
1724	8.13	48	-24	-2	Superior Temporal Gyrus, anterior division		GM Anterior intra-parietal sulcus hIP1 R	0.30	0.04					
					Superior Temporal Gyrus, posterior division		GM Inferior parietal lobule PF R	15.21	1.19					
					Middle Temporal Gyrus, anterior division		GM Inferior parietal lobule PFcm R	0.22	0.16					
					Middle Temporal Gyrus, posterior division		GM Inferior parietal lobule PFm R	12.41	3.35					
					Middle Temporal Gyrus, temporooccipital part		GM Inferior parietal lobule Pga R	11.64	5.45					
					Supramarginal Gyrus, posterior division		GM Inferior parietal lobule PGp R	10.70	0.07					
					Angular Gyrus		GM Primary auditory cortex TE1.0 R	8.78	0.07					
					Lateral Occipital Cortex, superior division		GM Primary auditory cortex TE1.1 R	0.06	0.12					
					Lateral Occipital Cortex, inferior division		WM Acoustic radiation R	0.01	0.21					
					Parietal Operculum Cortex		WM Callosal body	0.02	0.01					
					Planum Polare		WM Inferior occipito-frontal fascicle R	0.08	0.13					
					Heschl's Gyrus (includes H1 and H2)		WM Optic radiation R	0.03	0.86					
					Planum Temporale		GM Insula Id1 R	0.45	0.96					
					<i>Cerebral White Matter</i>		R GM Insula Ig1 R	30.46	0.04					
					<i>Cerebral Cortex</i>		R GM Insula Ig2 R	64.55	0.08					
					1707	7.07	-60	-46	28	Superior Temporal Gyrus, posterior division		GM Anterior intra-parietal sulcus hIP1 L	11.87	0.00
										Middle Temporal Gyrus, posterior division		GM Anterior intra-parietal sulcus hIP2 L	6.61	0.24
Middle Temporal Gyrus, temporooccipital part		GM Anterior intra-parietal sulcus hIP3 L	8.92	0.00										
Inferior Temporal Gyrus, posterior division		GM Inferior parietal lobule PF L	0.00	10.22										
Postcentral Gyrus		GM Inferior parietal lobule PFcm L	0.00	3.46										
Supramarginal Gyrus, anterior division		GM Inferior parietal lobule PFm L	1.45	6.17										
Supramarginal Gyrus, posterior division		GM Inferior parietal lobule PFop L	16.23	0.09										
Angular Gyrus		GM Inferior parietal lobule Pft L	9.14	0.01										
Lateral Occipital Cortex, superior division		GM Inferior parietal lobule Pga L	0.88	2.55										
Lateral Occipital Cortex, inferior division		GM Inferior parietal lobule PGp L	0.34	0.19										
Central Opercular Cortex		GM Primary auditory cortex TE1.0 L	0.01	0.00										
Parietal Operculum Cortex		GM Primary auditory cortex TE1.1 L	2.93	0.01										
		GM Secondary somatosensory cortex / Parietal operculum OP1 L	0.00	0.10										
Planum Temporale		WM Acoustic radiation L	2.43	0.06										

					<i>Cerebral White Matter</i>	24.45	L	WM Optic radiation L	0.18
					<i>Cerebral Cortex</i>	65.04	L	GM Insula Id1 L	0.01
422	6.8	8	2	66	Superior Frontal Gyrus	10.68		GM Primary motor cortex BA4a L	0.30
					Precentral Gyrus	4.46		GM Primary motor cortex BA4a R	0.09
					Juxtapositional Lobule Cortex	40.78		GM Premotor cortex BA6 L	33.78
					Paracingulate Gyrus	0.05		GM Premotor cortex BA6 R	41.19
					<i>Cerebral White Matter</i>	5.96	L	WM Corticospinal tract L	0.03
					<i>Cerebral Cortex</i>	35.45	L		
					<i>Cerebral White Matter</i>	6.94	R		
					<i>Cerebral Cortex</i>	29.41	R		
85	6.29	30	-94	-4	Lateral Occipital Cortex, superior division	0.01		GM Visual cortex V1 BA17 R	42.79
					Lateral Occipital Cortex, inferior division	5.45		GM Visual cortex V2 BA18 R	50.34
					Lingual Gyrus	0.27		GM Visual cortex V3V R	27.99
					Occipital Fusiform Gyrus	0.75		GM Visual cortex V4 R	2.44
					Occipital Pole	56.98		WM Optic radiation R	25.51
					<i>Cerebral White Matter</i>	26.88	R		
					<i>Cerebral Cortex</i>	65.24	R		
79	7.22	-48	26	2	Frontal Pole	0.30		GM Broca's area BA44 L	13.99
					Inferior Frontal Gyrus, pars triangularis	31.42		GM Broca's area BA45 L	22.18
					Inferior Frontal Gyrus, pars opercularis	11.15			
					Precentral Gyrus	0.03			
					Frontal Orbital Cortex	6.27			
					Frontal Operculum Cortex	16.13			
					<i>Cerebral White Matter</i>	21.61	L		
					<i>Cerebral Cortex</i>	75.23	L		
76	7.2	24	-10	-12	<i>Cerebral White Matter</i>	22.35	R	GM Amygdala_centromedial group R	25.08
					<i>Cerebral Cortex</i>	0.74	R	GM Amygdala_laterobasal group R	38.24
					<i>Putamen</i>	2.94	R	GM Amygdala_superficial group R	39.14
					<i>Pallidum</i>	3.06	R	GM Hippocampus cornu ammonis R	22.62
					<i>Hippocampus</i>	5.33	R	GM Hippocampus entorhinal cortex R	4.20
					<i>Amygdala</i>	59.86	R	GM Hippocampus dentate gyrus R	2.84
								GM Hippocampus hippocampal-amygdaloid transition area R	8.49
								GM Hippocampus subiculum R	10.18
								WM Acoustic radiation R	1.20
								WM Corticospinal tract R	0.25
								WM Fornix	0.17
								WM Optic radiation R	0.54
65	9.18	50	6	-22	Temporal Pole	41.37			
					Superior Temporal Gyrus, anterior division	8.60			
					Superior Temporal Gyrus, posterior division	0.32			
					Middle Temporal Gyrus, anterior division	9.17			

Middle Temporal Gyrus, posterior division	0.17	
Planum Polare	0.25	
<i>Cerebral White Matter</i>	31.89	R
<i>Cerebral Cortex</i>	67.80	R

**Table B.4: Happy emotional facial expressions vs. neutral facial expressions and moving geometric shapes.** Areas of activation with the cluster size (number of voxels), *T* value of the local maximum, MNI coordinates, the anatomical and functional areas within the cluster, and the probabilities of it being part of them, according to the relevant atlas.

**Happy emotional facial expressions vs. control conditions**

Size	<i>T</i> value	MNI coord. (mm)			Anatomic area	Side	Functional area	prob. (%)
		x	y	z				
256	6.75	48	-38	4	Superior Temporal Gyrus, posterior division		GM Inferior parietal lobule PFm R	0.04
					Middle Temporal Gyrus, posterior division		GM Inferior parietal lobule Pga R	0.02
					Middle Temporal Gyrus, temporooccipital part		GM Primary auditory cortex TE1.0 R	0.20
					Supramarginal Gyrus, posterior division		GM Primary auditory cortex TE1.1 R	0.15
					Angular Gyrus		WM Acoustic radiation R	0.29
					Planum Polare		WM Callosal body	0.10
					Heschl's Gyrus (includes H1 and H2)		WM Inferior occipito-frontal fascicle R	0.42
					Planum Temporale		WM Optic radiation R	0.86
					<i>Cerebral White Matter</i>		GM Insula Id1 R	2.24
					<i>Cerebral Cortex</i>		GM Insula Ig1 R	0.16
			GM Insula Ig2 R	0.28				
163	7.19	28	-100	8	Lateral Occipital Cortex, superior division		GM Visual cortex V1 BA17 R	49.42
					Lateral Occipital Cortex, inferior division		GM Visual cortex V2 BA18 R	48.02
					Lingual Gyrus		GM Visual cortex V3V R	21.21
					Occipital Fusiform Gyrus		GM Visual cortex V4 R	1.55
					Occipital Pole		WM Optic radiation R	25.93
					<i>Cerebral White Matter</i>			
					<i>Cerebral Cortex</i>			
14	7.64	-28	-98	6	Lateral Occipital Cortex, inferior division		GM Visual cortex V1 BA17 L	13.07
					Occipital Fusiform Gyrus		GM Visual cortex V2 BA18 L	29.86
					Occipital Pole		GM Visual cortex V3V L	40.93
					<i>Cerebral White Matter</i>		GM Visual cortex V4 L	6.00
					<i>Cerebral Cortex</i>		WM Optic radiation L	2.21

**Table B.5: All emotional facial expressions vs. neutral facial expressions and moving geometric shapes.** Areas of activation with the cluster size (number of voxels), *T* value of the local maximum, MNI coordinates, the anatomical and functional areas within the cluster, and the probabilities of it being part of them, according to the relevant atlas.

**All emotional facial expressions vs. control conditions**

Size	<i>T</i> value	MNI coord. (mm)			Anatomic area	Side	Functional area	prob. (%)
		x	y	z				
1777	9.54	52	-38	6	Superior Temporal Gyrus, anterior division		GM Anterior intra-parietal sulcus hIP1 R	0.08
					Superior Temporal Gyrus, posterior division		GM Inferior parietal lobule PF R	1.11
					Middle Temporal Gyrus, anterior division		GM Inferior parietal lobule PFcm R	0.22
					Middle Temporal Gyrus, posterior division		GM Inferior parietal lobule PFm R	4.14
					Middle Temporal Gyrus, temporooccipital part		GM Inferior parietal lobule Pga R	6.62
					Supramarginal Gyrus, posterior division		GM Inferior parietal lobule PGp R	0.12
					Angular Gyrus		GM Primary auditory cortex TE1.0 R	0.10
					Lateral Occipital Cortex, superior division		GM Primary auditory cortex TE1.1 R	0.20
					Lateral Occipital Cortex, inferior division		WM Acoustic radiation R	0.26
					Parietal Operculum Cortex		WM Callosal body	0.08
					Planum Polare		WM Inferior occipito-frontal fascicle R	0.14
					Heschl's Gyrus (includes H1 and H2)		WM Optic radiation R	1.60
					Planum Temporale		GM Insula Id1 R	1.13
					<i>Cerebral White Matter</i>		GM Insula Ig1 R	0.08
					<i>Cerebral Cortex</i>		GM Insula Ig2 R	0.13
1739	7.42	-60	-46	28	Superior Temporal Gyrus, posterior division		GM Anterior intra-parietal sulcus hIP2 L	0.01
					Middle Temporal Gyrus, posterior division		GM Inferior parietal lobule PF L	10.05
					Middle Temporal Gyrus, temporooccipital part		GM Inferior parietal lobule PFcm L	1.56
					Supramarginal Gyrus, anterior division		GM Inferior parietal lobule PFm L	8.70
					Supramarginal Gyrus, posterior division		GM Inferior parietal lobule Pga L	5.99
					Angular Gyrus		GM Inferior parietal lobule PGp L	1.22
					Lateral Occipital Cortex, superior division		GM Primary auditory cortex TE1.0 L	0.00
					Lateral Occipital Cortex, inferior division		GM Primary auditory cortex TE1.1 L	0.02
					Parietal Operculum Cortex		GM Visual cortex V5 L	0.00

					Heschl's Gyrus (includes H1 and H2)	0.00		WM Acoustic radiation L	0.11
					Planum Temporale	1.52		WM Optic radiation L	0.25
					<i>Cerebral White Matter</i>	22.07	L	GM Insula Id1 L	0.02
					<i>Cerebral Cortex</i>	64.20	L		
783	8.33	32	-94	-2	Lateral Occipital Cortex, superior division	0.27		GM Visual cortex V1 BA17 R	40.68
					Lateral Occipital Cortex, inferior division	7.54		GM Visual cortex V2 BA18 R	35.27
					Intracalcarine Cortex	0.06		GM Visual cortex V3V R	21.16
					Lingual Gyrus	0.37		GM Visual cortex V4 R	5.03
					Occipital Fusiform Gyrus	1.88		WM Optic radiation R	17.63
					Supracalcarine Cortex	0.01			
					Occipital Pole	47.58			
					<i>Cerebral Cortex</i>	0.02	L		
					<i>Cerebral White Matter</i>	21.02	R		
					<i>Cerebral Cortex</i>	59.76	R		
630	7.42	50	24	8	Frontal Pole	1.33		GM Broca's area BA44 R	8.75
					Insular Cortex	0.07		GM Broca's area BA45 R	44.41
					Middle Frontal Gyrus	0.19		GM Primary auditory cortex TE1.2 R	0.03
					Inferior Frontal Gyrus, pars triangularis	24.80			
					Inferior Frontal Gyrus, pars opercularis	10.06			
					Precentral Gyrus	0.42			
					Temporal Pole	0.05			
					Frontal Orbital Cortex	7.22			
					Frontal Operculum Cortex	6.08			
					Central Opercular Cortex	0.04			
					<i>Cerebral White Matter</i>	22.84	R		
					<i>Cerebral Cortex</i>	59.30	R		
554	10.6	-28	-96	-8	Lateral Occipital Cortex, superior division	0.01		GM Visual cortex V1 BA17 L	23.29
					Lateral Occipital Cortex, inferior division	7.63		GM Visual cortex V2 BA18 L	29.98
					Lingual Gyrus	0.05		GM Visual cortex V3V L	28.03
					Occipital Fusiform Gyrus	2.17		GM Visual cortex V4 L	10.90
					Occipital Pole	48.20		WM Optic radiation L	11.84
					<i>Cerebral White Matter</i>	22.38	L		
					<i>Cerebral Cortex</i>	59.71	L		
491	6.02	-50	24	2	Frontal Pole	6.39		GM Broca's area BA44 L	14.13

					Insular Cortex	0.00		GM Broca's area BA45 L	20.12
					Middle Frontal Gyrus	0.00		GM Secondary somatosensory cortex / Parietal operculum OP4 L	0.01
					Inferior Frontal Gyrus, pars triangularis	19.29			
					Inferior Frontal Gyrus, pars opercularis	11.48			
					Precentral Gyrus	1.87			
					Temporal Pole	0.48			
					Frontal Orbital Cortex	6.88			
					Frontal Operculum Cortex	6.18			
					Central Opercular Cortex	0.87			
					<i>Cerebral White Matter</i>	16.45	L		
					<i>Cerebral Cortex</i>	61.34	L		
309	6.59	6	2	66	Superior Frontal Gyrus	26.55		GM Premotor cortex BA6 L	6.32
					Precentral Gyrus	0.81		GM Premotor cortex BA6 R	55.40
					Juxtapositional Lobule Cortex	26.49			
					Paracingulate Gyrus	0.24			
					<i>Cerebral White Matter</i>	1.20	L		
					<i>Cerebral Cortex</i>	18.53	L		
					<i>Cerebral White Matter</i>	14.32	R		
					<i>Cerebral Cortex</i>	48.71	R		
267	7.24	24	-8	-8	Frontal Orbital Cortex	0.12		GM Amygdala_centromedial group R	20.10
					Parahippocampal Gyrus, anterior division	0.09		GM Amygdala_laterobasal group R	20.21
					<i>Cerebral White Matter</i>	27.69	R	GM Amygdala_superficial group R	32.34
					<i>Cerebral Cortex</i>	8.67	R	GM Hippocampus cornu ammonis R	13.93
					<i>Putamen</i>	5.90	R	GM Hippocampus entorhinal cortex R	3.13
					<i>Pallidum</i>	5.80	R	GM Hippocampus dentate gyrus R	2.95
					<i>Hippocampus</i>	4.41	R	GM Hippocampus hippocampal-amygdaloid transition area R	5.11
					<i>Amygdala</i>	37.88	R	GM Hippocampus subiculum R	5.67
								WM Acoustic radiation R	0.85
								WM Corticospinal tract R	1.93
								WM Fornix	0.28
								WM Inferior occipito-frontal fascicle R	0.00
								WM Optic radiation R	0.98

								WM Uncinate fascicle R	0.04
183	7.15	-18	-4	-10	Parahippocampal Gyrus, anterior division	0.15		GM Amygdala_centromedial group L	23.95
					<i>Cerebral White Matter</i>	29.24	L	GM Amygdala_laterobasal group L	22.52
					<i>Cerebral Cortex</i>	8.39	L	GM Amygdala_superficial group L	43.89
					<i>Putamen</i>	3.41	L	GM Hippocampus cornu ammonis L	11.69
					<i>Pallidum</i>	5.54	L	GM Hippocampus entorhinal cortex L	2.10
					<i>Hippocampus</i>	3.00	L	GM Hippocampus dentate gyrus L	2.83
					<i>Amygdala</i>	41.15	L	GM Hippocampus hippocampal-amygdaloid transition area L	5.46
					<i>Accumbens</i>	0.00	L	GM Hippocampus subiculum L	4.43
								WM Corticospinal tract L	2.02
								WM Fornix	0.16
								GM Lateral geniculate body L	0.09
								WM Optic radiation L	0.99
								WM Uncinate fascicle L	0.18
165	6.15	-30	18	-24	Frontal Pole	0.07		GM Amygdala_laterobasal group L	0.03
					Insular Cortex	1.91		GM Amygdala_superficial group L	0.17
					Temporal Pole	7.62		GM Hippocampus entorhinal cortex L	0.05
					Frontal Orbital Cortex	50.64		WM Inferior occipito-frontal fascicle L	0.84
					Parahippocampal Gyrus, anterior division	0.70		WM Uncinate fascicle L	0.38
					Planum Polare	0.02			
					<i>Cerebral White Matter</i>	10.44	L		
					<i>Cerebral Cortex</i>	73.64	L		
					<i>Putamen</i>	0.02	L		
					<i>Amygdala</i>	1.47	L		
81	5.09	32	8	-28	Insular Cortex	0.06		GM Amygdala_laterobasal group R	0.01
					Temporal Pole	26.16		GM Hippocampus entorhinal cortex R	0.17
					Frontal Orbital Cortex	36.36		GM Insula Id1 R	0.01
					Parahippocampal Gyrus, anterior division	0.65			
					Temporal Fusiform Cortex, anterior division	0.01			
					<i>Cerebral White Matter</i>	12.49	R		
					<i>Cerebral Cortex</i>	69.11	R		
					<i>Amygdala</i>	0.15	R		
56	6.79	52	8	-22	Temporal Pole	43.95			

					Superior Temporal Gyrus, anterior division	7.25			
					Superior Temporal Gyrus, posterior division	0.18			
					Middle Temporal Gyrus, anterior division	10.63			
					Middle Temporal Gyrus, posterior division	0.29			
					Planum Polare	0.04			
					<i>Cerebral White Matter</i>	29.16	R		
					<i>Cerebral Cortex</i>	70.31	R		
39	6.57	42	-44	-18	Inferior Temporal Gyrus, posterior division	2.18			
					Inferior Temporal Gyrus, temporooccipital part	13.87			
					Temporal Fusiform Cortex, posterior division	4.44			
					Temporal Occipital Fusiform Cortex	47.56			
					<i>Cerebral White Matter</i>	29.61	R		
					<i>Cerebral Cortex</i>	69.68	R		
12	7.18	-40	-44	-20	Inferior Temporal Gyrus, posterior division	10.00			
					Inferior Temporal Gyrus, temporooccipital part	10.50			
					Temporal Fusiform Cortex, posterior division	35.00			
					Temporal Occipital Fusiform Cortex	23.50			
					<i>Cerebral White Matter</i>	17.56	L		
					<i>Cerebral Cortex</i>	80.86	L		
9	5.27	-42	-2	-18	Insular Cortex	9.89		WM Inferior occipito-frontal fascicle L	0.56
					Temporal Pole	0.44		GM Insula Id1 L	2.00
					Planum Polare	49.11			
					<i>Cerebral White Matter</i>	21.27	L		
					<i>Cerebral Cortex</i>	75.17	L		
9	6.03	-22	-76	-38					
8	4.86	72	-44	30	Supramarginal Gyrus, posterior division	0.50			
					<i>Cerebral Cortex</i>	0.95	R		
4	5.73	20	10	10	<i>Cerebral White Matter</i>	80.64	R		
					<i>Caudate</i>	13.69	R		
					<i>Putamen</i>	5.67	R		
2	4.26	62	32	24	<i>Cerebral Cortex</i>	0.26	R		